



The Influence Of Wind On The Heat Losses From Solar Cavity Receivers

Ka Lok 'Leok' Lee

Thesis submitted for the degree of Doctor of Philosophy

School of Mechanical Engineering

Faculty of Engineering, Computer & Mathematical Sciences

The University of Adelaide, Australia

July 2018

Table of contents

Abstract IX

Declaration XI

Acknowledgement XIII

CHAPTER 1 Introduction1

1.1 Introductory background 2

1.2 Type of concentrated solar power technologies 4

1.3 Type of solar tower receivers 9

1.4 Type of heat transfer media 11

1.4.1 Gas receiver 11

1.4.2 Solid particle receivers 12

1.4.3 Liquid receivers 13

1.5 Convective heat losses from solar cavity receiver 13

1.6 Thesis aim and objectives 15

1.6.1 Aim 15

1.6.2 Objectives 15

1.7 Thesis outline 16

1.8 Format 20

CHAPTER 2 Literature Review 21

2.1 Heat loss from cavity solar receivers 22

2.1.1 Convective zone and stagnant zone for natural convection 23

2.1.2 Receiver tilt angle 25

2.1.3 Aspect ratio, aperture ratio and aperture displacement ratio 26

2.1.4	Effect of wind on heat losses from a receiver	31
2.1.5	Empirical relationships of convection	34
2.2	Experiment of convective heat losses from a heated cavity _____	37
2.3	Non-uniform temperature distribution _____	41
2.4	Ray tracing _____	41
2.5	Aperture features _____	42
2.5.1	Flow control aperture.....	42
2.5.2	Windowed aperture	43
2.6	Beam down solar system _____	45
2.7	Economic assessment _____	47
CHAPTER 3 Methodology		51
3.1	Numerical model _____	52
3.2	Experimental setup _____	54
CHAPTER 4 An Investigation Into The Effect Of Aspect Ratio On The Heat Loss From A Solar Cavity Receiver		59
CHAPTER 5 Experimental Investigation Of The Effects Of Wind Speed And Yaw Angle On Heat Losses From A Heated Cavity		75
CHAPTER 6 Experimental Investigation Of The Effects Of Wind Speed, Aperture Ratio And Tilt Angle On The Heat Losses From A Heated Cavity		89
CHAPTER 7 The Influence Of Wall Temperature Distribution, Wind Speed And Tilt Angle On The Heat Losses From A Heated Cavity		115
CHAPTER 8 Conclusions And Future Work		141
8.1	Key outcomes from the numerical study _____	142

8.2	Key outcomes from the experimental study	143
8.3	Future Work	146
	References	148

List of Figures

Figure 1.1: Schematic diagram of the incoming solar power of the Earth.	3
Figure 1.2: Figure of the yearly sum of Direct Normal Irradiation (DNI) from measured data of weather stations and satellites (Meteotest, 2010).	4
Figure 1.3: Schematic diagrams representation of the four types of solar concentrating technologies currently applied in commercial CSP plants: (a) parabolic trough collectors (PT), (b) linear Fresnel reflector systems (LF), (c) dish-engine systems (DE), and (d) central receiver power tower system (CR) system (Romero and Steinfeld, 2012).	5
Figure 1.4: Schematic diagram of a concentrating solar thermal power plant (James, 2011).	7
Figure 1.5: Schematic diagrams of (a) tubular external and (b) cavity receivers (Ho and Iverson, 2014).	10
Figure 1.6: Schematic diagram of a tubular air-turbine receiver (Ho and Iverson, 2014).	12
Figure 1.7: Schematic diagram of a design of a falling particle receiver system with integrated storage and heat exchange (Ho and Iverson, 2014).	12
Figure 2.1: Schematic diagram of a generic cylindrical cavity solar receiver.	23
Figure 2.2: Schematic diagram of the streamlines in a downward facing tilted cavity receiver for natural convection (Wu et al., 2010).	25
Figure 2.3: Cubic cavity orientations and definitions of L_a , which is the distance between the highest point of the aperture a cavity to the lowest point of the cavity (Clausing, 1983).	29

Figure 2.4: Schematic diagram of a solar cavity receiver.....	29
Figure 2.5: Schematic diagram of the tested cavity receiver in Ma’s experiment (Ma, 1993).	41
Figure 2.6: Schematic diagram of a pressurised volumetric receiver (REFOS type) (RÅkger et al., 2006).	44
Figure 2.7: Transmittance spectra of porous silica coatings on silica glass for different heat treatments in comparison to the uncoated silica glass (Helsch et al., 2010).	45
Figure 3.1: Schematic diagram of a) the heated cavity in the Thebarton wind tunnel and b) the detail of the receiver.	57
Figure 3.2: Photo of the heated cavity in the open section of the wind tunnel.....	58

Nomenclature

CFD	Computational Fluid Dynamics
CR	Central receivers
CSP	Concentrated Solar Power
HTF	Heat Transfer Fluid
DNI	Direct Normal Irradiation
LCOE	Levelised cost of electricity
LF	Linear Fresnel
PT	Parabolic Trough
PD	Parabolic dish

Symbols			
A	Area (m ²)	V	Wind speed (m/s)
β	Coefficient of thermal expansion (°C ⁻¹)	ν	Kinematic viscosity of air at reference temperature kg/(s.m)
D	Diameter (m)	α	Yaw angle or incoming wind direction (°)
ε	Emissivity coefficient of the internal walls surface	φ	Tilt angle of the cavity (°)
g	Gravity (m/s ²)		
Gr	Grashof number = $\frac{g\beta(T_{wall}-T_a)D_{cav}^3}{\nu^2}$	Subscript	
h_c	Convective heat transfer coefficient through the aperture (W/(m ² K))	a	Ambient
k	Thermal conductivity of air at reference temperature (W/(m.K))	as	Aspect
L	Length (m)	ap	Aperture
Nu	Nusselt number = $\frac{h_c D_{cav}}{k_{ref}}$	cav	Cavity

Q	Heat loss (W)	conv	Convection
R	Ratio	rad	Radiation
	Reynolds number =		
Re	$\frac{VD_{cav}}{\nu}$	ref	Reference
	Richardson number =		
Ri	$\frac{Gr}{Re^2} = \frac{g\beta(T_{wall} - T_a)D_{cav}}{V^2}$	tot	Total
T	Temperature (°C)	w	Wall

Abstract

The principal objective of the present study is to assess the influence of wind on the heat loss from a generic cavity solar receiver under different geometrical configurations and operating conditions. This understanding is needed to provide insight into approaches with which to increase the thermal efficiency of a solar cavity receiver. The results from this work can be used to reduce the cost of concentrating solar energy and increase the rate of penetration of sustainable and renewable energy sources.

A purpose built modular and cylindrical cavity receiver was mounted in a large-scale wind tunnel in order to quantify heat losses under the different conditions. The cylindrical cavity was lined up with 16 well controlled and separated heating strips to investigate the effect of the internal temperature and its distribution on heat losses. A systematic experimental study was performed to assess the influence of wind speed ($V = 0, 3, 6, 9$ and 12 m/s), yaw angle ($\alpha = 0^\circ, 22.5^\circ, 45^\circ, 77.5^\circ$ and 90°), tilt angle ($\varphi = 90^\circ, 45^\circ, 30^\circ, 15^\circ$ and -90°), cavity aperture ratio (0.33, 0.5, 0.75 and 1), internal walls temperature ($T = 100, 200, 300$ and 400 °C) and 4 combination of temperature distribution inside the cavity. The data was analysed, then the total heat loss, normalised heat loss, and heat loss distribution through the internal walls of the heated cavities are presented.

To further our understanding of the heat transfer and fluid flow inside and outside a cavity receiver, a numerical model of a solar cavity receiver was developed to assess the effect of aspect ratio (0.5 to 3) and head-on wind speed on the forced and natural (combined) convective heat loss and area-averaged convective heat flux

from a cylindrical solar cavity receiver. The temperature distribution and velocity of air in the cavity are also presented.

The present study found that increasing the cavity aspect ratio leads to a reduction in the influence of wind speed on the combined convective losses per unit of cavity internal area. Consequently, the overall efficiency of a solar cavity receiver increases with the cavity aspect ratio for the conditions assessed in this study (aspect ratio below 3). The influence of head-on wind speed on the heat losses was found to be ~ 4 times higher than the side-on wind for ($1/Ri > 19$). Decreasing the aperture ratio D_{ap}/D_{cav} from 1 to 0.33, acts to reduce the natural convective losses (at zero wind speed) by up of to a factor of 5, while the effect of this ratio diminishes as wind speed is increased. For high wind speed, the heat loss from the upward facing cases ($\varphi = -90^\circ$) is approximately 3 times lower than the downward tilted cases ($\varphi = 15^\circ$) for a head-on wind condition. The heat losses from the upward facing cases are similar with the side-on wind conditions. For a downward tilted solar cavity receiver, an “upper or rear surface hotter” cavity has less overall heat losses compared with the other cases. There is also a slight advantage with respect to heat loss in keeping the tilt angle of a solar cavity between 15° and 30° .

Declaration

I certify that this work contains no material which has been accepted for the award of any other degree or diploma in my name, in any university or other tertiary institution and, to the best of my knowledge and belief, contains no material previously published or written by another person, except where due reference has been made in the text. In addition, I certify that no part of this work will, in the future, be used in a submission in my name, for any other degree or diploma in any university or other tertiary institution without the prior approval of the University of Adelaide and where applicable, any partner institution responsible for the joint-award of this degree.

I acknowledge that copyright of published works contained within this thesis resides with the copyright holder(s) of those works.

I also give permission for the digital version of my thesis to be made available on the web, via the University's digital research repository, the Library Search and also through web search engines, unless permission has been granted by the University to restrict access for a period of time.

I acknowledge the support I have received for my research through the provision of an Australian Government Research Training Program Scholarship.

Ka Lok Lee _____ Date 02/07/2018

Supervisors' declaration

I solemnly and sincerely declare that I have reviewed this report and provided feedback.

Graham 'Gus' Nathan

Name

Signature

3/7/18

Date

Bassam Dally

Name

Signature

2-07-2018

Date

Alfonso Chinnici

Name

Signature

3/07/18

Date

Acknowledgement

Professor Graham 'Gus' Nathan, Professor Bassam Dally, Dr Alfonso Chinnici, Dr Maziar Arjomandi and Dr Mehdi Jafarian are thankfully acknowledged for the supervision, their time and helps toward this research and writing of this thesis.

I would like to gratefully acknowledge the University of Adelaide, Australian solar thermal research initiative (ASTRI) and Australian Renewable Energy Agency for their financial support. I would also like to thank the current and former staffs of the School of Mechanical Engineering and Centre for Energy Technology (CET). Lastly, I would like to thank my family for their support.

CHAPTER 1

Introduction

1.1 Introductory background

Due to the negative environmental impacts of fossil fuels, depletion of their reserves and, in some cases, an increase in their cost, the interest in renewable and sustainable energy sources is on the rise. Solar, wind, biomass, geothermal and hydroelectric energy are the most common potential alternative renewable energy sources (Salvadore and Keppler, 2010). Despite the urgent need to decrease the consumption of fossil fuels, it still accounts for about 82% of the present world energy demand (Biroi, 2017), because the technologies to utilize renewable energy are less mature than those to utilize fossil fuels, often leading to a higher cost of power generation. The sun, the world's primary source of energy with a surface temperature of 5800 K, is an unlimited source of energy. The radiation from the sun is also freely available with a smaller impact on ecology compared with fossil fuels (Price, 2003; Romero and Steinfeld, 2012). Therefore, the overall aim of the present research is to reduce the cost of harvesting and storing solar energy, to be used as an alternative energy source.

In looking at the scale of energy need, one finds that on the one hand, the global energy consumption is estimated to be 5.75×10^{20} J (Biroi, 2017), ~86% of which comes from non-renewable sources. On the other hand, there is $\sim 2.81 \times 10^{24}$ J (2.81YJ) of energy enters the atmosphere from the sun annually, a schematic diagram of the incoming solar power to the earth is shown in Figure 1.1 (International Energy Agency, 2013; Zhang et al., 2013). Solar energy is the largest energy sources available on earth and is about 4800 times greater than the energy consumption by humans. Therefore, there is a strong potential for solar energy to

become a dominant source of alternative energy for society. Figure 1.2 shows the yearly sum of DNI distribution on the earth surface. It shows that Australia is one of the countries with the highest annual solar insolation and hence a strong potential to use solar energy as one of the major energy sources.

However, solar energy is inherently intermittent, distributed unequally over the earth and highly diluted, due to the geometrical constraint of a large distance between the sun and the Earth (Romero and Steinfeld, 2012).

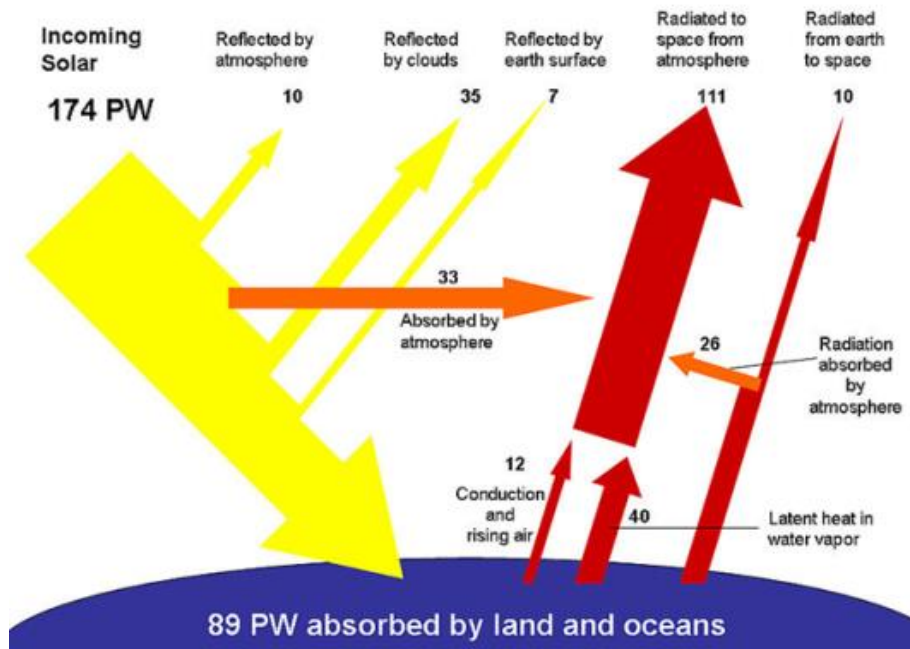


Figure 1.1: Schematic diagram of the incoming solar power of the Earth.

As a result, only about 1 kW/m² heat flux reaches the earth's surface. This flux is not high enough to heat a fluid to the temperatures required for large-scale electricity generation or mineral processing. Moreover, high temperature are required for high efficient power cycles. Optical concentrator devices are needed to enable sufficiently high solar radiative fluxes for this purpose. These devices

CHAPTER 1

typically use large reflective surfaces to concentrate the direct incident solar radiation onto a solar receiver, which typically heats a heat transfer fluid to drive concentrated solar power (CSP) technologies. The resulting concentration ratio is defined as the projected reflection surface area divided by the projected receiver aperture area.

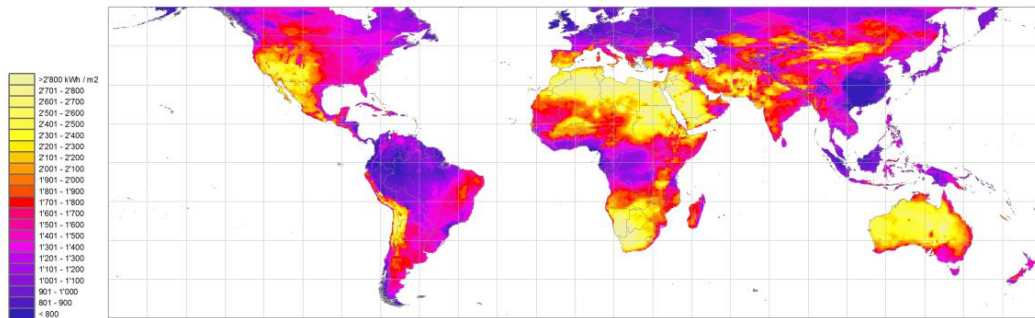


Figure 1.2: Figure of the yearly sum of Direct Normal Irradiation (DNI) from measured data of weather stations and satellites (Meteotest, 2010).

1.2 Type of concentrated solar power technologies

There are four types of commercially available CSP technologies, namely parabolic trough (PT) collectors, parabolic dish (PD) collectors, Linear Fresnel (LF) reflectors and the central receivers (CR) system (Barlev et al., 2011; IEA-ETSAP and IRENA, 2013; Johnston, 1995). These configurations are shown schematically in Figure 1.3. Parabolic trough and linear Fresnel systems are 2-D (linear) concentrating focus systems, which use thin and long segments of reflectors to focus the sunlight into a long receiver. Typically the range of concentration ratios for these systems varies from 30 to 80, depending on the size and number of the reflectors (Bader, 2011). The concentration ratio is defined as the projected reflection surface area divided by the projected receiver aperture area. Alternatively, CR and PD are 3-D or point concentrating systems, which focus the

incident solar radiation onto a single receiver. The typical ranges of concentration ratios of these systems are between 200 and 3000, which is higher than the 2-D PT and LF systems. Therefore, CR and PD systems can achieve higher output temperatures and higher efficiencies for power generation based on Carnot's law (Holman, 1997; Mills, 1999).

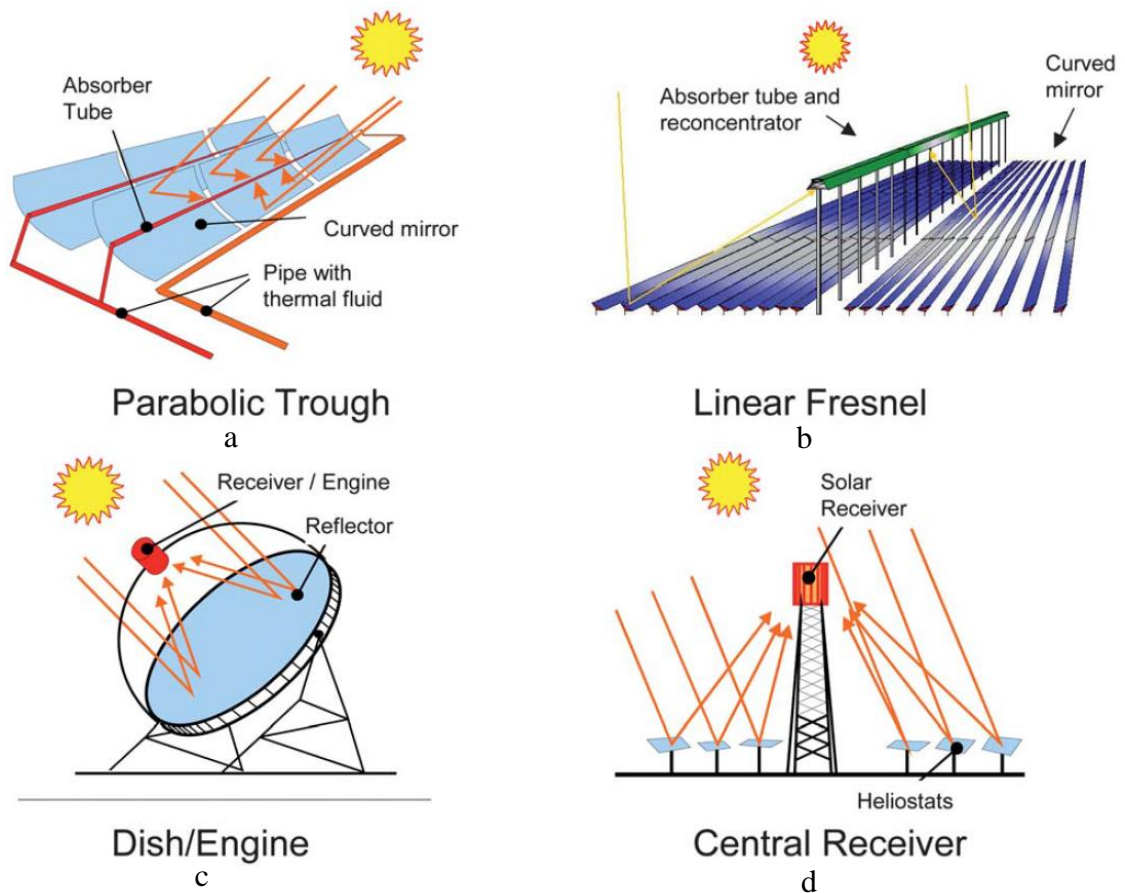


Figure 1.3: Schematic diagrams representation of the four types of solar concentrating technologies currently applied in commercial CSP plants: (a) parabolic trough collectors (PT), (b) linear Fresnel reflector systems (LF), (c) dish-engine systems (DE), and (d) central receiver power tower system (CR) system (Romero and Steinfeld, 2012).

In addition to the capability, CR systems can provide a larger thermal power output than PDs, (IEA-ETSAP and IRENA, 2013), and also have a potential to be integrated with a thermal energy storage system, which provides the system with a capacity to supply energy when sunlight is below the minimum required threshold

CHAPTER 1

of the solar insolation intensity for the receiver operation (Jafarian et al., 2013; Kueh et al., 2015). This enables CRs to have a higher capacity factor than the systems without thermal storage. The capacity factor is defined as the ratio of the actual output power of a plant, to that which would be achieved at maximum output power at full capacity over the same period of time. Consequently, a central receiver solar power tower systems has more potential to be used in large-scale power generation than other CSP technologies. CSP plant also has a strong potential to be used to power off-grid mines, remote towns and other industrial plants which require power. Solar power tower is one of the valuable CSP technologies which have a high potential to achieve compatible cost with conventional electricity generation especially when integrated with a thermal storage system (Kolb et al., 2011; Lovegrove et al., 2012). In addition, CR technologies can also be configured, either as a standalone power plant or be integrated with some existing power plants as a hybrid (Nathan et al., 2014). Moreover, a recent study shows that concentrated solar tower can be run in a hybrid mode which reduces the levelised cost of electricity (LCOE) by up to 17% and the net fuel consumption by up to 31%, depending on the operating conditions (Chinnici et al., 2018). Therefore, hybrid solar-combustion power tower systems have a very high potential to lower the LCOE in the future (Korzynietz et al., 2012; Nathan et al., 2014). Nevertheless, CST is also a very valuable option for standalone power generator with thermal storage, hence power can still be generated even when the sun is not shining. CST can also be used outside the power-generation area, such as in mineral processing and heating where thermal energy is required (ASTRI, 2017).

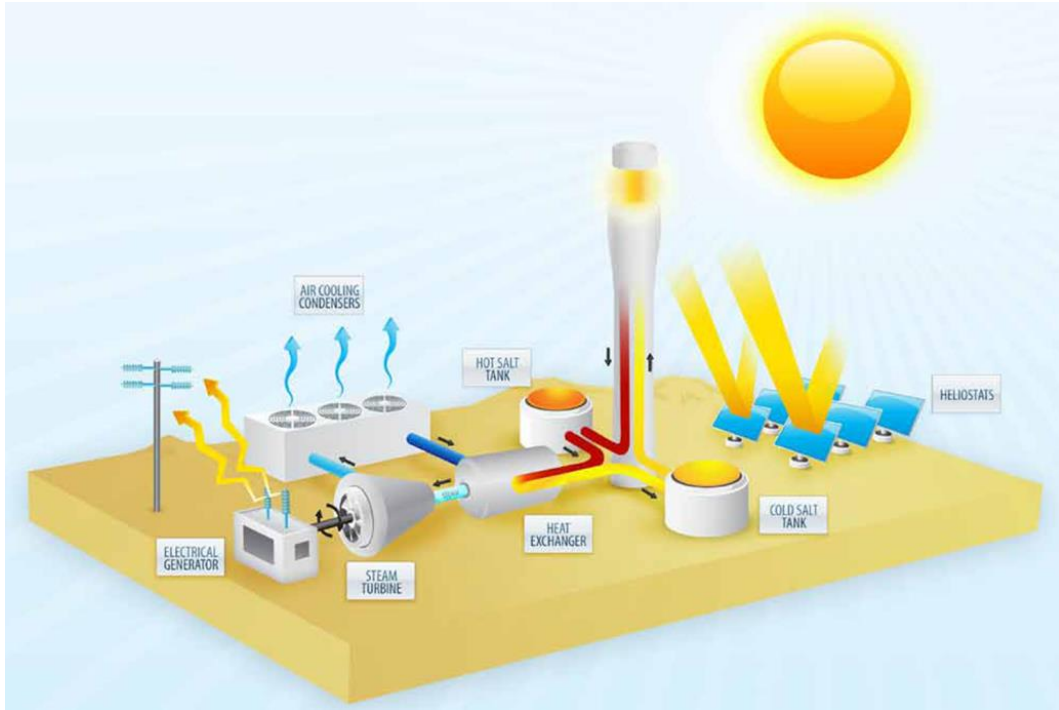


Figure 1.4: Schematic diagram of a concentrating solar thermal power plant (James, 2011).

A CR system consists of a tower with a mounted solar receiver, which is surrounded by a heliostats field to focus the solar radiation into the receiver (Behar et al., 2013; Müller-Steinhagen and Trieb, 2004). A typical concentrating solar thermal power plant is shown in Figure 1.4. A receiver absorbs the solar-focused irradiation energy and heats the heat transfer fluid. The heat transfer fluid is then typically used to heat a working fluid, or be directly applied to drive a turbine for power generation (Garbrecht et al., 2013). A receiver accounts for around 19% of the total cost of a CSP system (Kolb et al., 2011; Price, 2003). Therefore, an effective strategy for the decreasing of the cost of power generation from the CR systems is to decrease the size and cost of the heliostat field by increasing the efficiency of the solar receivers, if the cost of solar receivers cost remain similar. This can be achieved through the minimisation of the heat losses from the receivers and increasing its absorption and thermal efficiency. In light of the above need, the principal objective of the current

CHAPTER 1

research is to improve the solar to thermal efficiency of generic cavity solar receivers by providing the new understanding needed to enable industrial receivers to be designed more efficiently.

The overall efficiency of a central tower CSP system is strongly influenced by the receiver efficiency. Therefore, to effectively estimate the efficiency of a receiver, a sound understanding of the different types of the heat transfer from a receiver is necessary. Research over many year have shown that there are four main components of heat transfer from a receiver, three of which are associated with heat losses from a receiver and the fourth of which is to collect the useful energy (Ho and Iverson, 2014; Zhang et al., 2013). These three types of heat losses are; conductive heat loss from the wall of a receiver, convective heat loss from the cavity of a receiver and re-radiation through the receiver aperture. The conductive and radiative heat losses from a receiver can be reasonably well estimated with an analytical model. However, it is much more challenging to predict the convective losses from a cavity receiver. Analytical models are less suitable for such predictions since unlike conductive and radiative heat losses, convective losses can happen naturally through buoyancy effects and also influenced by wind speed, its direction and orientation to the receiver. This problem is further compounded when considering the effects of turbulence, mixing and fluid flow. In other words, convective heat losses from a cavity are strongly dependent on environmental conditions. For these reasons, convective heat losses from a solar receiver are hard to predict and are commonly determined experimentally (Ma, 1993).

1.3 Type of solar tower receivers

The absorbed thermal power from a solar receiver can be stored or used directly for power generation or industrial heat for mineral or chemical processing. The higher the temperature the higher efficiency of power cycles and the more suitable it is for a variety of industrial processes (Ho and Iverson, 2014; Kolb et al., 2011; Romero and Steinfeld, 2012). The type of receiver's geometry and absorption efficiency are all needed to be considered together to achieve the high temperature. Future systems are likely to use higher temperature heat transfer media, which may also be the storage media, to achieve a higher temperature (Garbrecht et al., 2013; Hasuike et al., 2006; Kolb et al., 2011). To achieve this, a solar receiver with a high concentration ratio and lower heat loss will be required (Holman, 1997; Mills, 1999).

The two main types of solar receivers for a tower system, are classified based on their geometry, namely; external (tubular) and cavity type. The schematic representation of these receivers is shown in Figure 1.5. An external type receiver absorbs radiation from all directions, but it also loses heat to all directions, as shown in Figure 1.5 (a). A cavity receiver receives a directional concentrated solar radiation into the a well-insulated enclosure containing the absorber and its losses are minimized due to the small aperture size where re-radiation and convection can occur and insulation of the receiver where conductive heat losses to the external wall then it lost to the surrounding shown in Figure 1.5 (b). As the result, the heat losses from a cavity receiver are less than those from an external type receiver (Falcone, 1986). A solar cavity receiver has a strong potential to reduce the heat

CHAPTER 1

loss from a receiver to achieve a high temperature. For that reason, this technology is the focus of this project.

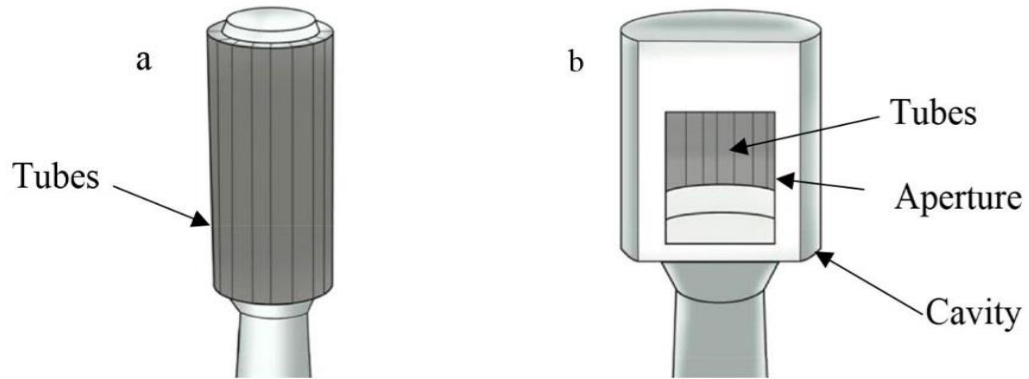


Figure 1.5: Schematic diagrams of (a) tubular external and (b) cavity receivers (Ho and Iverson, 2014).

1.4 Type of heat transfer media

There are three main types of solar cavity receivers classified by the phase of the heat transfer media and those are; gas, solid particle and liquid receivers.

1.4.1 Gas receiver

Within a gas receiver, gas is heated by absorbing the power from the concentrated sunlight, shown in Figure 1.6. The air is distributed by the distributor at the aperture to the absorber tubes. The solar power is absorbed by the absorber tubes then transferred to the gas in the tubes. After that the heated gas is collected by the collector and exit the cavity receiver. The gas is generally used to generate electricity directly with Rankine or Brayton cycles depending on the outlet temperature and pressure of the gas (Ávila-Marín, 2011; Ho and Iverson, 2014).

Volumetric air receivers and tubular gas receivers are the two main types of gas receivers. Due to the limited heat transfer capability of gas, gas solar receivers are often cavity receiver, otherwise it would lead to high losses if the receiver is built as external receiver. However, there are some issue with high temperature storage for gas. Therefore storage is more often used in the solid and liquid receiver.

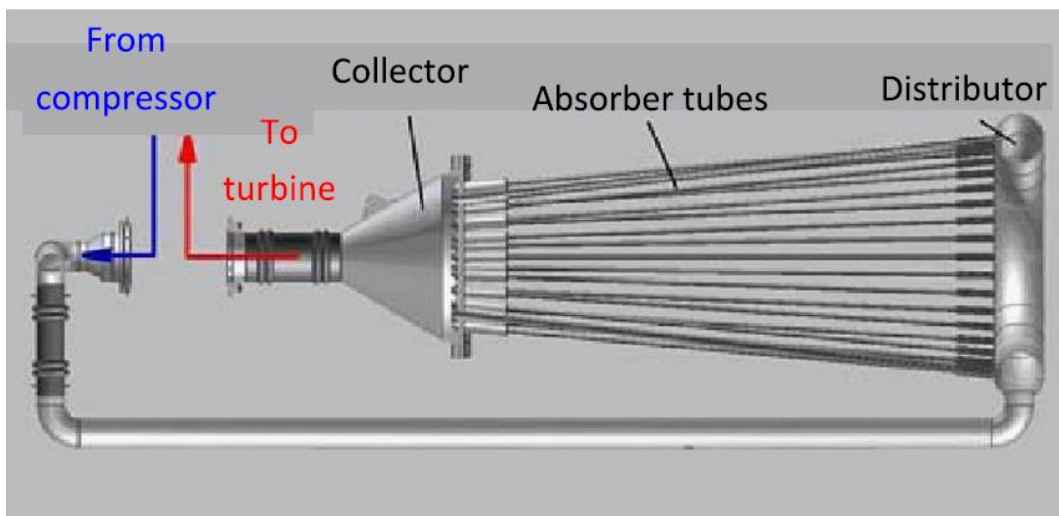


Figure 1.6: Schematic diagram of a tubular air-turbine receiver (Ho and Iverson, 2014).

1.4.2 Solid particle receivers

Solid particle receivers were proposed in the 1980s to increase the outlet temperatures of the receiver to over 1000 °C, which was unachievable by most of the gas and liquid receivers explored at that time (Falcone et al., 1985). This type of receiver typically uses ceramic particles flowing through a cavity receiver by forming a falling particle curtain, as shown in Figure 1.7. The particles are irradiated and absorb the concentrated sunlight directly. These heated particles can readily be stored and then used to heat a secondary heat transfer or working fluid. Although a number of studies have been performed on the particle type of receivers (Falcone et al., 1985; Ho et al., 2009; Siegel et al., 2010), the influence of wind on the heat loss from a particle cavity receiver is not known. Therefore further study of the solid particle cavity receivers is needed to improve the understanding of the heat losses from them.

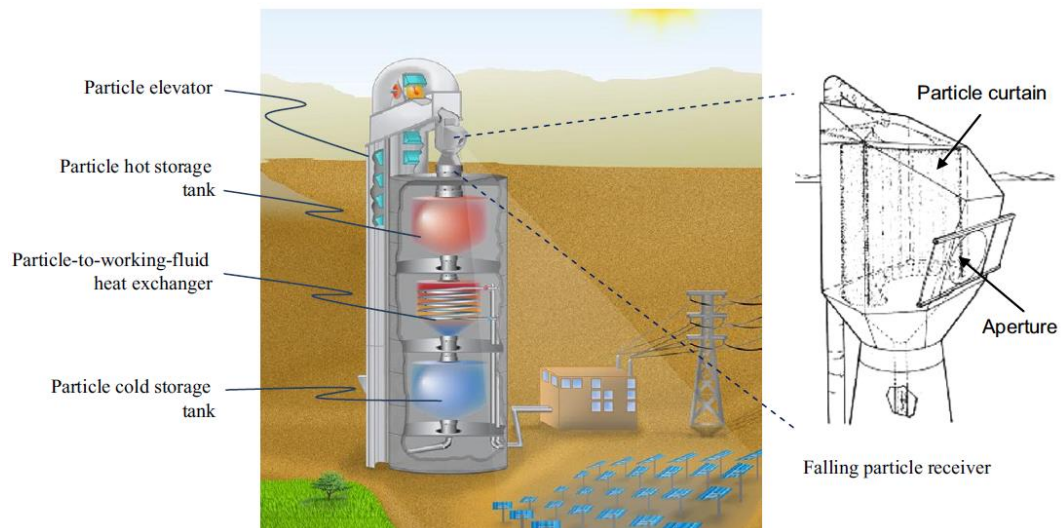


Figure 1.7: Schematic diagram of a design of a falling particle receiver system with integrated storage and heat exchange (Ho and Iverson, 2014).

1.4.3 Liquid receivers

Tubular liquid receivers are the main type of the liquid receivers that are used commercially. In these systems, the HTF is pumped through the tubes which are irradiated by concentrated sunlight. Consequently, the HTF indirectly absorb the concentrated solar power from the heated tubes (absorber) in the cavity. This is also known as indirectly irradiated receivers (Ho and Iverson, 2014). The HTF from these systems can be used directly as a heat source or stored directly as thermal storage.

1.5 Convective heat losses from solar cavity receiver

To understand the heat transfer performance of a cavity receiver, all three types of heat losses from a receiver need to be assessed. Typically more than 50% of the heat loss from a cavity solar receiver is due to the convection in the conditions with wind speed above 9 m/s in some given condition (Ma, 1993); and due to the complexity of the convective heat loss there is a lack of reliable and applicable knowledge in this field.

Typically, concentrated solar towers are built in remote areas and in very large flat fields, which usually have the propensity to strong wind. Furthermore, the location of a solar receiver on top of the solar tower, typically between 50 and 200m above the ground (Srilakshmi et al., 2015), exposes it to even higher wind speeds (Garcia et al., 1998; Li et al., 2010; Peterson and Hennessey Jr, 1978). Therefore, the surrounding conditions such as the ambient temperature and wind load can

CHAPTER 1

significantly affect a receiver's performance (Clausing, 1981, 1983; Kim et al., 2009; Ma, 1993; Xiao et al., 2012). While the effects of radiative and natural convective heat losses from a cavity receiver is relatively well understood, the effect of convective losses on the cavity's thermal efficiency and overall performance under a windy condition is still very limited. Hence, there is a gap of knowledge regarding the effects of wind on the heat loss from a receiver under different operating conditions in order to equip engineers and designers with the required understanding and the correlation to design more efficient receivers.

The convective heat loss from a cavity receiver, with a windowless aperture, mainly depends on the heat transfer rate to the air inside the cavity and the rate of mass exchange between the receiver and the environment. Some of the strategies that can help mitigate these heat losses would be to: 1) decrease the rate of mass exchange between the receiver and the environment, and 2) decrease the air circulation within the cavity. The air flow patterns inside cavities are an important factor of the convective heat loss from a receiver. For this reason, the effect of the receiver's geometry and surrounding conditions on the airflow patterns within a receiver needs to be particularly investigated in order to provide better understanding and data for models development and validation, which can be used to design an optimised cavity receiver.

From the brief discussion above, it is apparent, that improving the solar to thermal efficiency of a receiver has beneficial impact on reducing the cost of energy using CSP technology. The solar to thermal efficiency of a receiver is strongly dependent

on the convective heat loss from the receiver (Clausing, 1981). Therefore, the aim of the present work is to better understand the influence of a cavity receiver's geometries and surrounding conditions on the convective heat loss from it. These findings could be used for identification of novel configurations for a solar receiver with the optimised design and lower cost of solar energy.

1.6 Thesis aim and objectives

1.6.1 Aim

The overall aim of the present research is to provide the understanding of heat losses from a heated cavity, which is needed to enable engineers to more accurately predict the heat losses from alternative configurations of solar cavity receiver and, hence, to reliably optimise their receiver designs.

1.6.2 Objectives

The broad scientific objectives of the thesis are as follows:

- I. To understand the effect of wind and aspect ratio on the convective heat loss from cylindrical solar cavity receivers and the flow pattern inside the cavity;
- II. To determine the influence of Grashof number and Reynolds number on the heat losses through the aperture of cylindrical solar cavity receivers;
- III. To determine the influence of Reynolds number, wind direction, aperture ratio and tilt angle on the heat losses through the aperture of cylindrical cavity receivers for the conditions of solar tower system;

CHAPTER 1

- IV. To determine the influence of Reynolds number and temperature distribution over the internal walls of a solar cavity receiver on the heat losses through the aperture;
- V. To determine the influence of Grashof number, Reynolds number and temperature distribution over the internal walls on heat losses from an upward facing heated cavity for a beam-down solar receiver.

1.7 Thesis outline

The thesis is presented in eight chapters, comprised the introduction, literature review, methodology, then the collection of four papers that have been published already or are currently under review, and lastly the conclusions. The text below describe each chapter and its content.

Chapter 2 provides a critical review of literature related both to the natural convective and forced convective heat losses from the aperture of the heated cavity. The emphasis of the chapter is on the understanding of the effect of wind on heat loss and potential methods to reduce it. The research gap in each section has been identified.

Chapter 3 presents a summary of the research methods chosen to address the objectives, which comprises Computational Fluid Dynamics (CFD) models and wind tunnel experiments.

CHAPTER 1

Chapter 4 comprises of a copy of the first journal paper that resulted from this work publications. In this chapter, an investigation into the effect of aspect ratio on the heat loss from a solar cavity receiver is presented. The effect of aspect ratio and head-on wind speed on the forced and natural (which together are termed “combined”) convective heat loss from a cylindrical solar cavity receiver is reported, as assessed using three-dimensional computational fluid dynamics (CFD) models. This assessment was performed by assuming a uniform internal wall temperature. The numerical analysis predicted that there are ranges of wind speeds for which the combined convective heat losses are lower than the natural convective heat loss from the cavity and that this range depends on the aspect ratio of the cavity. In addition, the effect of wind speed on the area-averaged flux of convective heat loss from a heated cavity was predicted to be smaller for long aspect ratios than for short ones. This indicates that the overall efficiency of the solar cavity receiver increases with the aspect ratio for all conditions tested in this study. The temperature distribution and velocity of air in the cavity are also presented in this chapter.

Chapter 5 comprise the second journal paper from this work. The paper content is focussed on the measured influence of wind speed and yaw angle on heat losses from a reference configuration of a heated cavity. Conductive and radiative heat losses from the system were measured and recorded, to obtain the convective heat loss components. Wind speed and direction are the two major variables considered in this study. It was found that the convective heat losses through the aperture are approximately 4 times greater for the head-on wind case than for the side-on wind case, for high wind speed. Heat loss distributions from different sections of the

CHAPTER 1

cavity are also presented. Approximately 85% of the heat was lost from the lower half of the surface of the cavity for the no-wind condition. The heat loss and its distribution are also dependent on the aperture ratio.

Chapter 6 comprise the third journal paper resulting from this work. The paper content is focussed on measuring the effects of wind speed, aperture ratio and tilt angle on the heat losses from a heated cavity. It was found that the effect of aperture ratio on the convective heat losses is strongly coupled with the wind speed. In particular, the measured heat loss was found to have a weak correlation with the aperture ratio of the cavity, for high wind speed. However, for the no-wind condition, the total heat loss can vary by up to ~75% when varying the aperture ratio from 0.33 to 0.75. Tilt angle was found to have a relatively weak effect on the heat losses in comparison with the aperture ratio and wind speed. In addition, although heat losses were found to decrease with increasing the tilt angle for the no-wind condition, this statement does not hold for windy conditions.

Chapter 7 comprise the fourth paper that resulted from this work. The paper content focusses on assessing the effects of temperature distribution over the internal walls of the solar cavity, on the combined heat losses (radiation, natural and forced convection) through the aperture. It was found, for the no-wind condition, that the internal wall temperature distribution has tangible effects of the convective heat losses from the cavity reaching ~50% for the tested cases. Noteworthy, is that for cases with the high wind speeds from the head-on direction, the variations in heat loss does not exceed ~20%. In addition, an upward facing heated cavity has also

CHAPTER 1

been investigated in this study for the potential use in a beam-down solar receiver system. Results indicate that convective losses from an upward facing cavity are not dependent on wind direction and are not very sensitive to wind speed either. Hence this configuration has advantages in terms of convective heat losses in very windy locations.

Chapter 8 contains the conclusions from this research along with recommendations for further development and applications.

Journal papers:

- Lee, KL, Jafarian, M, Ghanadi, F, Arjomandi, M & Nathan, GJ , 'An investigation into the effect of aspect ratio on the heat loss from a solar cavity receiver', *Solar energy*, (2017), vol. 149, pp. 20-31.
- Lee, KL, Chinnici, A, Jafarian, M, Arjomandi, M, Dally, B & Nathan, G 'Experimental investigation of the effects of wind speed and yaw angle on heat losses from a heated cavity', *Solar energy*, (2018), vol. 165, pp. 178-188
- Lee, KL, Chinnici, A, Jafarian, M, Arjomandi, M, Dally, B & Nathan, G, 'Experimental investigation of the effects of wind speed, aperture ratio and tilt angle on the heat losses from a heated cavity', *Solar energy*, (2018), (Under review).

CHAPTER 1

- Lee, KL, Chinnici, A, Jafarian, M, Arjomandi, M, Dally, B & Nathan, G, 'The influence of wall temperature distribution, wind speed and tilt angle on the heat losses from a heated cavity', Solar energy, (2018), (Under review).

1.8 Format

The thesis has been submitted as a portfolio of the publications according to the formatting requirements of The University of Adelaide. The printed and online versions of this thesis are identical. The online version of the thesis is available as a PDF. The PDF version can be viewed in its correct fashion with the use of Adobe Reader 11.

CHAPTER 2
Literature Review

2.1 Heat loss from cavity solar receivers

Solar cavity receivers, as shown in Figure 1.3(d), Figure 1.5(b) and Figure 2.2, absorb the solar radiation from a heliostat field and transfer it to the Heat Transfer Fluid HTF. Reducing heat losses from the receiver is needed in order to maximise the solar to thermal efficiency η_{cav} , which is defined in equation (1).

$$\eta_{cav} = \frac{Q_{useful}}{Q_{CSP}}. \quad (1)$$

Here, Q_{useful} is the useful heat output from the solar cavity receiver and Q_{CSP} is the solar input from the heliostat field. The three components of heat losses from a solar cavity receiver are conduction through the internal to external walls of the receiver, then convection and radiation loss to the surrounding from the external wall of the receiver, together with the convection and radiation through the receiver aperture, with the latter comprising the re-radiation and reflection of the input concentrated solar radiation. Conduction through the internal walls to the outer surface, which then has heat losses via both convection and radiation to the surrounding, is much smaller than that through an aperture. This is because insulation is used between the internal walls of a cavity and the external surface of a receiver, which are shown in Figure 2.1. Hence, the dominant mechanisms of heat loss from a cavity solar receiver are convection and radiation through the aperture. Those solar receivers that are used in a tower system are expected to be subjected to higher wind speed than that near the ground (Garcia et al., 1998; Li et al., 2010; Peterson and Hennessey Jr, 1978). However, the significance between convection and radiation depends mainly on the operating and surrounding conditions. It is

expected that, for a solar receiver in high wind, convection becomes the dominant while radiation depends mainly on the temperature of the cavity wall (Falcone, 1986; Mills, 1999; Stalin Maria Jebamalai, 2016).

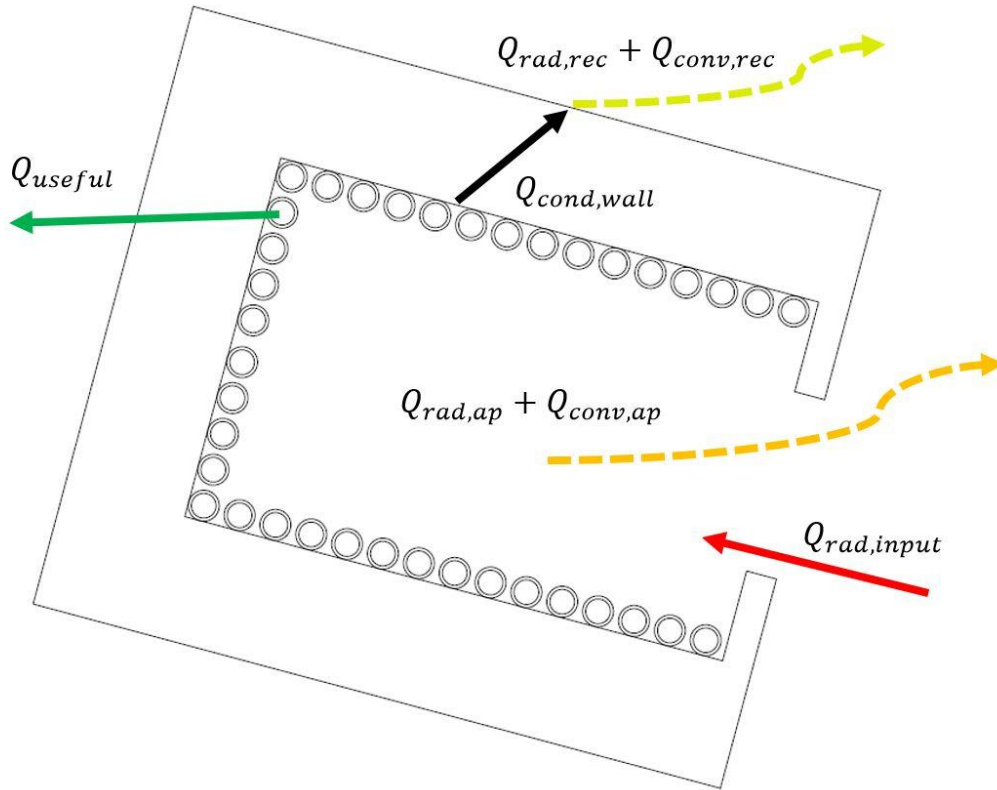


Figure 2.1: Schematic diagram of a generic cylindrical cavity solar receiver.

2.1.1 Convective zone and stagnant zone for natural convection

Due to the high temperature of the internal walls of a receiver, the density of the air inside a receiver or near a receiver's internal walls is lower than that of the surrounding ambient air (Clausing, 1981). Natural convection is a type of heat transport that is generated only by density differences in the fluid occurring due to temperature gradients (Clausing, 1983; Holman, 1997). Therefore, for a no-wind condition, the temperature difference in a heated cavity is the driving force for the

CHAPTER 2

circulation of the air inside a cavity receiver, which is the natural convective heat losses. The hot air may be trapped in the upper part of a cavity receiver depending on the geometry and the orientation of it. For these reasons, the volume within a receiver can be divided into two zones, called the convective and stagnant zones as shown in Figure 2.2 (Clausing, 1981, 1983; Wu et al., 2010). On the one hand, a convective zone is a region of air inside the cavity that has the central and counter-rotating eddies due to the driving force of natural convection. On another hand, a stagnant zone is a region of air inside the cavity that is both stratified and relatively stagnant compared with the convective zone (Clausing, 1981, 1983). The boundary between two zones is approximately horizontal and is aligned with the highest point of the aperture. A shear layer is generated between the movement of the convective zone and the stationary fluid in the stagnant zone as shown in Figure 2.2. The concept of the effects of the two zones was confirmed by an analytical prediction and an experiment with a generic cubic cavity receiver (Clausing, 1983). The results from the analytical prediction and experiment have a maximum difference of 20% (Clausing, 1983). Consequently, natural convective heat loss from a generic cavity receiver can generally be explained with the concept of the stagnant and convective zones. Convective heat loss from a solar receiver can be reduced by limiting the ratio of the convective zone to the stagnant zone, which is defined as the ratio of the volume of the convective zone to the volume of the stagnant zone. Some typical parameters that affect this ratio, are discussed in the following sections.

2.1.2 Receiver tilt angle

A receiver tilt angle φ or orientation is defined as the angle between the normal direction of the plane containing the aperture and the horizontal plane, shown in Figure 2.3. One of the ways to reduce the volume of the convective zone is to decrease the distance between the highest point of the aperture and the lowest point of a receiver L_a . This can be achieved by positioning the center of the aperture lower than that of the cavity, shown in Figure 2.4. Changing the tilt angle φ , results in changing L_a . Therefore, the tilt angle influences the flow pattern through its influence on the size of convection zone inside the cavity, which in turn influences the convective heat loss from a receiver.

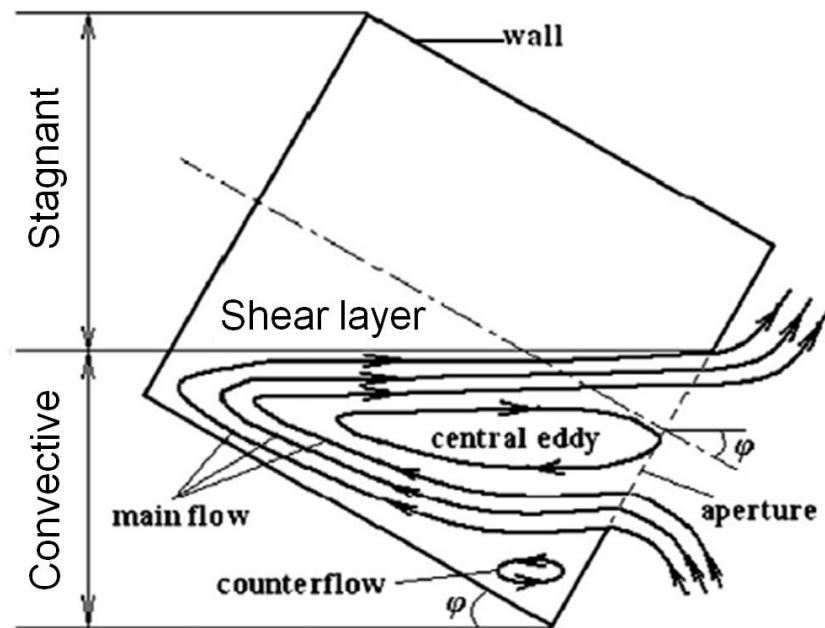


Figure 2.2: Schematic diagram of the streamlines in a downward facing tilted cavity receiver for natural convection (Wu et al., 2010).

If a receiver cavity is oriented downward ($\varphi = 90^\circ$), $L_a = 0$ so that stagnant zone almost fully occupies the receiver. This leads to the lowest natural convective heat

loss from a receiver (Taumoefolau and Lovegrove, 2002). For this orientation, the natural convective heat loss is negligible compared with other components of heat loss in most cases (Ma, 1993; Wu et al., 2010). The reason for this is that the hot air rises to the upper part of the cavity, which is farther away from the aperture, due to its lower density than the cool air near the aperture; hence the hot air is trapped in the cavity and forms a stable stratification. Two experimental studies were performed to assess the effect of tilt angle on the heat loss from a heat fluid heated cavity receiver (McDonald, 1995) and a heating element heated cavity receiver (Taumoefolau et al., 2004). They have a similar conclusion with each other about the effect of tilt angle on the heat losses from a heated cavity. For the case of a cavity receiver at 260 °C, decreasing its tilt angles from 90° to around -45° (tilting upward), the convective heat losses from the receiver increase (McDonald, 1995). This also agrees with Claus's statement about the maximum L_a (Clausing, 1983). The effects of tilt angle on the convective heat loss from the receiver, and the flow pattern inside a heated cavity for with wind conditions is still unclear. Therefore, the effects of tilt angle on forced convective heat loss from a solar receiver needs to be investigated.

2.1.3 Aspect ratio, aperture ratio and aperture displacement ratio

Aspect ratio R_{as} , aperture ratio R_{ap} and aperture displacement ratio R_{dis} are also important parameters for minimising convective heat loss from a solar cavity receiver and they are defined in equations (2) to (4) (Ávila-Marín, 2011; Kim et al., 2009; Wu et al., 2010). The schematic representation of a solar cavity receiver with these parameters is shown in Figure 2.4. These parameters are important for

CHAPTER 2

convective heat loss because they affect the ratio of the volume of the convective zone to the stagnant zone, hence the heat losses. If the aperture of the receiver is facing downward, increasing the aspect ratio of a cavity increases the ratio of the convective zone to stagnant zone. Therefore, for a set receiver diameter, increasing the length of the receiver also increases the volume of stagnant zone.

$$R_{ap} = \frac{D_{rec}}{L_{rec}}, \quad (2)$$

$$R_{as} = \frac{D_{ap}}{D_{rec}}, \quad (3)$$

$$R_{dis} = \frac{L_{ap}}{D_{rec}}. \quad (4)$$

Changing the aperture ratio changes the ratio of the volume of the convective zone to stagnant zone. Decreasing the aperture size does not only reduce the convective heat loss, it also reduces the re-radiative heat loss from a cavity receiver (Steinfeld and Schubnell, 1993; Wu et al., 2010; Wu et al., 2011). However, it also decreases the radiation power entering the receiver for a constant concentration ratio. Therefore, an optimum aperture ratio is a compromise between minimising the heat loss and maximising the solar input (Steinfeld and Schubnell, 1993). Lastly, the aperture displacement ratio R_{dis} has the effect on the ratio of the convective zone to stagnant zone. As the aperture displacement ratio is decreased, the volume of the convective zone decreases.

CHAPTER 2

An experimental study was undertaken on a cubical receiver for a few different cavity geometries to investigate the effect of aspect ratio, aperture ratio and aperture displacement ratio on the convective heat loss from the receiver (Kim et al., 2009). The natural and mixed convective heat losses from the receiver were obtained for various head-on wind speeds on different types of cavities. Four cavities types are investigated, comprising no cavity (external heater), open cavity, small centre cavity and small lower cavity. This study found that the convective heat loss from the receiver has a stronger relationship with the tilt angle, aperture ratio and wind speed than the aspect ratio and aperture displacement ratio. However, the correlation between tilt angle, aperture ratio and wind speed has not been well reported. In addition, the cavity was only heated at the rear part of it, hence their finding might not apply to a cavity, which has a hot side walls.

A numerical study for a non-fully open cylindrical isotherm solar receiver was performed by Wu et al., (2011). This study showed that moving the position of the aperture upward increases the aperture displacement ratio. This can increase the natural convective heat loss for aperture displacement ratio increasing from 0 to 0.6 and receiver tilt angle between 0° and 45° . Similarly, increasing the aperture size brings a stable increment of the natural convective heat loss (Wu et al., 2011). However, the effect of aperture size on the heat loss from a cavity receiver with wind conditions has not been reported.

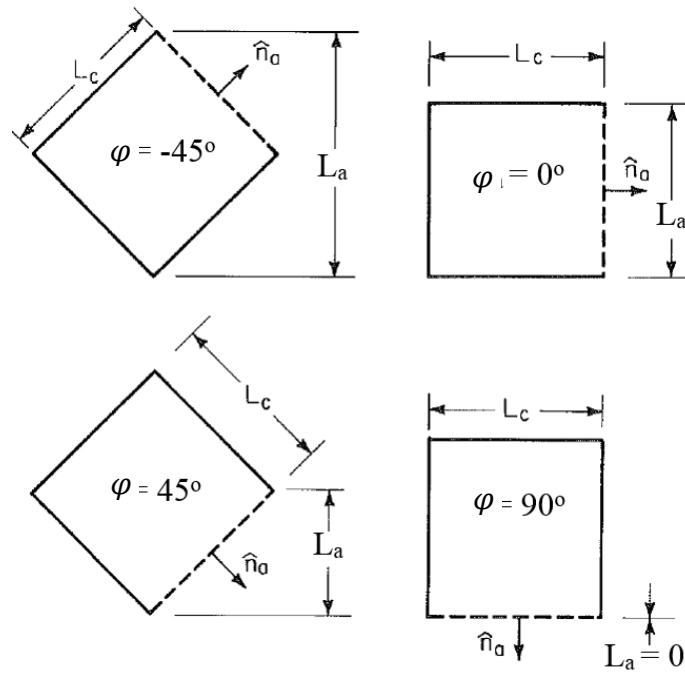


Figure 2.3: Cubic cavity orientations and definitions of L_a , which is the distance between the highest point of the aperture a cavity to the lowest point of the cavity (Clausing, 1983).

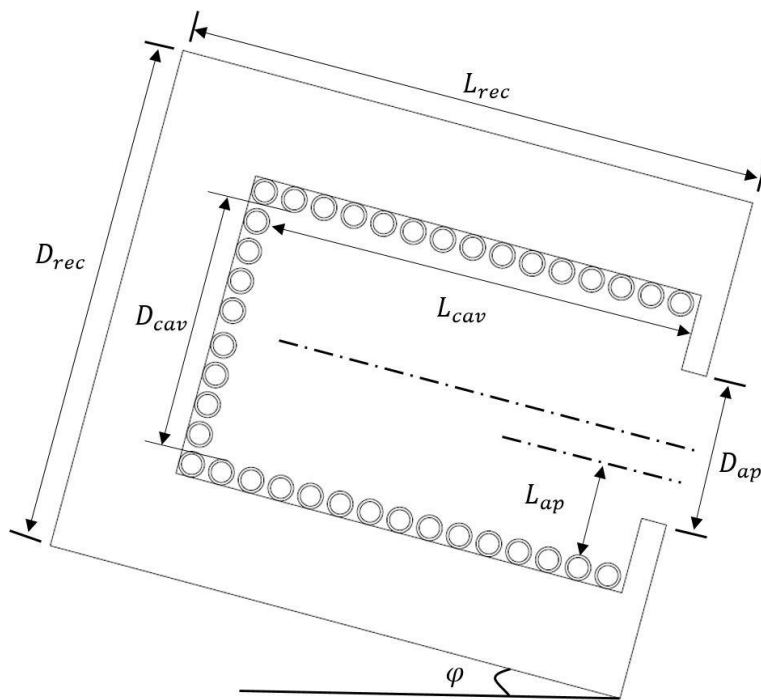


Figure 2.4: Schematic diagram of a solar cavity receiver.

CHAPTER 2

Another numerical study for the receivers with cross-section areas of 20m^2 and 400m^2 was performed (Paitoonsurikarn and Lovegrove, 2002, 2006) and compared with experiments (McDonald, 1995; Taumoefolau et al., 2004). A correlation for the calculation of the natural convective heat loss from a receiver as a function of the aspect ratio and aperture ratio was also suggested. This correlation suggests that natural convective heat loss from a solar receiver is increased as the tilt angle, length and diameter of the receiver and the diameter of the aperture are increased. However the interaction between the effect of wind, aspect ratio and aperture ratio is not known.

In summary, there are a large number of studies on the convective heat loss from a cavity receiver for the natural convective, hence the effects of these parameters on the convective heat loss from a cavity solar receiver for a no-wind condition are understood reasonably well. A summary of effects of the geometries of solar cavity receivers on natural convective heat loss is shown in Table 2.1. As tilt angle and aspect ratio are increased, the natural convective heat losses decrease. The natural convective heat loss from a cavity receiver is increased with its aperture ratio. It is important to note that, the reports above are only for a natural convective heat loss. However, a real solar cavity receiver is operated in a very high altitude location under a high wind condition, and the phenomenon of a forced convective from a solar cavity is not fully understood. Therefore, further investigation into the effect of wind on the heat losses from a solar receiver is needed.








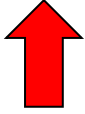
2.1.4 Effect of wind on heat losses from a receiver

Most of the receivers are operated in an outdoor environment, therefore the effects of wind on the receiver must be considered. The forced convective heat losses from a receiver are determined by the wind speed, wind direction, receiver geometries, and tilt angle of a receiver. The effects of wind on a receiver are complicated. Wind can increase or decrease the heat loss from a cavity depending on the wind speed and direction, and the effects of wind on a receiver were claimed to be explained by the following (Falcone, 1986):

- If the wind flow crease the air flow direction to be the same as the direction of natural convection of a cavity receiver, the wind reinforces the flow pattern of natural convection and the combined free forced convective heat losses are larger than the pure natural convective heat loss.
- If the wind flow prevents or is against the flow of natural convection of a cavity receiver, but the wind is not strong enough to determine or drive the air flow through the receiver cavity, then the combined free forced convective heat loss is less than the pure natural convection value.
- If the wind is strong enough to drive the air flow through a cavity receiver, regardless of the flow of the natural convective heat loss, the mixed convective heat losses are greater than the pure natural convective heat loss due to a much higher mass transfer throughout the receiver than that with the no-wind case.

CHAPTER 2

Table 2.1 table of the effects of geometries of solar cavity receivers on natural convective heat loss

Variables			Natural convective heat loss
Tilt angle	φ		
Aperture ratio R_{ap}	$\frac{D_{ap}}{D_{rec}}$		
Aspect ratio R_{as}	$\frac{L_{rec}}{D_{rec}}$		
Aperture displacement ratio R_{dis}	$\frac{L_{ap}}{D_{rec}}$		

To assess the effect of wind on a solar receiver, the conditions for the above situations need to be investigated. To investigate the behaviour of a receiver under wind load, a wind tunnel experiment was performed on a semi-cylindrical shape solar receiver at about 280 °C (Ma, 1993). The purpose of this experiment was to investigate the heat losses from the receiver under the various condition of the side-on wind speed (up to about 9 m/s), head-on wind speed (up to about 11 m/s) and receiver tilt angles. This investigation found that natural convective heat loss from a downward tilting solar receiver achieved its maximum value of about 2kW when the receiver aperture was faced horizontally. However, if the aperture was facing downward, the natural convective heat loss from the receiver was negligible, which

CHAPTER 2

is in agreement with the findings of another experiment by Prakash et al. (2009). Moreover, the forced convective heat loss from the receiver was claimed to be higher when the wind was blowing parallel to the aperture (side on wind) than blowing directly into the receiver (head on wind) for the same wind speed. This study also suggested two forced convective heat transfer coefficients as a function of receiver tilt angle and side on or head on wind speed, for this particular semi-cylindrical receiver and operational condition. However, this heat transfer coefficient does not apply to the generic cylindrical cavity receiver or the receiver which is operating in a high receiver temperature range. Therefore, there is a need for a systematic investigation of the different receiver temperatures, aperture sizes and receiver geometries to derive a better correlation for forced convective heat loss prediction, which considers all of those parameters. Another similar solar receiver experiment was performed for the side on and head on wind speed of 1m/s and 3 m/s with a different geometry (Prakash et al., 2009). This experiment was performed with low receiver temperatures which are about 50, 60 and 75 °C and repeated with receiver tilt angle of 0°, 30°, 45°, 60° and 90°. This study has an alternative conclusion to Ma's experiment (Ma, 1993). This study claimed that head-on wind had a higher convective heat loss than side on wind and the no-wind conditions. It also found that the no-wind convective heat loss was higher than the mix convective heat loss when the side on wind speed is between 1m/s and 3 m/s. This suggests the side on wind may prevent the hot air flow out from the receiver for low wind speed. Another experimental study was undertaken on a cubical receiver for a few different cavity geometries which are to cover the heater of the receiver (Kim, Yoon & Kang 2009). The heater is the only heat source of the

receiver with setpoint temperatures at 300, 400 and 500 °C. The purpose of this experiment was to assess the relationship between convective heat loss and aperture area, aperture position, the distance between aperture and heater, heater temperature, tilt angle and wind speed. This experiment claimed that forced convection is lower than natural convection in the lower tilt angle of 0° and 20° regardless of their tested wind speed. However, the effect of forced convection rapidly increases with wind speed for higher tilt angle. Moreover, it also found that the convective heat loss increases with increasing the heater temperature, receiver tilt angle, aperture area and wind speed. However, the convective heat loss is not strongly related to the distance between the aperture and the heater and the position of the aperture. Recalled that this experiment only focused on the head on wind direction, therefore its conclusions may not hold for the other wind directions.

2.1.5 Empirical relationships of convection

Empirical equation of convection heat transfer have been established for solar receivers. The Nusselt number is a dimensionless number used to estimate the convective heat loss from a receiver. A review of the Nusselt number correlations for a solar receiver was published by Wu et al. (2010). A new correlation obtained from experimental and numerical work was proposed by Paitoonsurikarn and Lovegrove (2006). This correlation was claimed to be simpler to be used and more reliable than most of the previous correlation in the most situation before 2006. This correlation is a function of the Nusselt number Nu_L , the Rayleigh number Ra_L , the Prandtl number Pr , the internal diameter of a receiver, the internal depth of a receiver and the aperture diameter, are shown in equations (5) and (6).

$$Nu_L = 0.0196Ra_L^{0.41} Pr^{0.13} \quad (5)$$

Here, Pr is the Prandtl number and L_s is define as follows:

$$L_s = \left| \sum_{i=1}^3 a_i \cos(\varphi + \psi_i)^{b_i} L_i \right| \quad (6)$$

Here, $L_1 = D_{cav}$ is the internal diameter, $L_2 = L_{cav}$ is the internal depth and $L_3 = D_{ap}$ is the aperture diameter of a receiver.

Table 2.2 Constants in Equation (6) for the evaluation of the ensemble cavity length scale L_s

i	a_i	b_i	ψ_i
1	4.08	5.41	-0.11
2	-1.17	7.17	-0.30
3	0.07	1.99	-0.08

Another empirical correlation, which is based on Taumoeofolau's experimental data from their model cavity receiver in 2002 and Xiao & Wu's CFD result, was proposed in two stages (Wu et al., 2011; Xiao et al., 2012). In the first stage, only natural convective heat loss from a receiver was considered. A correlation using Nusselt number to estimate the natural convective heat loss from a receiver was proposed in 2011 by Wu, Xiao and Li, as is shown in equation (7).

CHAPTER 2

$$Nu_n = 1.87845 \times 10^{-3} Gr^{\frac{1}{3}} \left(\frac{T_w}{T_a}\right)^{0.7090} (1 + \cos \varphi)^{4.7802} R_{as}^{1.9752} R_{ap}^{0.2749}. \quad (7)$$

This correlation is a function the Grashof number Gr , receiver wall temperature T_w , ambient temperature T_a , receiver tilt angle, dimensionless aperture size and dimensionless aperture position. At the second stage, wind effect was added to the model and a ratio of the with wind cases Nusselt number to the no-wind cases Nusselt number was suggested in 2012 by the same authors shown in equation (8).

$$\frac{Nu_t}{Nu_n} = 2.8205(2 + \cos \varphi)^{-5.8471}(3 + \sin \alpha)^{-0.0008} Re^{0.6310}. \quad (8)$$

Therefore, the combined convective heat loss can be estimated from the Reynolds number, the receiver inclination, the wind direction and the Nusselt number of the natural convective heat loss which was published in their previous article in 2011. This is the first correlation for combined convective heat loss from solar cavity receiver with that many variables. However, this numerical correlation has not been validated with another experiment; hence further experimental data is required to validate the reliability of the results.

Conversely, the study on the effect of wind on the heat losses from a cavity receiver is still at an early stage. Hence there is a limited correlation for forced convective heat loss from a receiver. To the best of the authors knowledge, the correlation from Xiao et al. (2012) study is the only correlation that has considered the effect of wind on a generic solar receiver. Therefore, this is the only correlation which can be used in the analytical investigation of this project. However, it should be used with care and more study is need on the correlation for forced or combined convective heat

loss from solar cavity receiver. In addition, experimental data is required to validate the correlation equation.

2.2 Experiment of convective heat losses from a heated cavity

An experimental study was performed to understand the convective heat losses from the heated cavity by Ma (1993). A heat transfer fluid was used to heat the cavity receiver to a set point temperature shown in Figure 2.5. The total heat input Q_{input} from the system was calculated from the temperature drop of the measured temperature between the inlet and outlet. The total heat loss Q_{loss} from the cavity is defined in equation (9). This is because there is not useful heat in the experiment, hence the input heat to the system equal to the total loss from the system. The $Q_{rad,ap}$ is the radiative heat loss from the aperture of the cavity. $Q_{conv,ap}$ is the combined convective heat loss from the aperture. $Q_{cond,w}$ is the loss through the insulation from the inside of the cavity to the outside of the receiver, then radiation and convective heat loss to the surrounding.

$$Q_{loss} + Q_{useful} = Q_{input}, \quad Q_{useful} = 0, \quad (9)$$

$$Q_{loss} = Q_{rad,ap} + Q_{conv,ap} + Q_{cond,wall}, \quad (10)$$

$$Q_{loss,non-conv} = Q_{rad,ap} + Q_{cond,w} = Q_{loss} - Q_{conv,ap}, \quad (11)$$

$$Q_{loss,conv} = Q_{conv,ap} = Q_{loss} - Q_{loss,non-conv}. \quad (12)$$

To assess the heat losses, the following steps were taken. The total heat loss Q_{loss} was determined using the required input power from the heat source at steady state. From the literature review, $Q_{rad,ap}$ and $Q_{cond,cav}$ are not very sensitive to receiver tilt angle and wind speed, and $Q_{conv,ap}$ is negligible if the aperture of the receiver is facing downward. Therefore, $Q_{loss,non-conv}$ was determined by tilting

CHAPTER 2

the receiver to face down and using equation (11), while $Q_{conv,ap}$ is negligible at that situation. After that, $Q_{loss,conv}$ was determined using equation (12) for various tilt angles and wind conditions. This experimental method was suggested by Ma (1993) and similar methods are using to in the later experimental studies to assess the heat losses from a cavity receiver. In addition, thermocouples were used to measure the temperature of the cavity to ensure the cavity was maintained at the set temperature. They claimed that, for the same wind speed, the convective heat loss for the side-on wind is higher than the head on wind direction and suggested few correlation equations. The natural convective heat transfer coefficient for a cavity receiver is given in equation 13 (Ma, 1993). The forced convective heat transfer coefficient of a cavity receiver for the side-on and head on wind is given in equation 14 and 15 (Ma, 1993). Then the combined convective heat loss from a cavity receiver can be estimated from equation (16).

$$\bar{h}_n = \frac{\overline{Nu}_L k}{L},$$

$$\overline{Nu}_L = 0.088 Gr_L^{\frac{1}{3}} \left(\frac{T_{cav}}{T_a} \right)^{0.18} (\cos\theta)^{2.47} \left(\frac{D_{ap}}{D_{cav}} \right)^s,$$

$$\text{Where } s = 1.12 - 0.982 \left(\frac{D_{ap}}{D_{cav}} \right),$$

T_{cav} =average temperature of the receiver

T_a =average ambient temperature

θ =receiver tilt angle

k =thermal conductivity

D_{cav} =receiver internal diameter

D_{ap} =receiver aperture diameter

(13)

$$\bar{h}_{f,side\ on} = 0.1967V^{1.849}, \quad (14)$$

$$\bar{h}_{f,head\ on} = (0.1634 + 0.7498 \sin\theta + 0.5023 \sin 2\theta + 0.3278 \sin 3\theta) V^{1.401}, \quad (15)$$

$$Q_{loss,conv} = A_{cav} \times \bar{h} \times (T_{cav} - T_a). \quad (16)$$

Recently, a low temperature heated cavity receiver was tested in a cryogenic wind tunnel, to analyse the influence of wind on convective losses of a cavity receiver for solar power tower system (Flesch et al., 2015). A low-temperature cavity is placed in a cold wind tunnel to have a similar Reynolds number of a large-scale solar cavity receiver. An ambient temperature of $-173\text{ }^{\circ}\text{C}$ was used in this experiment to match Gr and Re number of a solar cavity receiver with diameter = 2.4m. Five electric heating circuits with one power controller were used to maintain the average internal temperature = $60.4\text{ }^{\circ}\text{C}$. Tilt angle, wind speed and direction have been investigated in their study. They reported that, for some conditions, the minimum convective heat losses can occur at an intermediate wind speed, so that a low wind speed can reduce the losses to below the value of natural convection. This study also claimed that a side-on wind has a greater impact on the heat loss than a head-on wind case. Also worth noting, is that the effect of side-on wind is stronger than head-on wind only for the cases with tilt angle larger than 30° . Therefore the tilt angle is one of the parameters need to be considered when assessing the effect

CHAPTER 2

of yaw angle. Another experimental study was performed to assess the effect of the tilt angle, wind speed and direction on the convective heat losses from a heated cavity (Wu et al., 2015). Two electric heating circuits (constant heat flux) were used to heat the cavity to the given temperature without a fine feedback power controller. They claimed that there is no simple rule can describe the influence of wind incident angle exactly. And the impact of wind incident angle can be weakened at the high wind speed. In addition, an experimental correlation for the prediction of the heat losses in term of the Nu number is provided. However, their study has a blockage ratio $> 50\%$, hence this might reduce the accuracy of the results. It is because the air flow was affected from the large blockage ratio, as it introduces an artificial acceleration of the flow.

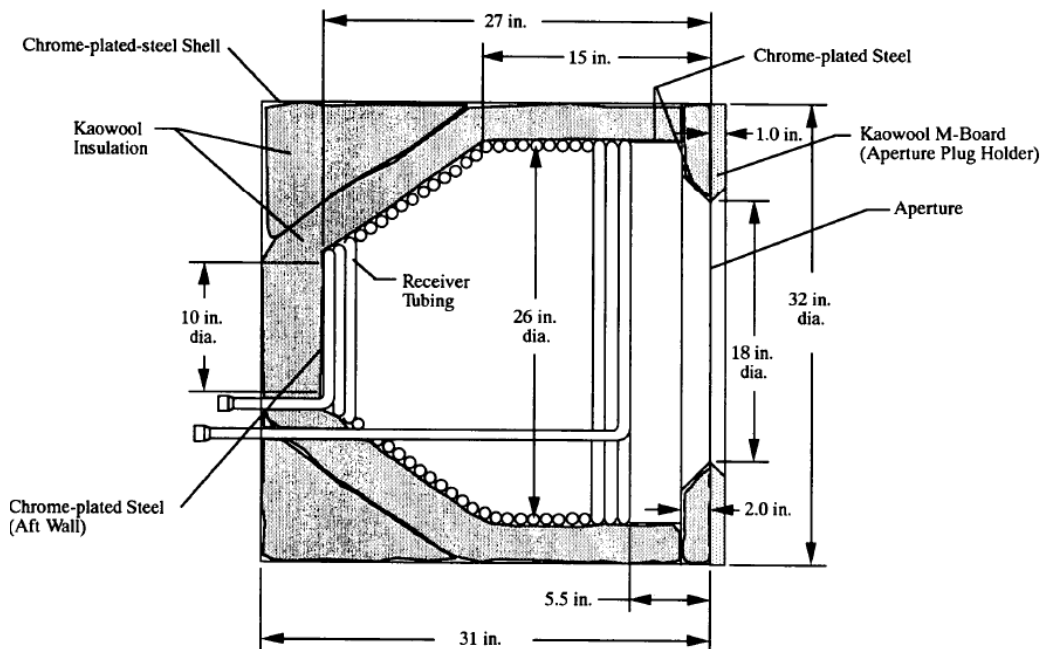


Figure 2.5: Schematic diagram of the tested cavity receiver in Ma's experiment (Ma, 1993).

2.3 Non-uniform temperature distribution

Several experimental studies were performed to investigate the heat losses from a solar receiver (Kim, Yoon & Kang 2009; Ma 1993; Prakash, Kedare & Nayak 2009; Taumoefolau & Lovegrove 2002). The experimental studies were performed for a range of different conditions, such as wind speed, tilt angle and aperture ratio. However, their methodologies for the heating of the cavity are similar with each other's. Their methodologies can be classified into two main categories of (a) conductive heating and (b) convective heating. Conductive heating is rising the temperature of a cavity receiver with heating element to a uniform internal temperature and convective heating is based on using a HTF to heat the cavity with a given HTF temperature. However, a solar receiver heated by concentrated solar radiation produced by the heliostats is exposed to a non-uniform radiative heat flux. This non-uniform heat flux together with the heat losses from the receiver lead to a non-uniform temperature distribution within the cavity of the receiver, which results in a complicated heat loss pattern from the receiver. Therefore, non-uniform temperature distribution over the internal walls is expected to have a critical effect on the heat loss from a solar receiver (Holman, 1997). Consequently, the effect of non-uniform heat flux distribution on heat loss from a solar cavity receiver needs to be investigated.

2.4 Ray tracing

Ray tracing techniques can be applied to cavities with non-uniform temperature distribution to determine the radiation loss from the receiver (Hogan et al., 1990).

Monte Carlo ray-tracing technique is one of the methods to estimate the re-radiative heat loss from a solar receiver (Siegel, 2001). Two rays tracing optical analysis' using Monte Carlo technique has been performed for a parabolic trough collector (Bader, 2011) and a parabolic dish cavity receiver (Steinfeld and Schubnell, 1993). However, both of the studies estimate the heat flux at the focus plane of a receiver, so only the temperature distribution at the focus plane was predicted. Thermal Finite element model with optical ray tracing was also use to assess the thermal efficiency of the solar cavity receivers (Uhlig et al., 2014). However, the convective heat losses from the solar cavity receivers were only estimated using some Nusselt number correlation, which have not been validated in the study. As the convective losses play an important role in the efficiency of a solar cavity receiver. The convective heat losses were evaluates using another CFD models in the same study. Therefore the effect of mixed convective heat losses on the temperature distribution has not been assess within the same thermal finite element model for the optical system. To the best knowledge of the author, a detailed ray tracing model for the entire solar tower central receiver system considering mixed convective heat loss when determining the temperature distribution over the internal walls within a same simulation has not been reported yet.

2.5 Aperture features

2.5.1 Flow control aperture

Active flow control system is one of the possible methods to reduce the convective heat loss from a cavity receiver. This type of system measures the surrounding conditions with a feedback control system to reduce the surrounding air flow into

the cavity, as well as keeping the hot air inside the cavity. A numerical study was performed to examine the use of an air curtain as a method of reducing the convective heat loss from a hot cavity (McIntosh et al., 2014). In this study, a two-dimensional model was conducted and the results show a reduction of about 34% of the heat loss from the cavity when air curtain directed across the aperture was used (McIntosh et al., 2014). However, the results have not been validated with a heated cavity experimentally. Therefore, further works are required to experimentally validate the result of the use of air curtain as well as develop a three-dimensional numerical model.

2.5.2 Windowed aperture

Alternatively, window cover is another possible way to reduce convective heat loss from a cavity receiver, however, to allow the solar power pass through and get into a receiver, a transparent or partially transparent cover is required. Therefore, a glass cover is used in some of the solar energy conversion systems (Deubener et al., 2009; Mande and Miller, 2011; RÄkger et al., 2006). One of the applications of glass cover in CSP system is that glass covers are required to hold the gas within a pressurised high-temperature volumetric close system receiver shown in Figure 2.6. At the same time, the glass cover also reduces the heat loss from the high-temperature receiver to keep the operating temperature above 800 °C (Gardon, 1961; Hensch et al., 2010; RÄkger et al., 2006; Rubin, 1982).

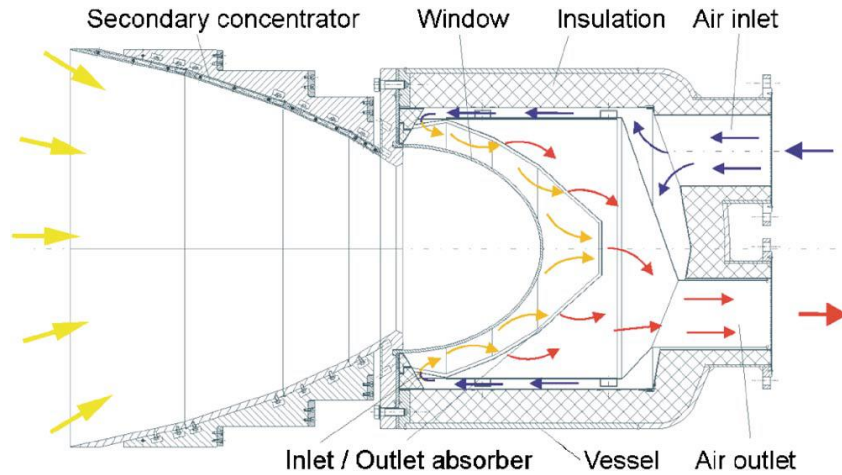


Figure 2.6: Schematic diagram of a pressurised volumetric receiver (REFOS type) (RÅkger et al., 2006).

Similarly, some special receivers called chemical reactors which are the others type of CSP system that required a glass cover to be operated. The cover separates the reactants within a receiver to the surrounding but only allow solar power to enter a receiver to provide power for the reaction (Deubener et al., 2009).

A glass cover is not generally used in tubular cavity receivers, because it does not require a window cover to be operational. However, a receiver with a window expected to have the lower radiative and convective heat losses than the one without the window (Mande and Miller, 2011; RÅkger et al., 2006; Rubin, 1982; Uhlig et al., 2014). Alternatively, the window blocks and reflects some of the solar power which leads to a high power wastage. This issue is addressed by the coating on the silica glass cover to increase its transmittance shown in Figure 2.7 (Helsch et al., 2010). Therefore, the study should still be continued to further increase its transmittance. Moreover the glass increase the capital, operating and maintenance cost of the plant, therefore, it is also a factor should be considered for the use of a

window on a tubular cavity receiver for CSP plant. Another assessment shows that, there is a reduction of electricity cost by using a window with 99% transmissivity 3% reflection losses (Uhlig et al., 2014). Therefore, future work may study further in this concept and also be focused the transmissivity, reflectivity and lifespan of the glass. However, the windowed cavities are not the focus of the present thesis.

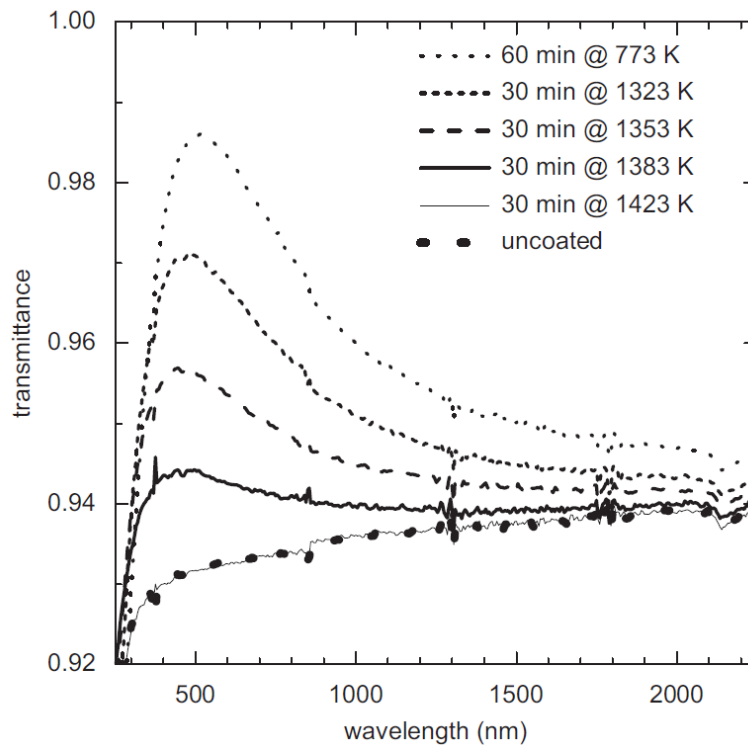


Figure 2.7: Transmittance spectra of porous silica coatings on silica glass for different heat treatments in comparison to the uncoated silica glass (Helsch et al., 2010).

2.6 Beam down solar system

A “beam down” optics or “solar tower reflector” system is a variation of central receiver plants with a secondary reflector on top of the central tower to redirect the concentrated solar beam from the heliostats again down toward a solar cavity

CHAPTER 2

receiver near ground level (Mokhtar, 2011; Segal and Epstein, 2008). The solar cavity receiver faces upward, hence a large receiver could be installed stably (Hasuike et al., 2006). Another advantage is that the effect of wind on this system could be less compared with a receiver located at the top of a high tower. The type of “beam down” system required new optical systems and knowledge of the receiver’s geometries. Therefore, there are many studies on these topics (Leonardi, 2012; Li et al., 2015; Mokhtar et al., 2014; Wei et al., 2013). However, the understanding of convective heat loss from a “beam down” solar cavity receiver is limited. The effect of wind on this type of system is not well known. In addition, the difference in heat losses between “beam up” and “beam down” is also needed to be investigated.

2.7 Economic assessment

The levelised cost of electricity (LCOE) is defined as the ratio of the cost of electricity generating from different energy sources or methods, and the energy it generates in the lifetime of the plant. It is one of the ways to quantitatively compare technologies. The key inputs for the LCOE calculation are capital costs, operations and maintenance (O&M) costs, fuel costs, financing costs, lifetime of the plant, discount factor and energy output in every year when the plant is operational (Price, 2003; Salvadore and Keppler, 2010). The LCOE from solar thermal technology was about 150 to 210USD/MWh in United States in 2010 (Kolb et al., 2011; Salvadore and Keppler, 2010), which is much higher than the cost of power from fossil fuel, which is about 30 to 60 USD/MWh (Nathan et al., 2014; Salvadore and Keppler, 2010). Therefore, power from CSP technology needs to be reduced to be more comparable in cost.

A recent study showed that CSP technology can achieve a cost of electricity about 60USD/MWh eventually by improving the technology (Price 2003), which is similar with the cost of power from fossil fuel. Another study shows that the solar receiver contributes to about 11% to the LCOE for a central receiver plant (Kolb et al., 2011). This study also suggests that increasing the efficiency of the receiver is the most effective way to reduce the LCOE. The efficiency of the receiver can be increased by 13% with the receiver temperature rise from 600 to 700 °C. However, the additional heat loss from the receiver due to the increase of temperature has not been mentioned in this study.

CHAPTER 2

If the solar to thermal power efficiency is increased, the capacity of the plant is also increased. Therefore, it also increases the overall energy output from the plant, hence the reduction of LCOE is not limited to the 11% cost contribution from the solar receiver. The valuations of different receiver structure and feature are compared using LCOE. Therefore, a good understanding of the LCOE model is required and the factors which have the major effect on LCOE was identified. The model used in this project to investigate the effect of the efficiency of a receiver on the LCOE is defined as below (Salvadore and Keppler, 2010):

$$LCOE = \frac{\sum_t \frac{C_t + M_t}{(1+r)^t}}{\sum_t \frac{E_t}{(1+r)^t}}. \quad (17)$$

For the purpose of this project, only capital and operating and maintenance cost were considered. In addition, the energy output from the system is a function of the receiver efficiency. Therefore, it is important to assess and improve the receiver efficiency to compare the LCOE of the different receiver.

In conclusion, even though a cavity receiver has been used in the solar tower systems, further investigation is required to reduce the heat losses from the system, hence to increase efficiency and reduce LCOE. In addition, although the aperture features, such as active flow control aperture and windowed aperture, have been introduced to reduce the heat losses from a solar receiver system, the understanding for the mechanisms, which affect the convective heat losses is not enough. This

CHAPTER 2

understanding is required for the engineers to design an active flow control aperture or windowed aperture for a heat losses reduction. Therefore, there is a need for further analysis to better understand the effect of the cavity's geometry, wind condition and temperature distribution over the internal walls on the heat losses from a solar cavity receiver and to develop the knowledge required to enable engineers to more accurately predict the heat losses from alternative configurations of solar cavity receiver and, hence, to reliably optimise their receiver designs.

CHAPTER 3

Methodology

Numerical and experimental methods were used to achieve the objectives shown in section 1.6.2. A numerical method was used to achieve objective I (see Section 1.6.2). It was the first assessment of this thesis to identify which aspect ratio of a cavity receiver to perform the in the experimental part of this thesis as well as providing some understanding of the flow-field inside a cavity receiver. Then wind tunnel experiments were performed to achieve objectives II to V (see Section 1.6.2) which mostly quantify the effects of the different geometrical configurations and operating conditions on the heat losses from the cavity.

3.1 Numerical model

Computational Fluid Dynamics (CFD) models were used to assess the effects of wind speed and aspect ratio on the heat losses from a heated cavity with uniform temperature. The aspect ratio was investigated in this study, because it was previously identified as one of the key configurations parameters that affect heat losses from a cavity receiver. Also, the aspect ratio is more difficult to be studied experimentally as it requires to change in the geometry of the main body of the cavity receiver which can be costly and technically difficult. In addition, the flow-field information inside a cavity is also very difficult to measure experimentally, without disturbing the flow field and affecting the fidelity of the measurements. As a result, CFD modelling was performed first to help achieve objective I, and then to identify the aspect ratio which would be used in the experiments.

CHAPTER 3

The commercial software ANSYS Fluent Release 17.0 was employed for the 3D numerical simulations of the combined natural and forced convective heat loss from the solar cavity receiver (Fluent, 2018). The cavity was placed at the middle of a computational domain. The extent of the domain around the solar receiver was chosen to be 20 times larger than the diameter of the cavity in both the radial and axial direction, a size that has been found to be sufficient to approach the unconfined atmosphere. A grid independence study was performed on five different meshes of $\sim 0.1, 0.2, 0.5, 1, 2$ and 3×10^6 elements (combination of hexahedral and tetrahedral elements). The grid convergence index (GCI) was below 1% for the selected mesh; The model was deemed to have converged when the total heat loss from all the walls of the cavity exhibited less than a 0.1% variation over the previous 50 iterations. The realizable $k - \varepsilon$ turbulence with standard wall function model was used to simulate the heat transfer and flow field following from a previous study (Xiao et al., 2012). The formulation for the turbulent viscosity and the wall functions are reported elsewhere (Fluent, 2016, 2018; Shih et al., 1995). Mesh independence study was also performed and approximately 2×10^6 elements is sufficient. More details of the CFD model can be found in CHAPTER 4.

A fully open cylindrical cavity receiver was chosen for the present CFD study, to match the available experimental data of the heat losses from a cylindrical cavity receiver at that time (Taumoefolau and Lovegrove, 2002; Taumoefolau et al., 2004). These data were used to validate the prediction of the heat losses from the calculations of the CFD model. Since the effect of the cavity's aspect ratio on its convective heat loss was the focus of this study, only one tilt angle (15°) and wind

direction (head-on) was employed, as they have been numerically studied previously (Flesch et al., 2014; Wu et al., 2011; Xiao et al., 2012). The details of the methodology, validation and limitations for the CFD model can be found in CHAPTER 4.

3.2 Experimental setup

Three experimental campaigns were conducted in this project as explained here below. In the first experimental study, the influence of internal walls temperature and wind conditions on the heat losses through the aperture of cylindrical solar cavity receivers were assessed. This addresses objective II of this work. The second experimental campaign addresses objective III of this work by studying the influence of Reynolds number, wind direction, aperture ratio and tilt angle on heat losses from the cavity. And the third experimental campaign, which addressed objective IV and objective V was focussed on understanding the influence of Reynolds number and internal walls temperature distribution, of the solar cavity receiver, on the heat losses through the aperture, as well as the comparison of heat losses between a downward tilted heated cavity and an upward facing heated cavity. Only an overview of experimental will be presented in this section, the detail of each experimental setup is reported in each publication shown in Chapter 5, 6 and 7.

Figure 3.1a and Figure 3.2 presents an overview of the experimental arrangement used in the three studies of this thesis. An electrically heated cavity was placed

CHAPTER 3

within the open section of the wind tunnel at University of Adelaide's Thebarton laboratory. This provides well-controlled variation in wind speed with negligible blockage, which is low even without the open section. The projected area of the external dimensions of the cavity ($\sim 0.249 \text{ m}^2$) is $\sim 4.1\%$ of the cross-sectional dimensions area of the wind tunnel ($2.75 \text{ m} \times 2.19 \text{ m}$), which is also ~ 330 times larger than the cross-section area of the aperture ($\sim 0.018 \text{ m}^2$). The key dimensions of the cavity with its reference case condition are shown in Figure 3.1b. The cavity has an inner diameter $D_{cav} = 0.3\text{m}$ and inner length $L_{cav} = 0.45\text{m}$ with an aspect ratio $R_{as} = L_{cav}/D_{cav} = 1.5$ and aperture diameter $D_{ap} = 0.15$. The internal walls of the cavity are made from copper, because of its high thermal conductivity and safe operating temperature.

A systematic study of the influence on the heat losses was assessed for variations in wind speed $V = 0, 3, 4, 6$ and 9 m/s , aperture ratio $R_{ap} = D_{ap}/D_{cav} = 0.33, 0.50, 0.75$ and 1.00 , tilt angle $\varphi = -90^\circ, 15^\circ, 30^\circ, 45^\circ$ and 90° , yaw angle $\alpha = 0^\circ, 22.5^\circ, 45^\circ, 77.5^\circ$ and 90° , uniform temperature $T_{cav} = 100, 200, 300$ and $400 \text{ }^\circ\text{C}$ and various temperature distribution over the internal walls ("upper, lower, front and rear hotter cases"). A list of the experimental conditions are shown in Table 3.1. This leads to a total of 310 combinations of conditions. Of these 155 conditions correspond to the case with an open aperture to measure the convective and radiative heat losses, and the other 155 cases for the closed aperture to measure the heat loss through the walls. Total of 108 combinations of wind speed, orientation and uniform wall temperature are presented in the journal publication shown in Chapter 5. Following by total of 90

CHAPTER 3

combinations of wind speed, tilt angles and aperture ratios are presented in the journal publication shown in Chapter 6. Finally, total of 112 combinations of wind speed, tilt angle, yaw angle and temperature distribution over the internal walls are presented in the journal publication shown in Chapter 7. The details of the methodology and conditions used in each experimental study can be found in the methodology section of CHAPTER 5 to CHAPTER 7.

A summary and discussion based on the finding across the few studies of this thesis can be found in CHAPTER 8. Although the CFD model used in this thesis has a different geometry from the experiments of this work, the current numerical model can be further developed based on the additional data from the experiment. The details of it are discussed in the future work section of CHAPTER 8.

Table 3.1 List of experimental conditions

Velocity (V , m/s)	Yaw angle (α°)	Tilt angle (φ°)	Temperature of the wall (T_w , $^\circ\text{C}$)	Aspect ratio ($\frac{L_{cav}}{D_{cav}}$)	Aperture ratio ($\frac{D_{ap}}{D_{cav}}$)
0,3,6,9 and 12	0,22.5, 45 77.5 and 90	-90, 0, 15, 30, 45 and 90	100, 200, 300, 400	1.5	0.00, 0.33, 0.50, 0.75, 1.00

CHAPTER 3

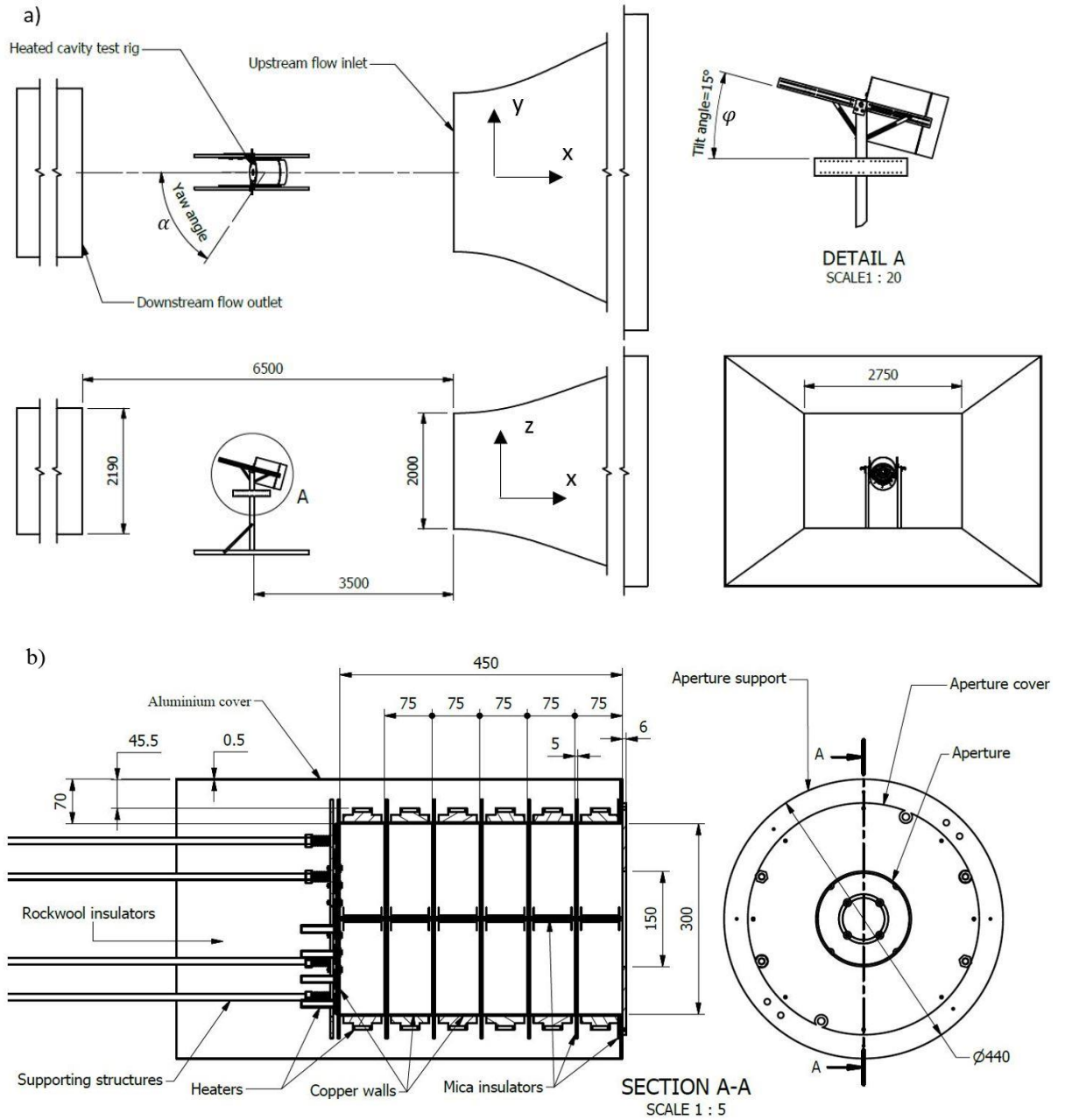


Figure 3.1: Schematic diagram of a) the heated cavity in the Thebarton wind tunnel and b) the detail of the receiver.

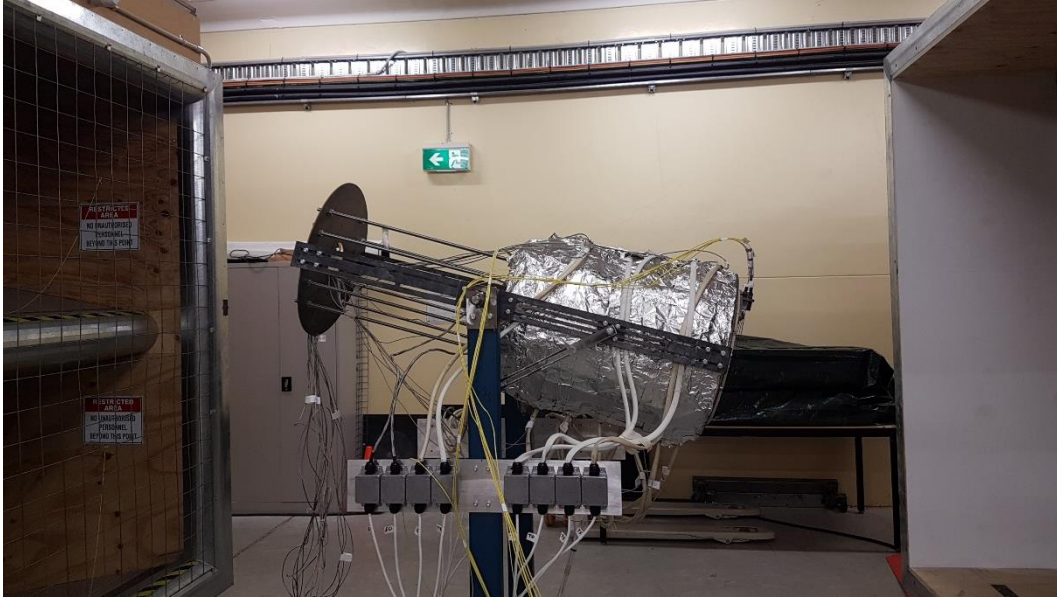


Figure 3.2: Photo of the heated cavity in the open section of the wind tunnel.

CHAPTER 4

An Investigation Into The Effect Of Aspect Ratio On The Heat Loss From A Solar Cavity Receiver

Statement of Authorship

Title of Paper	An investigation into the effect of aspect ratio on the heat loss from a solar cavity receiver
Publication Status	<input checked="" type="checkbox"/> Published <input type="checkbox"/> Accepted for Publication <input type="checkbox"/> Submitted for Publication <input type="checkbox"/> Unpublished and Unsubmitted work written in manuscript style
Publication Details	Lee, KL, Jafarian, M, Ghanadi, F, Arjomandi, M & Nathan, GJ , 'An investigation into the effect of aspect ratio on the heat loss from a solar cavity receiver', Solar energy, (2017), vol. 149, pp. 20-31.

Principal Author

Name of Principal Author (Candidate)	Ka Lok Lee		
Contribution to the Paper	Developed the numerical model, performed analysis on all data, interpreted data, wrote manuscript and acted as corresponding author.		
Overall percentage (%)	65%		
Certification:	This paper reports on original research I conducted during the period of my Higher Degree by Research candidature and is not subject to any obligations or contractual agreements with a third party that would constrain its inclusion in this thesis. I am the primary author of this paper.		
Signature		Date	29/06/2018

Co-Author Contributions

By signing the Statement of Authorship, each author certifies that:

- i. the candidate's stated contribution to the publication is accurate (as detailed above);
- ii. permission is granted for the candidate to include the publication in the thesis; and
- iii. the sum of all co-author contributions is equal to 100% less the candidate's stated contribution.

Name of Co-Author	Mehdi Jafarian		
Contribution to the Paper	Supervised development of the work , helped to evaluate and edit the manuscript		
Signature		Date	02/07/2018.

Name of Co-Author	Farzin Ghanadi		
Contribution to the Paper	helped to evaluate and edit the manuscript		
Signature		Date	02/07/2018

CHAPTER 4

Name of Co-Author	Maziar Arjomandi	
Contribution to the Paper	Supervised development of the work , helped to evaluate the manuscript	
Signature	_____	

	Date	2/07/2018

Name of Co-Author	Graham Jerrold Nathan	
Contribution to the Paper	Supervised development of the work , helped to evaluate and edit the manuscript	
Signature	_____	

	Date	3/7/18



An investigation into the effect of aspect ratio on the heat loss from a solar cavity receiver



Ka Lok Lee*, Mehdi Jafarian, Farzin Ghanadi, Maziar Arjomandi, Graham J. Nathan

School of Mechanical Engineering, The University of Adelaide, SA 5005, Australia

ARTICLE INFO

Article history:

Received 9 September 2016

Received in revised form 28 March 2017

Accepted 31 March 2017

Keywords:

Solar receiver

Solar thermal power

Heat loss

Concentrated solar thermal radiation

Aspect ratio

Wind

ABSTRACT

The effect of aspect ratio and head-on wind speed on the forced and natural (combined) convective heat loss and area-averaged convective heat flux from a cylindrical solar cavity receiver has been assessed using three dimensional computational fluid dynamics (CFD) simulations. The cavity assessment was performed with one end of the cavity open and the other end closed, assuming a uniform internal wall temperature (i.e. the cavity walls were heated). The numerical analysis shows that there are ranges of wind speeds for which the combined convective heat losses are lower than the natural convective heat loss from the cavity and that this range depends on the aspect ratio of the cavity. In addition, the effect of wind speed on the area-averaged flux of convective heat loss from a heated cavity is smaller for long aspect ratios than for short ones, which indicates that the overall efficiency of the solar cavity receiver increases with the aspect ratio for all conditions tested in this study.

© 2017 Elsevier Ltd. All rights reserved.

1. Introduction

Solar thermal power is expected to play an important role in the mix of power generators of the future owing to the foreseeable development of low-cost thermal energy storage system, relative to electrical energy storage system (Kolb et al., 2011). Solar thermal power plants typically use a receiver to transfer the energy of the highly concentrated solar radiation to an internal fluid which is then used for power generation. Recent research has sought to develop systems to achieve higher operating temperatures than what is available from the state-of-the-art, which lead to a higher power generation efficiency, larger solar power plants and an anticipated lower cost (Ávila-Marín, 2011; IEA-ETSAP and IRENA, 2013; Lovegrove et al., 2012; Price, 2003; Segal and Epstein, 2003; Steinfeld and Schubnell, 1993). One of the challenges to be overcome to enable higher temperatures of the solar receiver is to decrease the heat losses from the solar receiver, since heat loss increases with temperature. However, the underlying mechanisms that control the heat losses from a receiver are highly complex and remain poorly understood. Hence, there is a need to further increase the understanding of the mechanisms of heat loss from solar receivers.

One of the geometric configurations being developed for solar thermal systems is a cavity receiver. Previous studies have shown

that cavity-type receiver configurations are the most suitable configuration for high temperature receivers, owing to their lower radiation losses, which is significant given the trend in research to increase the temperature of the solar thermal system (Collado, 2008; Segal and Epstein, 2003). However, an increase in the operating temperature will also increase the heat losses from the receiver (Ho and Iverson, 2014). Hence, to achieve high operating temperatures, there is a need to lower heat losses. One advantage of external receivers is the relatively low surface area compared with cavity receivers. However, in addition to their high radiative losses, both external receivers and very short cavity receivers have high convective heat losses, particularly in windy conditions. Furthermore, their heat losses are very complex, since they include conductive heat loss through insulated walls as well as radiative and convective heat losses through the aperture. Conductive and radiative heat losses can be estimated analytically using a typical wall temperature of the cavity, emissivity and absorptivity, shape factors and the properties of the insulation material (Holman, 1997; Mills, 1999). However, convective heat losses are more difficult to estimate due to the complexity of the temperature and flow fields in and around the cavity. In addition, convective heat losses include both natural convection, which is driven by buoyancy, and forced convection, which is driven by any wind currents. Therefore, the primary objective of the present work is to assess the convective heat loss mechanisms from a fully open heated cavity.

Natural convective heat losses from heated solar cavities were first studied by Clausing (1981). He concluded that convective heat

* Corresponding author.

E-mail address: ka.lee@adelaide.edu.au (K.L. Lee).

loss is governed by two factors: (1) the transfer of energy and mass across the aperture and (2) the transfer of heat to the air inside the cavity. Due to the high internal wall temperatures, the density of air inside the receiver or near to its internal surfaces is lower than that of the ambient air because of the high temperature of the internal walls, which are exposed to concentrated solar radiation. Depending on the configuration, this leads to natural circulation of the air inside the cavity receiver, resulting in natural convective heat loss. They also found that, for certain receiver configurations, hot air is trapped in the upper part of the receiver, dividing the volume within the receiver into a convective (non-stagnant) and a stagnant zone. The boundary between the two zones lies approximately at the horizontal plane, passing through the highest end point of the aperture and is sometimes also referred to as a shear layer (Clausing, 1981, 1983). Similarly, Quere et al. (1981) evaluated the convective heat loss from a cubical cavity with one face open and isothermal conditions numerically. They observed that the convective heat loss is strongly dependent on the inclination (tilt angle φ) of the cavity, which is defined as the angle between the horizontal plane and the normal direction of the aperture, as shown in Fig. 1. Ma (1993) presented detailed experimental data for combined convective heat loss from a cylindrical receiver. He showed that wind directions parallel to the aperture (side-on wind) have a greater impact on the convective heat loss than those normal to the aperture (head-on wind). Other studies (Leibfried and Ortjohann, 1995; Paitoonsurikarn and Lovegrove, 2003) found that some wind can even have reduce the convective heat losses, depending on its speed and direction, together with the cavity geometry. Paitoonsurikarn and Lovegrove (2006) also investigated the effects of various angles of incident wind on the flow field inside the cavity and on the convective heat losses for a parabolic dish structure. They showed that the magnitude of heat loss for side-on wind is higher than head-on wind, similar to the experimental observations of Ma (1993). In contrast, the study by Prakash et al. (2009) found that a head-on wind generates convective heat losses from a cylindrical cavity receiver than the side-on wind for the wind speeds of 1 m/s and 3 m/s. Xiao et al. (2012) investigated the effects of wind incident angle and receiver inclination on the combined free-forced convective heat loss from a solar cavity receiver. They showed that the combined convective heat loss decreases with an increase in inclination for low wind speeds. However, this rate of decrease reduces as the wind speed increases, while the convective heat loss does not vary much with the tilt angle of the cavity for high wind speeds.

The literature shows that, while the effects of wind on the heat loss from the solar cavity have been studied extensively, the effects of geometry on the combined convective heat loss from solar cavity receivers is not well known. There are studies on the effect of wind direction on the heat loss (Flesch et al., 2014; Xiao et al.,

2012). Previous studies have also shown that forced convective heat loss could result in an increment of up to 2.5 times the heat loss from a cavity relative to the minimum convective heat loss for the same wind speed (Xiao et al., 2012; Yu et al., 2012). Head on and side on wind are the most commonly used wind directions for this type of simulation. It has also been shown that wind with a direction parallel to the aperture may possibly has a reduction effect on the heat loss as it inhibits hot air from leaving the cavity (Flesch et al., 2014; McIntosh et al., 2014; Prakash et al., 2009). Nevertheless, there are conflicting results in a number of investigation (Ma, 1993; Paitoonsurikarn and Lovegrove, 2006; Prakash et al., 2009) regarding the effects of head-on and side-on wind on the combined convective heat loss from the heated cavity, which is possibly due to the different cavity configurations, temperatures of the walls and wind conditions used in the respective studies. Furthermore, it has been found that the larger the aspect ratio of the cavity, the smaller the mean air flow speed inside the cavity (Rockwell and Naudascher, 1978; Tam and Block, 1978).

The aforementioned discussion shows that, while the effects of wind on the heat loss from a solar cavity have been studied extensively for head-on and side-on wind directions, the effect of the cavity geometry on the combined convective heat loss from solar cavity receivers is not well understood. Furthermore, the effect of aspect ratio on solar cavity receivers in terms of its combined convective heat loss is also not well known. Therefore, the principle objective of this work is to assess the effects of aspect ratio of a cavity on its combined convective heat loss for various wind speeds.

2. Methodology and model validation

A fully open cylindrical cavity receiver, as shown schematically in Fig. 1, was chosen for the present study. The experimental data on the heat losses from the smaller cylindrical cavity receivers used in solar dish systems (Ma, 1993; McDonald, 1995; Prakash et al., 2009; Taumoeofolau and Lovegrove, 2002) was chosen for validation in the absence of any publically available larger scale data. Comparing those experimental studies, Taumoeofolau and Lovegrove's study was chosen for this project, as the effect of the cavity's aspect ratio on its convective heat loss is the focus of this study. Since the effect of tilt angle of solar cavity and wind direction have already been assessed numerically (Flesch et al., 2014; Wu et al., 2011; Xiao et al., 2012). This work is not repeated. Instead only one tilt angle and wind direction was employed.

Validation of the model was performed through comparison of the model predictions with the experimental data reported by Taumoeofolau et al. (2004). In this experiment, a simple cylindrical solar cavity receiver was used with an outer diameter $D_{receiver}$ of 280 mm, an outer length $L_{receiver}$ of 320 mm, an inner diameter D of 70 mm and inner length L of 155 mm. The comparison was undertaken for tilt angles φ from 0° to 90° . Of these, a tilt angle of 15° was chosen as a reference case, since it is within the suitable range for large solar towers (Wei et al., 2010a,b). The modelled small-scale cavity receiver has an inner cavity length where L is 155 mm, similar to the experimental study undertaken by Taumoeofolau et al. (2004). For the present work, L was varied from 35 mm to 210 mm with increments of 35 mm to alter the aspect ratios (the ratio of cavity length to the cavity diameter), from 0.5 to 3 with increments of 0.5. Furthermore, a parametric analysis of the effects of changing the head on wind velocities (2, 4, 7 and 10 m/s) was also performed.

An isothermal boundary of 400°C for the inner cavity walls was chosen, following the approach of previous numerical studies (Paitoonsurikarn et al., 2004; Wu et al., 2011; Xiao et al., 2012). This avoids the challenge of addressing the complex coupling

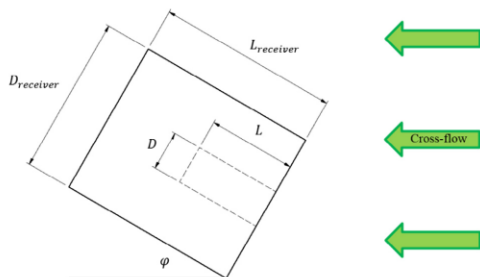


Fig. 1. Schematic diagram of the configuration chosen for investigation, with a fully open cylindrical solar cavity receiver in the presence of a uniform cross-flow.

between the non-uniform radiative heat flux from the solar field and the convective cooling, which has not been undertaken previously for both natural and forced convection. For example, previous models that have directly calculated radiative losses have only been performed for natural convection or have assumed a uniform convective heat loss (Asselineau et al., 2014; Gil et al., 2015). However, for validation the internal wall temperature was set to a slightly higher temperature 445 °C, while the circular end plate was set to 408 °C following Taumoeofalou et al. (2004). The outer walls of the receivers were assumed to be adiabatic, so that heat loss through the insulation by conduction and convection was ignored. This is because the wall losses have no influence on the internal convective losses for the case in which the temperature of the internal walls is assumed to be isothermal. That is, the topic of heat losses through the wall was considered to be beyond the scope of the present investigation. The wind was assumed to have uniform free stream velocity in the horizontal direction, as is described in more detail within the numerical section below. All the other walls of the domain were chosen to be pressure outlets with an ambient temperature of 27 °C. A summary of these numerical parameters is presented in Table 1.

2.1. Radiative heat loss

The radiative heat loss from each cavity was calculated both analytically and numerically. The analytical approach was performed using simple view factor to determine the ratio of convective heat loss and total heat loss. This allows comparison with published experimental results. The net radiative heat loss $Q_{radiation}$ from the cavity was calculated using Eq. (1), following Holman (1997):

$$Q_{radiation} = F_{w_{\infty}} A_w \sigma \epsilon_w (T_w^4 - T_{\infty}^4). \tag{1}$$

Here $F_{w_{\infty}}$ is the shape factor for the inner wall surface of the cavity and its environment, A_w is the total area of the inner heated wall, σ is the Stefan-Boltzmann constant for radiation and ϵ_w is the surface emissivity of the heated cavity wall. For the cavity wall, a uniform wall temperature of 445 °C and emissivity of unity was chosen.

For a cavity with a uniform surface temperature, the cavity shape factor can be simplified to Eq. (2) and the net radiative heat loss can be simplified to a function of the area of the aperture $A_{aperture}$, as shown in Eq. (3):

$$F_{w_{\infty}} = \frac{A_{aperture}}{A_w}, \tag{2}$$

$$Q_{radiation} = A_{aperture} \sigma \epsilon_w (T_w^4 - T_{\infty}^4). \tag{3}$$

The surface to surface radiation model in ANSYS Fluent Release 17.0 was also used to calculate the radiative losses. View factors for all surfaces were computed for each geometry and grids, notably for cavity lengths of 70, 140 and 210 mm.

2.2. Numerical model

The commercial software ANSYS Fluent Release 17.0 was employed for the 3D numerical simulations of the combined natural and forced convective heat loss from the solar cavity receiver. The cavity was placed at the middle of a computational domain. The extent of the domain around the solar receiver was chosen to be 20 times larger than the diameter of the cavity in both the radial and axial direction, a size that has been found to be sufficient to approach the unconfined atmosphere (Paitoonsurikarn and Lovegrove, 2002).

A grid sensitivity analysis was carried out to ascertain that the selected mesh density was of sufficient resolution to minimize spatial discretization errors. The analysis revealed that a grid size of approximately 2×10^6 elements is sufficient to capture the salient features of the simulation. The mesh density was significantly greater inside the cavity and gradually decreased toward the enclosure domain wall, as illustrated in Fig. 2. Hexahedral mesh elements were used inside the cavity to achieve fast convergence rates, whilst tetrahedral mesh elements were used for the remainder of the domain. Moreover, inflation layers were employed on all the walls of the receiver to model the boundary layer. A sketch for the typical mesh structure for a fully open solar cavity with an aspect ratio = 1 is shown in Fig. 2.

Table 1
Dimensions, parameters and boundary conditions used in the present study.

Items	Reference case ^a	Numerical model validation	Numerical assessment
Inner cavity length L (mm)	155	155	35, 70, 105, 140, 175 and 210
Inner cavity diameter D (mm)	70	70	70
Outer receiver length $L_{receiver}$ (mm)	320	320	$L + 165$
Outer receiver diameter $D_{receiver}$ (mm)	280	280	280
Aspect ratio (L/D)	2.21	2.21	0.5, 1, 1.5, 2, 2.5 and 3
Tilt angle ϕ	0°, 15°, 30°, 45°, 60°, 75° and 90°	0°, 10°, 12.5°, 15°, 17.5°, 20°, 30°, 45°, 60°, 75° and 90°	15°
Head-on wind speed (m/s)	0	0	0, 2, 4, 7 and 10
<i>Boundary condition</i>			
Cylindrical section of the cavity	Isothermal wall 445 °C	Isothermal wall 445 °C	Isothermal wall 400 °C
Circular end plate of the cavity	Isothermal wall 408 °C	Isothermal wall 408 °C	Isothermal wall 400 °C
External wall of the receiver	Adiabatic wall	Adiabatic wall	Adiabatic wall
Upstream boundary of the domain	Isothermal wall 27 °C	Pressure outlet condition Gauge Pressure = 0 Pa Backflow total temperature = 27 °C with 5% turbulent intensity and turbulent viscosity	Inlet condition Inlet temperature 27 °C Velocity magnitude $V = 0, 2, 4, 7, 10$ m/s with 5% turbulent intensity and turbulent viscosity ratio of 10
Other boundaries of the domain	Isothermal wall 27 °C	Pressure outlet condition Gauge pressure = 0 Pa Backflow total temperature = 27 °C with 5% turbulent intensity and turbulent viscosity	Pressure outlet condition Gauge pressure = 0 Pa Backflow total temperature = 27 °C with 5% turbulent intensity and turbulent viscosity

^a Taumoeofalou and Lovegrove (2002) and Taumoeofalou et al. (2004).

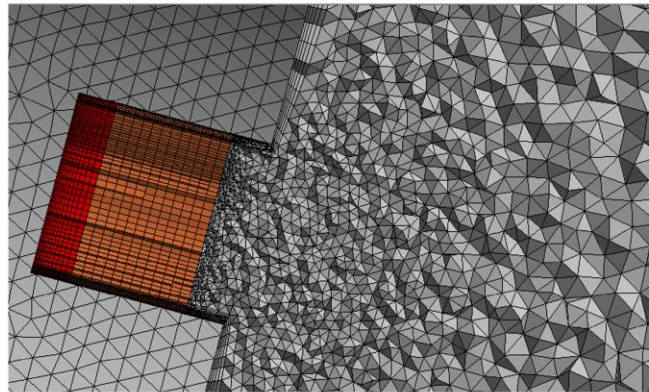


Fig. 2. Typical grid topology for a fully open solar cavity used in the current work (Aspect Ratio = 1).

Air properties such as density, specific heat capacity at constant pressure, thermal conductivity and dynamic viscosity were evaluated at their local temperatures. The air properties of each cell in the domain were calculated using a temperature dependent polynomial or piecewise-polynomial function using thermodynamic data (Mills, 1999).

The realizable $k - \epsilon$ turbulence model was used to simulate the heat transfer and flow field. The formulation for the turbulent viscosity and the wall functions are reported elsewhere (Fluent, 2016; Shih et al., 1995). The entire computational domain was initialised to a uniform velocity, temperature and turbulent viscosity for a steady state simulation. The convective heat loss $Q_{Convection}$ from all walls of the cavity was obtained with Eq. (4).

$$Q_{Convection} = \int h_c(T_w - T_\infty)dA \quad (4)$$

It is calculated by the amount of power required to maintain the given wall temperature. The model was deemed to have converged when the total heat loss from all the walls of the cavity exhibited less than a 0.1% variation over the previous 20 iterations. This typically occurred after 3000 iterations. All boundary conditions used in this study are also summarised in Table 1.

2.3. Model validation

The validity of the CFD model was assessed by comparison with the previous experimental and numerical data that are available from the literature. These are the experimental and numerical assessment of losses from natural convection by (Paitoonsurikarn et al., 2004) and Taumofolau and the flow visualisation study of Taumofolau et al. (2004). Nevertheless, full validation has not been possible due to the absence of a direct assessment of either the effects of forced convection or aspect ratio in the literature. In addition, no experimental data are available for an isothermal wall, although numerical results are available for the case of natural convection. Hence the absolute accuracy of the calculations for force convection as a function of aspect ratio remains unknown, although the trends can be expected to be reasonable.

2.3.1. Natural convective heat loss

The present calculations for natural convective heat loss have been compared with the experimental and numerical work by Taumofolau et al. (2004) in Fig. 3. Also shown are the available estimates for convective heat loss obtained with correlation equations by Clausing (1983), Paitoonsurikarn and Lovegrove (2006), Paitoonsurikarn et al. (2011), Stine and McDonald (1989), Koenig

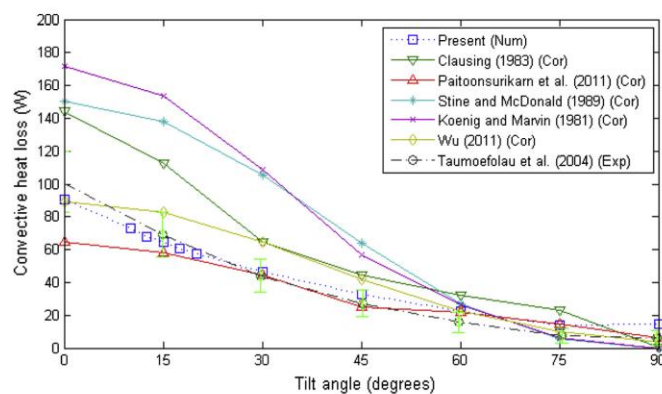


Fig. 3. Comparison of the present calculations of natural convective heat loss against previous work for a fully open cavity with various tilt angles.

Table 2
Comparison of present predictions of natural convective heat loss from a fully open cavity with previous numerical and experimental.

Receiver tilt angle (degrees)	Convective heat loss (W)			Differences (%)		
	Present ^a	Numerical ^b	Experimental ^b	Present ^a VS Exp ^b (%)	Present ^a VS Previous Num ^b (%)	Previous Num ^b VS Exp ^b (%)
0	90.9	101.0	100.6	-9.7	-10.0	0.3
10	72.8	84.6	79.5	-8.4	-14.0	6.4
15	64.5	76.4	69.0	-6.5	-15.6	10.8
20	57.6	68.2	60.5	-4.7	-15.5	12.7
30	46.5	51.9	43.6	6.6	-10.5	19.1

^a Present numerical study.
^b Taumoefolau et al. (2004).

and Marvin (1981) and Wu et al. (2011). It can be observed that the current numerical simulations agree reasonably well with the experimental data. Furthermore, as shown in Table 2, the numerical estimations from the present study are closest to the experimental data for tilt angles between 15° and 30°. This is the range of tilt angles most relevant to a solar tower and is the target for the present investigation. The improvement in the present numerical model over previous work is attributed firstly to the use of a Realizable $k-\varepsilon$ turbulence model instead of the one-equation Spalart-Allmaras, which only solves a single conservation equation. Secondly, the boundary condition for the outer walls of the domain is a pressure outlet with a backflow temperature of 27 °C, instead of a wall with a constant temperature, which leads to a blockage effect. The difference between the present study and the experimental values are less than 10% for small tilt angles and is within the error bars of the experimental data, as is shown in Table 2.

2.3.2. Qualitative validation

An instantaneous Schlieren image from the previous experiments of Taumoefolau et al. (2004) are compared in Fig. 4 with the present calculations of velocity field at the symmetry plane for a fully open heated cavity receiver for a tilt angle of 30° is shown. The Schlieren image shows that the heated air exits the cavity through the upper part of the aperture, attached to the front edge of the receiver. Above this, it spreads out and mixes with the cooler ambient air. The numerical velocity field exhibits good qualitative agreement with the experiments, exhibiting the same trends. This gives confidence that the main qualitative features of the flow are reproduced by the model.

Fig. 5 presents a close-up view of the previous experiments at the plane of the aperture together with the transverse view of the velocity field normal the aperture obtained from the present numerical study. The figure depicts the outflow region through

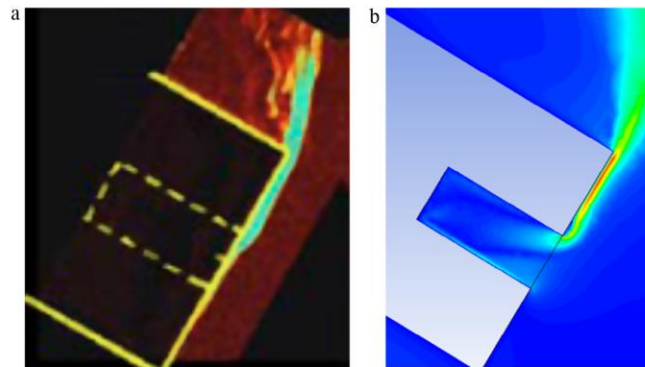


Fig. 4. Flow field in the vicinity of an open cavity at a 30° tilt angle: (a) Schlieren image (Taumoefolau et al., 2004), (b) numerical velocity contour plot.

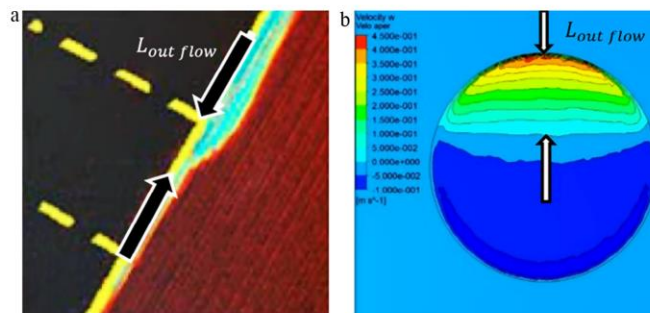


Fig. 5. Close-up view of the open cavity at a 30° tilt angle: (left) Schlieren image (Taumoefolau et al., 2004), (right) numerical results of the aperture's normal velocity profile.

the aperture, defined as the zone where the normal velocity is positive. Also shown is the line of zero velocity, dividing the inflow from the outflow regions. The fraction of the aperture where the air flows out through the aperture $f_{out\ flow}$ is defined as the ratio between the length of outflow $L_{out\ flow}$ and the diameter of the aperture, also illustrated in both images of Fig. 5. The fractions of outflow $f_{out\ flow}$ of the Schlieren image and numerical velocity contour plot are 0.359 and 0.361 respectively. Table 3 presents this ratio for the three cases for which experimental data are available, namely for tilt angles of 0°, 30° and 60°. The results in this section show that the convective heat loss and associated flow patterns simulated within the present numerical model are in excellent agreement with the experimental study by Taumoefolau et al. (2004). Therefore, based on these validation studies, the present numerical model is deemed to be acceptable for estimating the natural convective heat losses for the cavity receiver.

2.4. Radiative heat loss

For a heated cavity with a uniform surface temperature, the radiative heat loss is a function of the area of the aperture. Therefore changing the aspect ratio of the cavity has no effect on the radiative heat loss based on the analytical model. Table 4 compares

the radiative heat loss as estimated for different aspect ratios. It can be seen that the numerical estimates of the radiative heat loss agreed with the analytical values to within 0.1% for aspect ratios varying from 1 to 3. Therefore, the aspect ratio of the cavity has virtually no effect on its radiative heat loss, which also agrees with the study by Asselineau et al. (2014).

The experimental results from Taumoefolau et al. (2004) are used for further validation. In the experiments, the radiative heat loss from the heated cavity was noted to be 53.4 ± 3.1 W with a surface emissivity of 0.87 for a cavity temperature of 445 °C. This is approximately 61.4 ± 3.7 W for a heated cavity with a surface temperature of 445 °C and an emissivity of 1. The mean deviation between the experimental and analytical value is about 8.36% with a lower deviation of 2.48%. On the other hand, the deviation between the analytical and numerical value is approximately 0.41%. The larger deviation between the experimental values and the analytical/numerical values may be caused by a systematic offset from the experiments, such as the non-uniform temperature of the cavity surface in the experiment. Therefore, the overall deviation from the experiments is considered acceptable and the analytical value of radiative heat loss from heated cavities with uniform wall temperatures and a set diameter of aperture is used in the present study.

3. Results and discussion

3.1. Natural convection

The variations in the predicted convective heat loss from a heated cavity with aspect ratio is presented in Fig. 6 for the case of wind speed = 0 m/s, a wall temperature of 400 °C and a tilt angle of 15°. The aspect ratio was varied though changes to the cavity length, with the aperture and cavity diameter kept constant. It can be observed that the total convective heat losses from a heated

Table 3 Comparisons between the fractions of out flow of a fully open cavity.

Receiver tilt angle (degrees)	Fraction of out flow $f_{out\ flow}$		Differences (%)
	Numerical ^a	Experimental ^b	
0	0.446	0.435	1.1
30	0.359	0.361	-0.2
60	0.363	0.358	0.5

^a Present study.
^b Taumoefolau et al. (2004).

Table 4 Comparisons between the analytical, numerical and experimental results of radiative heat loss from the model receiver for various aspect ratios.

	Cavity length L (mm)	Aspect ratio (L/D)	Emissivity	Radiative heat loss (W)
Analytical	155	2.21	1	56.27
Numerical	70	1	1	56.02
Numerical	140	2	1	56.05
Numerical	210	3	1	56.04
Experimental (Taumoefolau et al., 2004)	155	2.21	0.87	53.4 ± 3.1

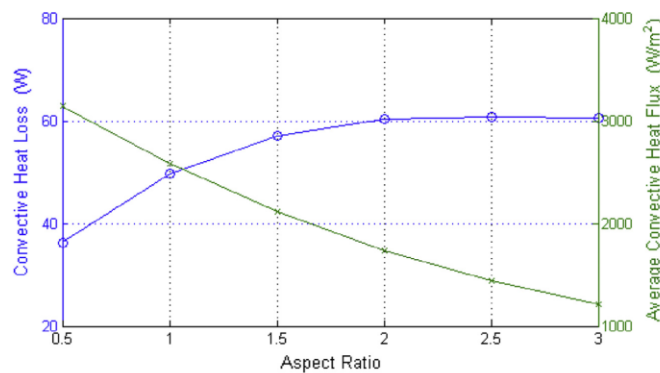


Fig. 6. Variation of convective heat loss and average convective heat flux over the walls of a cavity with an aspect ratio (wind speed = 0 m/s, wall temperature = 400 °C and tilt angle = 15°).

cavity increases non-linearly with the aspect ratio. That is, heat losses increase by more than 50% when the length to diameter ratio of the cavity increases from 0.5 of its diameter to 1.5, but by less than 2.5% difference when the aspect ratio is increased from 2 to 3. Therefore further incremental increases of the aspect ratio are expected to have a weak effect on the convective heat loss of a heated cavity.

Increasing the aspect ratio by varying the cavity length results in an increase of the surface area not only on the air side of the heat exchanger driving convective heat loss; but also of the area exposed to the heat transfer fluid, driving useful heat gain for conversion to heat power. Therefore, increase in aspect ratio can have potential to increase efficiency. Fig. 6 also depicts the dependence of the average convective heat loss flux \bar{q}_{conv} over the internal heat exchange surface of the cavity on the aspect ratio. Here the average flux of convective heat loss, \bar{q}_{conv} is defined as the total integrated convective heat loss from all the walls of the cavity $Q_{conv} = \int_{conv} (A) dA$ divided by the total heat exchange surface area of the cavity A_{HX} . It can be seen that the average heat loss flux \bar{q}_{conv} from the heat exchange surface of the cavity decreases strongly with an increase in aspect ratio. This demonstrates that, for the case of a uniform surface temperature, an increase in aspect ratio will increase the efficiency of the receiver due to greater incremental increase to surface area than that of the convective heat loss from the cavity. Nevertheless, care should be taken in extrapolating this finding to the case of a non-uniform wall temperature, since the actual wall temperature profile in a solar receiver will be non-uniform.

3.2. Combined convection

Fig. 7(a) presents the dependence of convective heat loss on wind speed for several values of constant aspect ratio, also for the case of a uniform wall temperature of 400 °C and a tilt angle of 15°. It can be observed that an increase in the wind speed from zero initially reduces the convective heat loss from the heated cavities for all aspect ratios. For wind speeds above this local minima, the convective heat loss increases approximately linearly with an increase in wind speed. This minimum was also observed in a previous study by Xiao et al. (2012) and has been attributed to the competition at low wind speeds between the wind, pushing fluid into the cavity, and buoyancy, pushing hot air out from the cavity.

It can also be observed from Fig. 7 that, for an aspect ratio of 0.5, a wind speed of approximately 3 m/s is required for the convective heat loss to increase above the case of natural convection (wind

speed = 0 m/s). Furthermore, the critical wind speed for which convective heat loss is predicted to only increase significantly above the natural convection case that depends upon the aspect ratio. For an aspect ratio of 0.5, the critical wind speed is 2.5 m/s, while for aspect ratios of 2–3, the critical wind speed is 5 m/s/. That is, an increase in the aspect ratio increases the resilience of the cavity to heat losses from wind. It can also be seen from Fig. 7 that, despite the general trend of the convective heat loss increasing with aspect ratio, the trend is different the aspect ratio of 2.5. Interestingly, this case has the highest overall convective heat loss for all tested cases and, in particular, is higher than for the aspect ratio of 3. This highlights a potential benefit of long cavities – at least for the case of uniform wall temperature.

Fig. 7(b) presents the calculated dependence of the convective heat loss per unit of area from the walls of the cavity as a function of wind speed, for different a series of different aspect ratios, also for a wall temperature of 400 °C and a tilt angle of 15°. The plot shows that the area-averaged flux of convective heat loss decreases consistently with an increase in aspect ratio for a given wind speed. Therefore, receiver with a smaller aspect ratio has a larger effect of wind, hence the rate of change of the average convective heat loss per unit area with respect to the wind speed is larger for a short cavity than a long one.

Fig. 8(a) presents the simulated dependence of total convective heat loss on aspect ratio for several values of constant wind speed. Here again, the wall temperature was kept constant at 400 °C and the tilt angle was 15°. This shows that the rate at which the combined convective heat loss from the heated cavities increases with aspect ratio is significantly lower for each values of wind speed than it is for natural convection case. This gives further evidence of the shielding effect of a longer cavity for the case of some wind. It can also be seen that, even at the maximum wind speed of 10 m/s, the ratio between total convective losses to that of natural convection is ~2 for low aspect ratios and decreases to ~1.5 at the longer aspect ratios. For wind speeds of 2 m/s, the combined convective heat losses from the cavities are lower than for the natural convective heat losses for all the tested aspect ratios, while for 4 m/s it is lower for all aspect ratios greater than unity.

It can also be observed that the convective heat loss remains approximately uniform at 4 m/s for all aspect ratios, with a variation of approximately 2.5%. This may indicate that 4 m/s is a unique wind speed for the aperture diameter of 0.07 m where the combined convective heat loss from a heated cavity at 400 °C

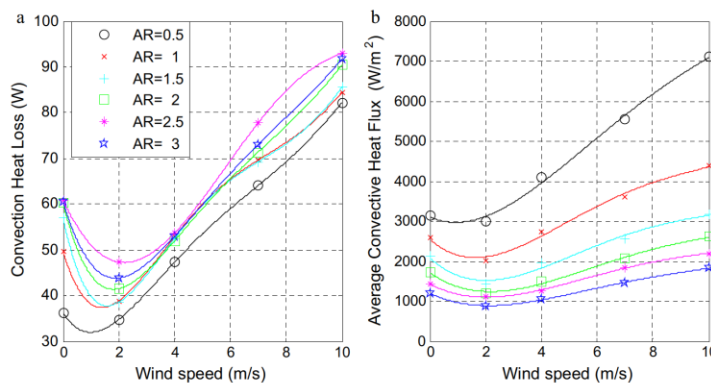


Fig. 7. The calculated dependence on wind speed of (a) total convective heat loss and (b) average convective heat loss over the walls of the cavity. The wall temperature is uniform at 400 °C and the tilt angle = 15°.

and tilt angle of 15° is independent of the aspect ratio of the cavity.

Fig. 8(b) presents the dependence of the area-averaged flux of convective heat loss from the walls of the cavity on aspect ratio for various values of wind speed, also for case of uniform wall temperature of 400 °C and a tilt angle of 15°. The convective heat loss per unit area is greater for smaller aspect ratios, even though the total heat loss is greater for large cavities. For wind speeds of 10 m/s, the area-averaged flux of convective heat loss drops by 74% from 7108 W/m² to 1831 W/m². The rate of reduction of the area-averaged convective heat loss flux decreases with increase in aspect ratio. Table 4 presents the value of radiative heat loss, which is independent of aspect ratio and wind speed. Comparing Fig. 8 and Table 4, they can be seen that the value of the natural

convective heat loss is similar to the radiative heat loss from the heated cavity for case of uniform wall temperature of 400 °C.

3.3. Temperature and velocity distributions

Fig. 9 presents a cross sectional image of the distribution of temperature through the vertical axis of the heated cavity for head on winds at various speed. It can be observed that the presence of wind is predicted to inhibit the penetration of cold fluid into the cavity, so that the area occupied by cold fluid decreases. That is the lowest temperature of air within the cavity for all cases occurs with natural convection only, where it is pure ambient air at ~27 °C for a wind speed of 0 m/s, while even a wind speed of 2 m/s increase the minimum temperature air in the cavity to

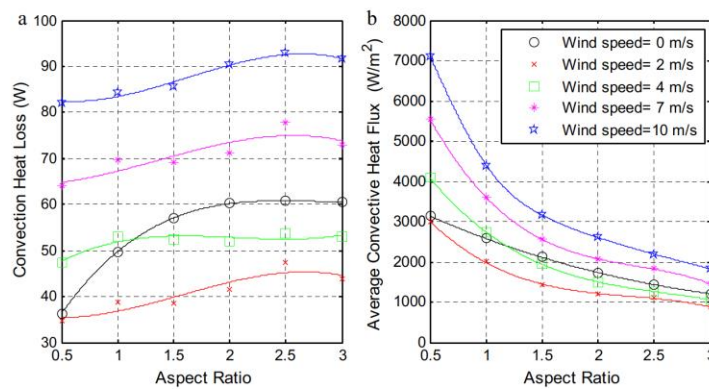


Fig. 8. Calculated dependence on aspect ratio for various values of constant wind speed of (a) total convective heat loss and (b) average flux of convective heat loss over the walls of the cavity. The wall temperature is uniform at 400 °C and the tilt angle = 15°.

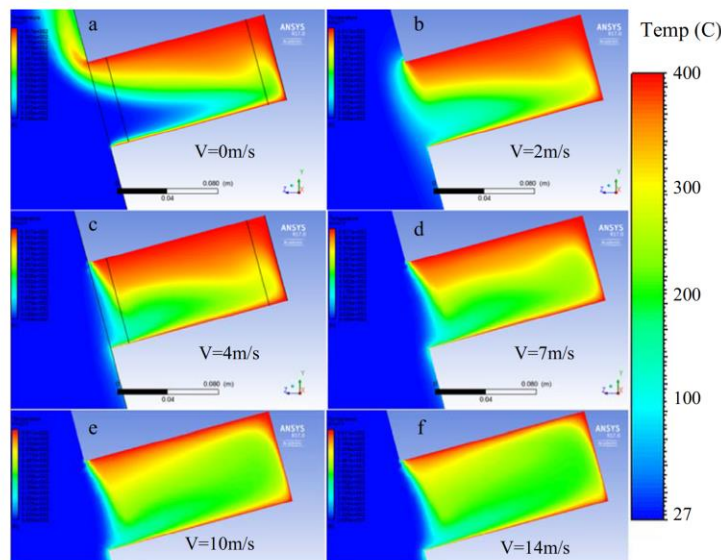


Fig. 9. Cross sectional image of the distribution of the predicted temperature through the vertical axis for the heated cavity with at wall temperature = 400 °C, tilt angle = 15° and aspect ratio = 2, for various cases of head on wind speed V = (a) 0 m/s, (b) 2 m/s, (c) 4 m/s, (d) 7 m/s, (e) 10 m/s and (f) 14 m/s.

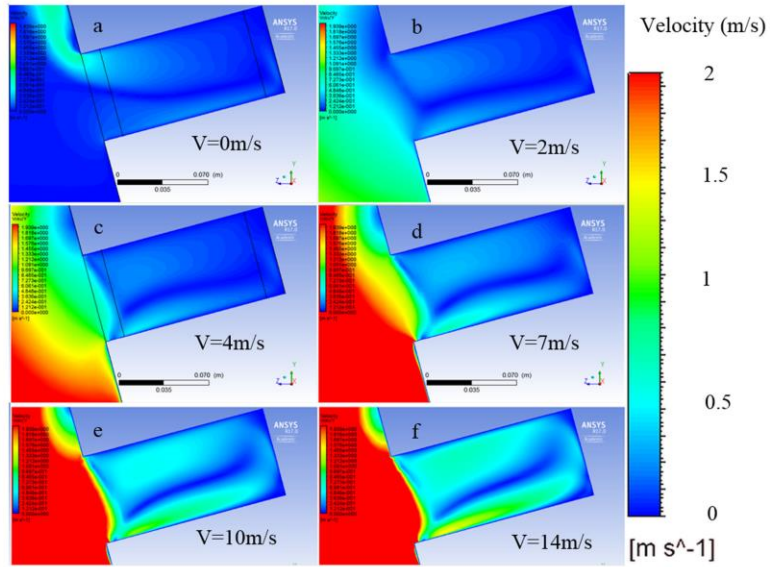


Fig. 10. Cross sectional image of the distribution of the predicted velocity through the vertical axis for the heated cavity with at wall temperature = 400 °C, tilt angle = 15° and aspect ratio = 2, for various cases of head on wind speed $V =$ (a) 0 m/s, (b) 2 m/s, (c) 4 m/s, (d) 7 m/s, (e) 10 m/s and (f) 14 m/s.

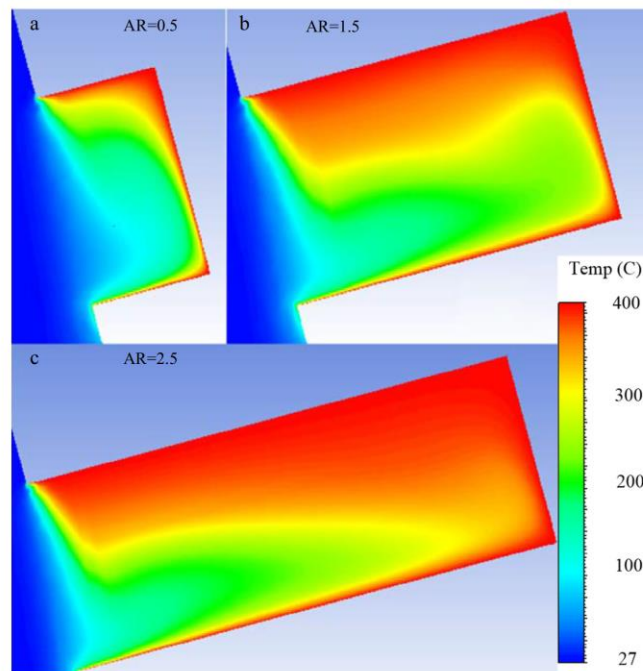


Fig. 11. Cross sectional image of the distribution of the predicted temperature through the vertical axis for the heated cavity with at wall temperature = 400 °C, tilt angle = 15° and head on wind speed = 4 m/s, for various cases of aspect ratio $AR =$ (a) 0.5, (b) 1.5 and (c) 2.5.

~100 °C. This explains the reason why the combined convective heat losses from the cavity is lower with some wind than for the natural convective case.

Fig. 10 presents the cross sectional image of velocity through the central vertical cross section of the heated cavity, also with head on wind of various speeds. It can be seen that introducing a wind speed of 2 m/s reduces the velocity relative to the case of natural convection only, particularly in the region near to the top of the aperture (Fig. 10a and b). However, as wind speed is increased, the velocity over the lower surface increases (Fig. 10c and d). For wind speeds above 10 m/s, the velocity over the surface continues to increase, consistent with increased significance of forced convection (Fig. 10e and f). This provides a qualitative explanation for the observed trends, in which an increase in wind speed increases the convective cooling from the heat exchange surfaces.

Fig. 11 presents the analogous image of temperature through the vertical plane of the heated cavity, but for various aspect ratios. Once again wind is directed heat on, but the wind speed is 4 m/s. The increased shielding effect with increased cavity length is clearly evident, with the thickness of the thermal boundary layer increasing with increased cavity length. It can also be seen that the air temperature is lowest over the lower surface, which is consistent with the orientation of the cavity causing the wind to impinge on the lower surface.

Fig. 12 presents the corresponding cross sectional image of velocity through the vertical plane of the heated cavity. It can be observed that a recirculating interior flow is generated inside the heated cavity for all aspect ratios, with the flow entering the lower side and recirculating upward from the back of the cavity to leave from the upper side. However, the magnitude of velocity over the

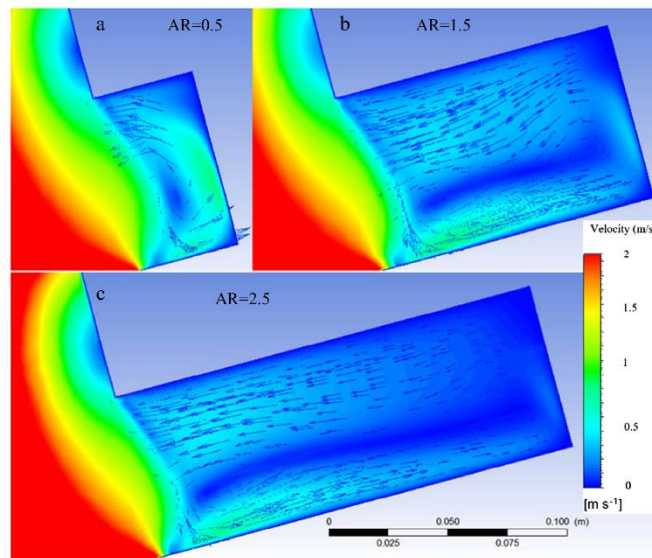


Fig. 12. Cross sectional image of the distribution of the predicted velocity through the vertical axis for the heated cavity with at wall temperature = 400 °C, tilt angle = 15° and head on wind speed = 10 m/s, for various cases of aspect ratio AR = (a) 0.5, (b) 1.5 (c) 2.5.

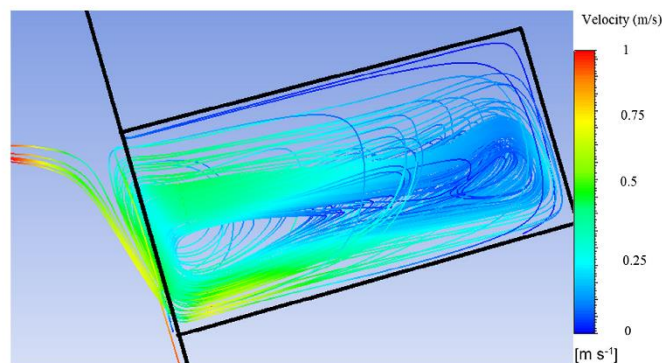


Fig. 13. Image of the streamlines of 10 seeded particles started from the centre of a cavity for a heated cavity with the wall temperature = 400 °C, tilt angle = 15°, aspect ratio = 2 and head on wind speed = 2 m/s.

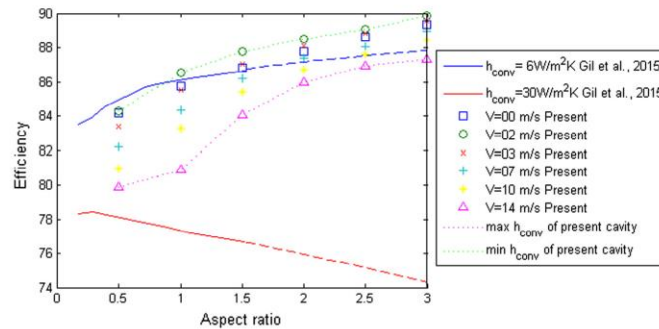


Fig. 14. Efficiency as a function of aspect ratio, as calculated both with the present and for a radiatively heated cavity by Gil et al. (2015) for a cavity with aperture radius = 10.13 cm and receiver radius = 15.98 cm for two values of assumed convective heat loss thermal transmittances to the air in the cavity. The solid lines represent their calculated data, which is available for aspect ratios = <1.5, while the dashed lines extrapolated. The data points and dotted lines represent are from the present work. The efficiency of the present study has been linearly interpolated using the corresponding aspect ratio and thermal transmittance for wind speeds from 0 to 14 m/s.

surface decreases with an increase in aspect ratio. This further explains why an increase in aspect ratio decreases the average convective heat transfer. That is, increasing the aspect ratio causes the temperature of the fluid that is recirculated over the surface to increase in temperature, reducing convective losses.

Fig. 11c indicates that the air close to the end of the cavity is above 350 °C, while Fig. 12c shows that the velocity of air there is less than 1 m/s. The combination of low velocity and high temperature is consistent with low convective heat losses from the rear of the cavity for aspect ratios greater than 2.5.

The streamlines in the flow, which were derived from ten hot particles seeded into the mid plane half way (backward and forward) along the length of the cavity for AR = 2 and wind speed = 2 m/s, is presented in Fig. 13. This provides further information of the recirculating hot air within the cavity. This can be attributed in part to the orientation of the chamber and in part by the role of buoyancy. It can be seen that the circulation is somewhat three dimensional, with a weak swirl generated in some locations. Furthermore, the same fluid has a long residence time, with some streamlines exhibiting many circulation before exiting from the cavity. A long residence time is consistent with a low convective heat loss. This mechanism provides a potential explanation for the reduction in convective heat loss for the introduction of a low velocity heat on wind speed of 2 m/s relative to the case of natural convection.

The absolute convective heat loss from a heated cavity increases with the aspect ratio due to the increase in total area of the heated surface. However, increasing aspect ratio at constant wall temperature corresponds to an increase in the total solar input to the cavity, which is different from an increase in aspect ratio with constant solar thermal input. Given the absence of experimental data on this topic, it is difficult to extrapolate the present findings to the case of aspect ratio with a constant solar input. Nevertheless, the effect of aspect ratio on efficiency can be assessed for the present cases.

It is instructive to compare the present results with those calculated previously for a radiatively heated cavity Gil et al. (2015). Fig. 14 presents the dependence of the efficiency on aspect ratio for both the present solar cavity receiver with uniform wall temperature and for the radiatively heated cavity receiver of Gil et al. for various assumed values of convective heat loss to the air that is induced into the cavity. The cavity thermal efficiency is defined as the ratio between energy transmitted to the engine working fluid and energy received from the concentrator. It can be seen that the present data agrees reasonably well with Gil et al.'s model for the case in which the assumed convective heat

transfer coefficient is 6 W/m² K, but disagrees with their case for which it is 30 W/m² K, which exhibits the opposite trend. There is large difference of efficiency for a cavity which has a great variation of convective heat transfer coefficient. Therefore this highlights the importance of correctly predicting the convective heat transfer coefficient. For reference, the range of convective heat transfer coefficients from the present study are 2.4 W/m² K to 23.2 W/m² K. For aspect ratio of 0.5, the range of convective heat transfer coefficients is 8.1–23.2 W/m² K with efficiency varying from 79.9 to 84.3%. For aspect ratio of 3.0, the range of convective heat transfer coefficients is 2.4–6.9 W/m² K with efficiency varying from 87.3 to 89.9%. It can be seen that the average efficiency of the cavity receiver is calculated to increase with aspect ratio. In addition, the effect of wind speed on the efficiency decrease with increasing the aspect ratio of a cavity. This provides further evidence for the advantages in efficiency of a longer cavity.

4. Conclusions

It has been found that, for the present scenario of uniform temperature of the cavity walls, a small increase in wind speed from zero reduces the combined convective heat loss below the value for the natural convection (i.e. a wind speed of zero). The “critical” value of wind speeds, below which heat loss is reduced below the case of natural convection is found to be at least 2 m/s for all cases and to increase with the aspect ratio. Furthermore, the higher the aspect ratio, the smaller is the effect of wind speed on the combined convective losses per unit area. This is, an increase in aspect ratio increases the shielding provided by the cavity. It was also found that there is a critical wind speed at which the variation of the combined convective heat loss is less than 2.5% over all the tested aspect ratios. At this wind speed of about 4 m/s, the combined convective heat loss from a heated cavity is nearly independent of the aspect ratio for aspect ratio greater than unity. However, the heat flux of the combined convective loss drops by approximately 74% when the aspect ratio is increased from 0.5 to 3 for a wind speed of 10 m/s. In short, the overall efficiency of a solar cavity receiver increases with the aspect ratio of the cavity for the conditions assessed here.

These trends are explained by the nature of the wind-induced flow-field, which is calculated to comprise a recirculating flow that moves to the back of the chamber along the lower wall and to recirculate along the upper wall. The direction of recirculation is broadly similar for the cases of natural and forced convection,

but the structure at the aperture plane is very different, explaining why the forced convection competes against the natural convection at low wind speeds. In addition, some three dimensionality occurs, with a weak swirl in some locations. The recirculation was found to induce a relatively long residence time that appears to increase with aspect ratio. This increase in residence time is a plausible explanation for the increased efficiency with aspect ratio. The general agreement with the model study of Gil et al. (2015) for the case of low convective heat transfer coefficient gives some confidence that these trends will also extend to the case with a radiatively heated cavity, although more work is required to quantify these effects.

The present work highlights the advantage of using even a short cavity in mitigating the deriving a benefit from a low velocity wind in competing against natural convection. Nevertheless, care should be taken in extrapolating the present results too far for practical solar receiver designs, since these typically have a higher temperature at the front of the receiver. Hence, while the trends may still apply, further work is required to better assess the case of non-uniform wall temperature profiles. In addition, the effects of wind, such as wind direction, turbulent intensity and the turbulent viscosity ratio also need to be assessed.

Acknowledgments

This research has been financed by the Australian Renewable Energy Agency (ARENA) and the University of Adelaide, through the Australian Solar Thermal Research Initiative (ASTRI), ARENA 1-SR1002. We would also like to acknowledge Dr. Amanullah Choudhry for editing this work. We also wish to acknowledge the valuable contributions from the anonymous reviewers.

References

- Asselineau, C.-A., Abbassi, E., Pye, J., 2014. Open cavity receiver geometry influence on radiative losses. In: Proceedings of Solar 2014, 52nd Annual Conference of the Australian Solar Energy Society, Solar 2014, ed., Melbourne, 2014.
- Ávila-Marín, A.L., 2011. Volumetric receivers in solar thermal power plants with central receiver system technology: a review. *Sol. Energy* 85 (5), 891–910.
- Clausing, A., 1981. An analysis of convective losses from cavity solar central receivers. *Sol. Energy* 27 (4), 295–300.
- Clausing, A., 1983. Convective losses from cavity solar receivers—comparisons between analytical predictions and experimental results. *J. Sol. Energy Eng.* 105 (1), 29–33.
- Collado, F.J., 2008. Quick evaluation of the annual heliostat field efficiency. *Sol. Energy* 82 (4), 379–384.
- Flesch, R., Stadler, H., Uhlrig, R., Pitz-Paal, R., 2014. Numerical analysis of the influence of inclination angle and wind on the heat losses of cavity receivers for solar thermal power towers. *Sol. Energy* 110, 427–437.
- Fluent, A., 2016. *FLUENT User's Guide 17.0*. Ansys Corporation.
- Gil, R., Monné, C., Bernal, N., Muñoz, M., Moreno, F., 2015. Thermal model of a dish stirring cavity-receiver. *Energies* 8 (2), 1042–1057.
- Ho, C.K., Iverson, B.D., 2014. Review of high-temperature central receiver designs for concentrating solar power. *Renew. Sustain. Energy Rev.* 29, 835–846.
- Holman, J., 1997. *Heat Transfer*. McGraw-Hill, New York.
- IEA-ETSAP, IRENA, 2013. *Concentrating Solar Power Technology Brief*.
- Koenig, A., Marvin, M., 1981. Convection Heat Loss Sensitivity in Open Cavity Solar Receivers. Final Report, DOE Contract No. EG77-C-04-3985, Department of Energy, Oak Ridge, Tennessee.
- Kolb, G.J., Ho, C.K., Mancini, T.R., Gary, J.A., 2011. Power Tower Technology Roadmap and Cost Reduction Plan. Sandia National Laboratories, Livermore, CA, Technical Report No. SAND2011-2419.
- Leibfried, U., Ortjohann, J., 1995. Convective heat loss from upward and downward-facing cavity solar receivers: measurements and calculations. *J. Sol. Energy Eng.* 117 (2), 75–84.
- Lovegrove, K., Watt, M., Passey, R., Pollock, G., Wyder, J., Dowse, J., 2012. Realising the Potential of Concentrating Solar Power in Australia: Summary for Stakeholders. Australian Solar Institute Pty, Limited.
- Ma, R.Y., 1993. Wind Effects on Convective Heat Loss From a Cavity Receiver for a Parabolic Concentrating Solar Collector. Sandia National Laboratories.
- McDonald, C.G., 1995. Heat Loss From An Open Cavity. Sandia National Labs., Albuquerque, NM (United States); California State Polytechnic Univ., Pomona, CA (United States). Coll. of Engineering.
- McIntosh, A., Hughes, G., Pye, J., 2014. Use of an Air Curtain to Reduce Heat Loss from an Inclined Open-Ended Cavity.
- Mills, A.F., 1999. *Basic Heat and Mass Transfer*. Prentice hall, Upper Saddle River, NJ.
- Paitoonsurikarn, Lovegrove, K., 2003. On the study of convection loss from open cavity receivers in solar paraboloidal dish applications. In: Proceedings of 41st Conference of the Australia and New Zealand Solar Energy Society (ANZSES), Melbourne, Australia.
- Paitoonsurikarn, S., Lovegrove, K., 2002. Numerical investigation of natural convection loss in cavity-type solar receivers. In: Proceedings of Solar.
- Paitoonsurikarn, S., Lovegrove, K., 2006. Effect of paraboloidal dish structure on the wind near a cavity receiver. In: Proceedings of the 44th Annual Conference of the Australian and New Zealand Solar Energy Society, Canberra.
- Paitoonsurikarn, S., Lovegrove, K., Hughes, G., Pye, J., 2011. Numerical investigation of natural convection loss from cavity receivers in solar dish applications. *J. Sol. Energy Eng.* 133 (2), 021004.
- Paitoonsurikarn, S., Taumofolau, T., Lovegrove, K., 2004. Estimation of convection loss from paraboloidal dish cavity receivers. In: Proceedings of 42nd conference of the Australia and New Zealand Solar Energy Society (ANZSES), Perth, Australia.
- Prakash, M., Kedare, S., Nayak, J., 2009. Investigations on heat losses from a solar cavity receiver. *Sol. Energy* 83 (2), 157–170.
- Price, H., 2003. Assessment of Parabolic Trough and Power Tower Solar Technology Cost and Performance Forecasts. Sargent & Lundy LLC Consulting Group, National Renewable Energy Laboratory, Golden, Colorado.
- Quere, P.L., Humphrey, J.A., Sherman, F.S., 1981. Numerical calculation of thermally driven two-dimensional unsteady laminar flow in cavities of rectangular cross section. *Numer. Heat Transf.* 4 (3), 249–283.
- Rockwell, D., Naudascher, E., 1978. Review—self-sustaining oscillations of flow past cavities. *J. Fluids Eng.* 100 (2), 152–165.
- Segal, A., Epstein, M., 2003. Optimized working temperatures of a solar central receiver. *Sol. Energy* 75 (6), 503–510.
- Shih, T.-H., Liou, W.W., Shabbir, A., Yang, Z., Zhu, J., 1995. A new k- ϵ eddy viscosity model for high Reynolds number turbulent flows. *Comput. Fluids* 24 (3), 227–238.
- Steinfeld, A., Schubnell, M., 1993. Optimum aperture size and operating temperature of a solar cavity-receiver. *Sol. Energy* 50 (1), 19–25.
- Stine, W.B., McDonald, C., 1989. Cavity receiver heat loss measurements. In: Proc. of ISES World Congress, Kobe, Japan.
- Tam, C.K., Block, P.J., 1978. On the tones and pressure oscillations induced by flow over rectangular cavities. *J. Fluid Mech.* 89 (02), 373–399.
- Taumofolau, T., Lovegrove, K., 2002. An experimental study of natural convection heat loss from a solar concentrator cavity receiver at varying orientation. In: Proceedings of Solar.
- Taumofolau, T., Paitoonsurikarn, S., Hughes, G., Lovegrove, K., 2004. Experimental investigation of natural convection heat loss from a model solar concentrator cavity receiver. *J. Sol. Energy Eng.* 126 (2), 801–807.
- Wei, X., Lu, Z., Wang, Z., Yu, W., Zhang, H., Yao, Z., 2010a. A new method for the design of the heliostat field layout for solar tower power plant. *Renew. Energy* 35 (9), 1970–1975.
- Wei, X., Lu, Z., Yu, W., Wang, Z., 2010b. A new code for the design and analysis of the heliostat field layout for power tower system. *Sol. Energy* 84 (4), 685–690.
- Wu, S.-Y., Xiao, L., Li, Y.-R., 2011. Effect of aperture position and size on natural convection heat loss of a solar heat-pipe receiver. *Appl. Therm. Eng.* 31 (14), 2787–2796.
- Xiao, L., Wu, S.-Y., Li, Y.-R., 2012. Numerical study on combined free-forced convection heat loss of solar cavity receiver under wind environments. *Int. J. Therm. Sci.* 60, 182–194.
- Yu, Q., Wang, Z., Xu, E., 2012. Simulation and analysis of the central cavity receiver's performance of solar thermal power tower plant. *Sol. Energy* 86 (1), 164–174.

CHAPTER 5

Experimental Investigation Of The Effects Of Wind Speed And Yaw Angle On Heat Losses From A Heated Cavity

Statement of Authorship

Title of Paper	Experimental investigation of the effects of wind speed and yaw angle on heat losses from a heated cavity
Publication Status	<input checked="" type="checkbox"/> Published <input type="checkbox"/> Accepted for Publication <input type="checkbox"/> Submitted for Publication <input type="checkbox"/> Unpublished and Unsubmitted work written in manuscript style
Publication Details	Lee, KL, Chinnici, A, Jafarian, M, Arjomandi, M, Dally, B & Nathan, G 'Experimental investigation of the effects of wind speed and yaw angle on heat losses from a heated cavity', Solar energy, (2018), vol. 165, pp. 178-188.

Principal Author

Name of Principal Author (Candidate)	Ka Lok Lee		
Contribution to the Paper	Developed the experiment, performed analysis on all data, interpreted data, wrote manuscript and acted as corresponding author.		
Overall percentage (%)	60%		
Certification:	This paper reports on original research I conducted during the period of my Higher Degree by Research candidature and is not subject to any obligations or contractual agreements with a third party that would constrain its inclusion in this thesis. I am the primary author of this paper.		
Signature		Date	29/06/2018

Co-Author Contributions

By signing the Statement of Authorship, each author certifies that:

- i. the candidate's stated contribution to the publication is accurate (as detailed above);
- ii. permission is granted for the candidate to include the publication in the thesis; and
- iii. the sum of all co-author contributions is equal to 100% less the candidate's stated contribution.

Name of Co-Author	Alfonso Chinnici		
Contribution to the Paper	Supervised development of the work , helped to evaluate and edit the manuscript		
Signature		Date	03/07/18

Name of Co-Author	Mehdi Jafarian		
Contribution to the Paper	Supervised development of the work , helped to evaluate the manuscript		
Signature		Date	02.07.2018.

CHAPTER 5

Name of Co-Author	Maziar Arjomandi		
Contribution to the Paper	Supervised development of the work , helped to evaluate the manuscript		
Signature		Date	2/07/2018

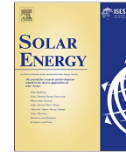
Name of Co-Author	Bassam Dally .		
Contribution to the Paper	Supervised development of the work , helped to evaluate and edit the manuscript		
Signature		Date	2-07-2018

Name of Co-Author	Graham Jerrold Nathan		
Contribution to the Paper	Supervised development of the work , helped to evaluate and edit the manuscript		
Signature		Date	3/7/18



Contents lists available at ScienceDirect

Solar Energy

journal homepage: www.elsevier.com/locate/solener

Experimental investigation of the effects of wind speed and yaw angle on heat losses from a heated cavity



Ka Lok Lee^{*}, Alfonso Chinnici, Mehdi Jafarian, Maziar Arjomandi, Bassam Dally, Graham Nathan

School of Mechanical Engineering, The University of Adelaide, SA 5005, Australia

ARTICLE INFO

Keywords:
Solar receiver
Solar thermal power
Heat loss
Concentrated solar thermal
Temperature distribution
Wind

ABSTRACT

An experimental investigation of the effects of wind speed (0–12 m/s) and yaw angle (0°–90°) on the convective heat losses from a cylindrical cavity heated with a uniform wall temperature, is presented. The cavity is heated with 16 individually controlled copper surface elements, so that both the heat losses and the heat flux distribution can be measured and subjected to a controlled convective environment in the open section of a wind tunnel. It was found that the convective heat losses through the aperture are ~4 times greater for the head-on wind case than for the side-on wind case, when the inverse of Richardson number ($1/Ri$) > 77 (wind speed > 12 m/s). For the no-wind condition, ~85% of the heat was lost from the lower half of the surface of the cavity, while for $1/Ri > 43$ (wind speed > 9 m/s), the heat loss was more uniformly distributed over the surface of the cavity. For head-on-wind conditions and for $1/Ri > 19$ (wind speeds > 6 m/s), the convective heat losses are ~2 times greater than for side-wind conditions. The correlations between the mixed (natural and forced) convective heat losses, Nusselt number and Richardson number are also reported.

1. Introduction

Solar thermal power is expected to play an important role in the mix of power generators of the future owing to the growing development of thermal energy storage technology, which has a low-cost relative to electrical energy storage counterparts (Kolb et al., 2011; Philibert, 2010; Tanaka, 2010). Solar thermal power plants typically use a receiver to transfer the energy of the highly concentrated solar radiation to a heat transfer medium, such as fluid, which is then transferred to storage and then to the working fluid of a power cycle. Recent research has sought to develop systems to achieve higher operating temperatures than are commercially, since higher temperatures will enable a higher power generation efficiency, larger solar power plants and an anticipated further reduction in cost (Ávila-Marín, 2011; IEA-ETSAP and IRENA, 2013; Jafarian et al., 2013; Lovegrove et al., 2012; Price, 2003; Segal and Epstein, 2003; Steinfeld and Schubnell, 1993). One of the challenges to be overcome to enable higher temperatures of the solar receiver is to decrease the heat losses from the solar receiver, since heat losses also increase with the temperature. However, the underlying mechanisms that control the heat losses from a receiver are highly complex and remain poorly understood. Hence, there is a need to further increase the understanding of the mechanisms of heat loss from solar receivers.

Solar cavity receivers are one class of geometric configurations being developed for solar thermal systems. Previous studies have shown that cavity receivers are the most suitable configuration for high temperature receivers, owing to their radiation losses being lower than for surround-field or billboard receivers. This is significant because of the above-mentioned trend in research to develop solar thermal system to operate at higher temperatures (Collado, 2008; Segal and Epstein, 2003). The mechanisms controlling heat losses from a solar receiver are complex, comprising both radiative and convective components through the walls and aperture, which are linked by conductive heat transfer through insulated walls. Conductive and radiative heat losses can be estimated analytically using a typical wall temperature of the cavity, emissivity and absorptivity, shape factors and the properties of the insulation material (Holman, 1997; Mills, 1999). However, the convective heat losses are more difficult to estimate due to the complexity of both the temperature and flow fields inside and around the cavity. Importantly, convective losses can be expected to be significant in windy sites because cavity receivers are typically mounted on a tower, where wind speed is higher than on the ground due to the shape of the atmospheric boundary layer. However, these effects are yet to be assessed systematically and very little experimental data are available in the literature. Therefore, the primary objective of the present work is to advance understanding of the convective heat loss mechanisms from

^{*} Corresponding author.

E-mail addresses: ka.lee@adelaide.edu.au (K.L. Lee), alfonso.chinnici@adelaide.edu.au (A. Chinnici), mehdi.jafarian@adelaide.edu.au (M. Jafarian), maziar.arjomandi@adelaide.edu.au (M. Arjomandi), bassam.dally@adelaide.edu.au (B. Dally), graham.nathan@adelaide.edu.au (G. Nathan).

<https://doi.org/10.1016/j.solener.2018.03.023>

Received 14 November 2017; Received in revised form 4 March 2018; Accepted 9 March 2018
0038-092X/ © 2018 Published by Elsevier Ltd.

Nomenclature			
Symbols		<i>Ri</i>	Richardson number = $\frac{Gr}{Re^2} = \frac{g\beta(T_{wall} - T_0)D_{cav}}{\nu^2}$
<i>A</i>	area (m ²)	<i>T</i>	temperature (°C)
β	coefficient of thermal expansion (°C ⁻¹)	<i>V</i>	wind speed (m/s)
<i>D</i>	diameter (m)	ν	kinematic viscosity of air at reference temperature kg/(sm)
ϵ	emissivity coefficient of the internal wall surface	α	yaw angle or incoming wind direction (°)
<i>g</i>	gravity (m/s ²)	ϕ	tilt angle of the cavity (°)
<i>Gr</i>	Grashof number = $\frac{g\beta(T_{wall} - T_0)D_{cav}^3}{\nu^2}$	Subscript	
<i>h_c</i>	convective heat transfer coefficient through the aperture (W/(m ² K))	<i>a</i>	ambient
<i>k</i>	thermal conductivity of air at reference temperature (W/(m K))	<i>as</i>	aspect
<i>L</i>	length (m)	<i>ap</i>	aperture
\overline{Nu}	mean Nusselt number = $\frac{h_c D_{cav}}{k_{ref}}$	<i>cav</i>	cavity
<i>Q</i>	heat loss (W)	<i>conv</i>	convection
<i>R</i>	Ratio	<i>rad</i>	radiation
<i>Re</i>	Reynolds number = $\frac{VD_{cav}}{\nu}$	<i>ref</i>	reference
		<i>tot</i>	total
		<i>w</i>	wall

a solar cavity receiver as a function of wind direction and speed.

Convective heat losses from heated solar cavities were first studied by Clausing (1981), who found that the convective flow pattern in a heated cavity receiver can be divided into two zones, which are the stagnant and the convective zones. The stagnant zone means that, the air in that region move very slow due to the trapped hot air in the upper part of the cavity. On the other hand, air moves quickly in the lower part of the cavity when compared to the air in the stagnant zone. Therefore the heat transfer coefficient is higher in the convective zone than the stagnant zone. Ma (1993) was the first to present detailed experimental data for combined convective heat loss from a hot heat transfer fluid (Syltherm@ 800, Dow Coming) within a heated cylindrical receiver to a temperature of ~277 °C and a wind speed up of to 8.9 m/s. He reported that wind directions normal to the axis (side-on wind) have a greater impact on the convective heat loss than those parallel to the axis (head-on wind). More recently, Flesch et al. (2015) reported that, for some conditions, the minimum convective heat losses can occur at an intermediate wind speed, so that a low wind speed can reduce the losses to below that of natural convection. A low temperature cavity is placed in a cold wind tunnel to have a similar Reynolds number of a large scale solar cavity receiver. A similar experimental approach was used in the present study with a much wider range of temperatures. This study also found that a side-on wind has a greater impact on the heat loss than does a head-on wind. In the following year, a CFD simulation was performed, and it reported similar findings to those measured experimentally (Jafarian et al., 2013). However, the results from the CFD model are about 20–25% lower than the experiment, which may be due to the fact that the boundary conditions of the

CFD model are difference to the experiment, such as wall temperature and hence heat fluxes. Also worth noting, is that the effect of side-on wind is stronger than head-on wind only for cases tilt angle larger than 30°. Therefore the tilt angle may also be one of the parameters when assessing the effect of yaw angle. In contrast, the study by Prakash et al. (2009) found that a head-on wind generates greater convective heat losses from a cylindrical cavity receiver than does a side-on wind. Another recent study found that there is no simple rule to describe the influence of wind yaw angle reliably (Wu et al., 2015). However, a reduction in the effect of yaw angle on convective losses was measured at wind speeds of ~5.7 m/s, relative to a lower wind speed. This apparently contradictory mix of information shows that the effect of yaw angle on the convective heat loss from a solar cavity receiver is not fully understood. The summary of the tested key parameters, methods and findings for previously measured combinations of forced and free convective heat loss from the heated cavities are shown in Tables 1 and 2. Importantly, for each of these measurements, only the total heat loss from the system is reported. Other details about the flow are not available.

The convective heat losses from cavity receivers have also been investigated numerically, both for natural convection (Paitoonsurikarn and Lovegrove, 2002; Paitoonsurikarn et al., 2011; Wu et al., 2011) and for mixed convection (Flesch et al., 2014; Hu et al., 2017; Lee et al., 2017; Paitoonsurikarn and Lovegrove, 2003; Xiao et al., 2012). Despite their value, these numerical studies have only been partially validated due to the lack of experimental data. As can be seen from Table 1, the provision of only single value of total convective heat loss is insufficient for reliable model validation.

Table 1
List of key operating conditions and measured parameters for the experimental studies combined forced and free convective heat loss from heated cavities.

Studies	Wall temperature T_w (°C)	Wind speed <i>V</i> (m/s)	Diameter of cavity D_{cav} (m)	Diameter of aperture D_{ap} (m)	R_{as}	R_{ap}	Re	$\frac{1}{Ri}$	Tilt angle ϕ (°)	Yaw angle α (°)	Blockage ratio
Ma (1993)	277	0, 2.7, 3.6 and 8.9	0.66	0.46	1.05	0.70	2.08×10^5	0–20.1	0, 30, 60 and 90	0 and 90	36%
Prakash et al. (2009)	75	0, 1 and 3	0.33	0.33	1.52	1.00	5.04×10^4	0–16.2	0, 30, 45, 60 and 90	0 and 90	22%
Wu et al. (2015)	39–128	1.15, 1.84, 2.94 and 5.69	0.105	0.105	1.82	1.00	3.18×10^4	0–101	0, 15, 30, 45, 60, 75 and 90	0, 15, 30, 45, 60, 75 and 90	58%
Flesch et al. (2015)	60.4	0, 1, 3, 5 and 7	0.66	0.36	1.11	0.55	5.20×10^5	0–7.02	0, 30, 60 and 90	0, 30, 60, 90, 135 and 180	N/A
Present	100, 150, 200, 300 and 400	0, 3, 4, 6, 9 and 12	0.3	0.15	1.50	0.50	8.78×10^4	0–204	15	0, 22.5, 45, 77.5 and 90	4.1%

Table 2
List of the various methods and findings from experimental studies for combined forced and free convective heat loss from heated cavities.

Studies	Heating method	Measuring method	Convective heat loss power	Heat flux	Wind tunnel type	Which wind direction have a greater impact on the heat loss
Ma (1993)	Hot pipe heated by Sytherm@ 800, Dow Corning	Calculated overall receiver heat loss based on the measured temperature drop of the heat transfer fluid	Yes	N/A	1.2 × 1.2 m wind tunnel	Side-on wind
Prakash et al. (2009)	Hot pipe heated by water	Calculated overall receiver heat loss based on the measured temperature drop of the heat transfer fluid	Yes	N/A	0.6 m circular blower tunnel	Head-on
Wu et al. (2015)	Two electric heating circuits (constant heat flux) without any power controller	$Q_{conv} = Q_{total} - Q_{rad} - Q_{cond}$, where Q_{total} is constant and Q_{rad} and Q_{cond} is estimated using the measured temperature data on the receiver	Yes	N/A	~0.3 m circular blower tunnel	The impact of wind yaw angle is very small
Flesch et al. (2015)	5 electric heating circuits with one power controller to maintain at an average temperature	$Q_{conv} = Q_{total} - Q_{rad} - Q_{cond}$, conductive losses is measured when the aperture opening was blocked with a cover. The radiative losses are calculated with a simple view factor approach with assuming same temperature for all inner surfaces	Yes	5 sections	Cryogenic wind tunnel at -173 °C	Side-on wind
Present	16 electric heating circuits with 16 individual power controllers to maintain all 16 heated surfaces at the set temperature	See Section 2 Method	Yes	16 sections	Open section of a wind tunnel with incoming wind size 2.5 m × 2.5 m	Gaps Whether the head-on or side-on wind speed have larger impact Whether the impact of wind yaw angle is large or small

Moreover, most of the previous experiments of heat transfer were performed with only a single temperature controller for the entire internal surface (Table 2). This makes it impossible to achieve a truly uniform internal temperature distribution because the heat transfer across the entire surface is controlled to a single temperature set-point, even though it varies locally. As a result, it is difficult to reliably validate numerical models with existing data because previous validations were typically done with the assumption of a uniform internal wall temperature (Flesch et al., 2014; Hu et al., 2017; Lee et al., 2017; Paitoonsurikarn et al., 2004; Wu et al., 2011; Xiao et al., 2012). Therefore, there is a need for new experimental data that more accurately reproduces a uniform internal wall temperature for the development and validation of numerical models.

In light of the above gaps in understanding and in available data, the principle objective of the present investigation is to provide direct measurements of the influence of wind speed and yaw angle on the mixed convection heat losses from a heated cavity receiver with uniform wall temperature. In addition, we aim to resolve the following questions: (1) whether heat flux increases or decrease with yaw angle; (2) how the yaw angle influences the contribution of convective heat losses to total heat losses; (3) how wind speed and yaw angle influence the distribution of heat flux within the cavity; and (4) the relative significance of buoyancy and inertial forces on the convective heat losses from the cavity.

2. Methodology

The experimental arrangement is shown in Fig. 1a. An electrically heated cavity is placed within the open section of the wind tunnel at the University of Adelaide’s Thebarton laboratory to provide well controlled variation in wind speed with air as the working fluid. The wind velocities were measured using Cobra Probe with Turbulent Flow Instrumentation (Chen et al., 2000). The average wind velocities were used in the test location for the testing. The projected area of the external dimensions area of the cavity (~0.249 m²) is ~4.1% of the cross-sectional dimensions area of the wind tunnel (2.75 m × 2.19 m), which is also ~330 times larger than the cross-section area of the aperture (~0.018 m²) to provide uniform flow around the cavity. Moreover, since the cavity is placed in the open section of the wind tunnel, the effect of blockage is even lower. The main dimensions of the cavity are shown in Fig. 1b). The cavity has an inner diameter of 0.3 m with $R_{as} = 1.5$ and $R_{ap} = 0.5$. The internal walls of the cavity are made from copper, because of its high thermal conductivity and operating temperature. This was surrounded by with 40 mm of mineral fibre insulation, which is made from melted rock (known as Rockwool) and an outer layer of aluminium foil to reduce conductive heat loss from the sides and end of the cavity.

The internal surface was lined with 16 segments of heating elements that are each individually controlled. They are also made from copper to provide high conductivity, as shown in Figs. 1 and 2. The photos of the experimental setup in the wind tunnel are also shown in Fig. 3. These segments are arranged to comprise 6 annular rings of 12 heaters, each covering a 180° arc along the length of the chamber to measure separately the upper and lower half, together with another 4 circumferential rings on the back wall. Each heater is controlled with a feedback controller, which controls the set-point temperature to the desired value and records the power to do so. Mica insulators are used to minimise the conductive heat transfer between each heater. Thermocouples are attached to each copper wall surface to measure its temperature, which is assumed to be uniform due to the high thermal conductivity of copper. The thermocouples which were used in this study are K – type with washer/ring attachment to attach to the copper surface. The temperature is recorded by Datalogger DT85. They are also used for the temperature feedback control system using Matlab and Simulink. The output power signal from the computer is converted into DMX signal by Arduino, then control by the DMX lighting system power

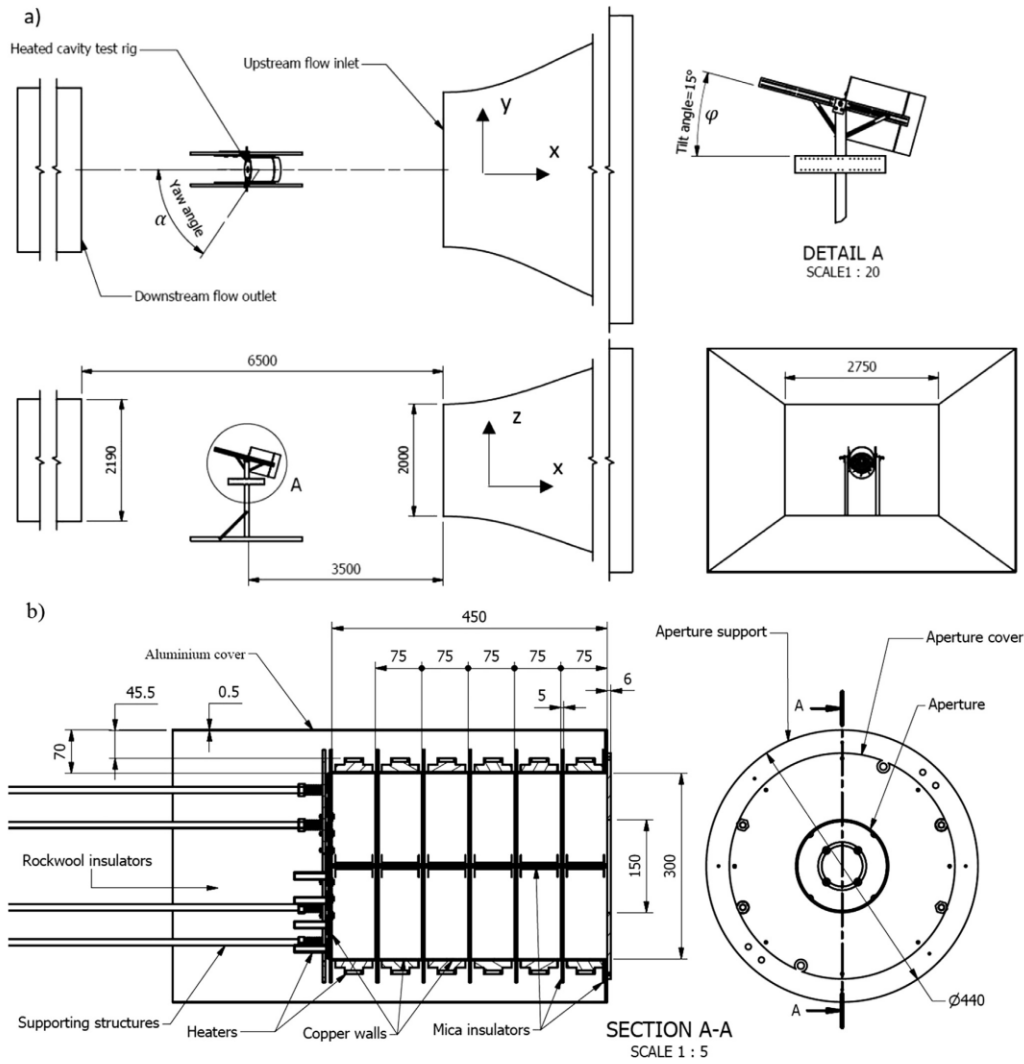


Fig. 1. Schematic diagram of (a) the heated cavity in the Thebarton wind tunnel and (b) the detail of the receiver.

controllers. The steady-state power required to maintain the system at the set point temperature is measured and to provide a measure of the total heat loss from the system. Stead-state is considered to have been reached when the following conditions are met for 300 s: (1) the variation of each measured temperature is below ± 0.5 °C; and (2) the variation of total heat loss is less than $\pm 5\%$ of the total power required for that condition if the total heat loss is above 2 kW or ± 100 W if the power is below 2 kW.

The individual components of convective and radiative heat losses from the receiver are isolated in a series of steps. First the radiative heat loss is determined, because it is independent of the cavity's orientation. This was performed with the cavity oriented vertically downward ($\varphi = 90^\circ$), because this position minimises convective heat loss. The total heat losses were measured both with aperture to the cavity opened and closed. The power loss for the aperture closed corresponds to the

wall losses Q_{wall} . After that, the aperture was opened and the total power loss Q_{total} was recorded again. The difference between the opened and closed aperture cases yields the heat loss through the aperture

$$Q_{aper} = Q_{total} - Q_{wall} = Q_{rad} + Q_{conv} \quad (1)$$

These measurements were performed for a series of temperatures from 100 °C to 400 °C.

A Medtherm 64 series gauge (Medtherm, 2000) was used to measure the direct radiative heat loss through the aperture. The convective heat loss through the aperture Q_{conv} was then determined by subtraction. A cross check was performed using the different proportionality constant for radiation, which scales with ΔT^4 , while convection scales with ΔT following previous works (Holman, 1997; Siegel, 2001).

Internal wall temperature, wind yaw angle ($\alpha = 0-90^\circ$) and wind speed ($V = 0-12$ m/s) were varied in this study. The internal wall

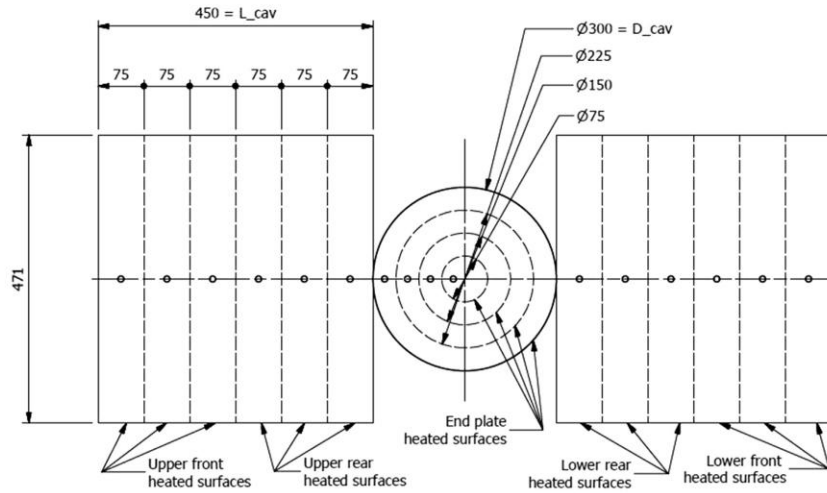


Fig. 2. Schematic diagram of the simplified configuration of the internal copper wall surface of the heated cavity (shown unrolled view). The thermocouples are shown as circular symbols.

temperature was varied over the 100–400 °C. Only one tilt angle of 15° downward was employed because this parameter has already been assessed numerically (Flesch et al., 2014; Wu et al., 2015, 2011), it is not repeated in this study. Instead a total of 108 combinations of wind speed, orientation and wall temperature were tested, the details of which are shown in Table 3. Of these, were 54 conditions were for an

opened heated cavity to measure the convective heat losses, and the other 54 for the corresponding closed aperture to measure the reference heat loss through the walls.

The temperature of each heated copper surface was individually measured and controlled, which allows the heating power of each individual surface to be recorded. This, in turn, allow the heat flux

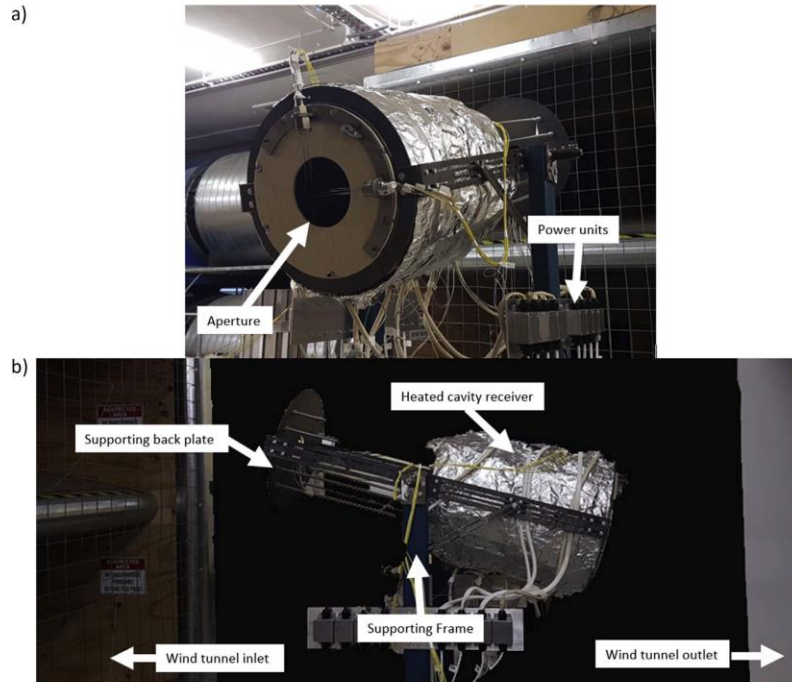


Fig. 3. Photos of the heated cavity in Thebarton wind tunnel.

Table 3
List of experimental conditions.

Velocity (V)	Yaw angle (α)	Tilt angle (φ)	Temperature of the wall (T_w)	Aspect ratio ($\frac{L_{cav}}{D_{cav}}$)	Aperture ratio ($\frac{D_{ap}}{D_{cav}}$)
0	0	90	100, 200, 300 and 400	1.5	0 and 0.5
0, 3, 6, 9 and 12	0	15	100, 150, 200, 300 and 400	1.5	0 and 0.5
0, 3, 6, 9 and 12	0, 22.5, 45, 77.5 and 90	15	300	1.5	0 and 0.5

distribution within the cavity to be measured.

The inverse Richardson number was selected as the key dimensionless parameter that accommodated the effect of scale, wind speed and temperature difference on the relative roles of the buoyancy and inertia forces. This study will cover a large range of inverse of Richardson numbers, which enables the finding from this study to not only apply to a single equivalent scaled cavity, but to a large range of scaled cavity depending on the operating temperature and cavity size. In the present investigation, we varied only the wind speed and the temperature difference and did not change the physical scale of the cavity. These variations were performed with the cavity aligned head-on to the wind, because wind speed has the greatest impact on the heat losses for this orientation. The inverse of Richardson number $1/Ri$ can be expressed as a combination of the Grashof and Reynolds numbers, shown in Eq. (2).

$$1/Ri = \frac{\text{Flow shear term}}{\text{Buoyancy term}} = \frac{Re^2}{Gr} = \frac{V^2}{g\beta(T_w - T_a)D_{cav}} \quad (2)$$

Typically, a heated surface is dominated by natural convection for $Ri < 0.1$, and by forced convection for $Ri > 10$, while both are important for $0.1 < Ri < 10$ (Huhn, 2006). However, this range is used as a reference only and it might vary with conditions.

The mean Nusselt number \overline{Nu} was calculated as follow:

$$\overline{Nu} = \frac{\text{total heat transfer}}{\text{conductive heat transfer}} = \frac{Q_{conv}D_{cav}}{A_{total,cav}(T_{wall} - T_a)k_{ref}} \quad (3)$$

where the total inner surface area $A_{total,cav} = 0.495 \text{ m}^2$ and conductivity at the reference temperature are a function of reference temperature T_{ref} , which is defined as

$$T_{ref} = \frac{T_{wall}}{2} + \frac{T_a}{2} \quad (4)$$

The cavity is heated with 16 by the heaters, each of which has a maximum output power of 800 W. The maximum uncertainty of each heater is $\pm 25 \text{ W}$ ($\sim 3.1\%$), which includes the uncertainty from the power and temperature measuring instrument, the variation in the measured temperature for each steady-state condition, and the influence of the feedback controller.

3. Results

The influence of internal wall temperature on the heat losses from a downward facing heated cavity is shown in Fig. 4. The total losses, as measured for both cases with the aperture opened and closed, are shown Fig. 4a. The difference between them corresponds to the sum of

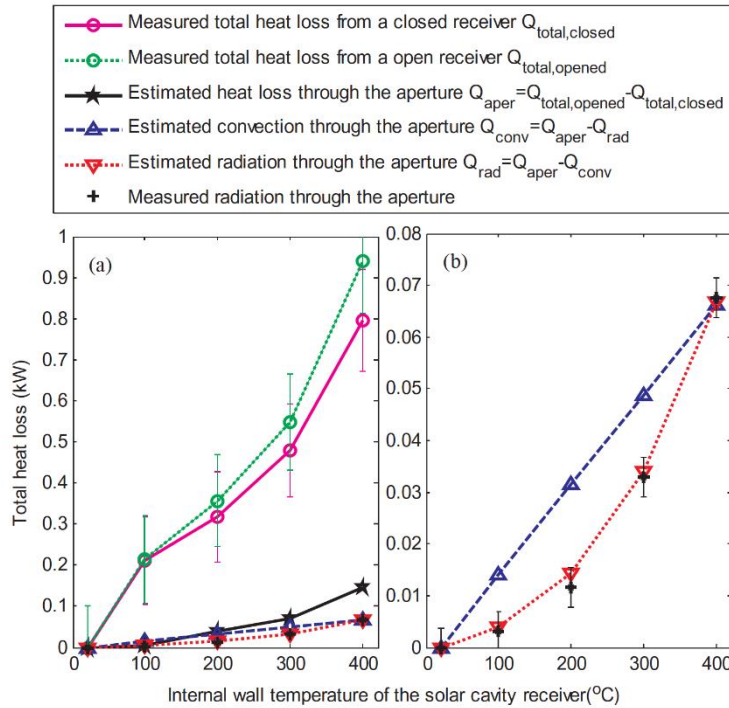


Fig. 4. Variation of heat loss from the system with the internal wall temperature of a downward facing solar cavity receiver with the tested condition shown in test 1 in Table 3: (a) scaled from 0 to 1 kW (b) scaled from 0 to 0.08 kW.

the convective and radiative heat losses through the aperture. The details of the convective and radiative heat losses through the aperture are shown in Fig. 4b. The radiative heat losses are measured directly with the Infrared radiometer. Additionally, the proportions of the heat losses through the aperture are also estimated using their relationship to temperature, which is proportional to the surface temperature for convective heat loss and temperature to the fourth power for radiative heat loss. The emissivity coefficient ϵ of the internal wall surface are found to be approximately 0.34. The radiation heat losses from both methods agreed with each other to within 8% of the heat loss through the aperture for the corresponding temperature, shown in Fig. 4b. Since the radiative heat loss depends only on the surface wall temperature here, it is constant for a given wall temperature across all conditions. This allows the convective heat losses to be determined for the other conditions, such as variations in the angle of tilt and yaw and the wind speed. For no wind condition, convective heat losses are higher than radiation heat losses for temperatures below 400 °C, however their values are similar at 400 °C and radiation is expected to dominate for high temperatures. Nevertheless, convective heat losses are also very important for high temperature condition, especially for high wind speed location.

The influence of wind speed on the convective heat losses from the heated cavity is presented in Fig. 5a for various values of internal wall temperature and for the case $\alpha = 0^\circ$, $\varphi = 15^\circ$, $R_{as} = 1.5$ and $R_{ap} = 0.5$ with maximum error of approximately $\pm 3\%$. It can be seen that the convective heat losses increase with both the wind speed and with cavity temperature, which is consistent with expectation. However, the influence of wind speed on convective losses is weak below 3 m/s, so that convective heat loss is almost independent of wind speed for these conditions. The influence of wind speed on convective heat loss increases above ~ 6 m/s. This shows that forced convection starts to dominate above that wind speed. The influence of wind speed on the ratio between the convective and radiative heat losses, through the aperture and for various values of the internal wall temperature is shown in Fig. 5b. The ratio of radiative to convective heat losses is strongly dependent on the internal temperature, because radiative heat loss is a function of temperature to the power of 4. However, for a constant temperature the radiative losses are constant. So that the wind speed only influences the convection losses. It can be seen from Fig. 4 that, the effect of temperature on the convective heat loss is linear, and

that informed the analytical calculations of convective heat loss. Also worth noting is that, the symbols represent the measured data in the experiment, and the lines represent the analytically calculated results by assuming a solar cavity receiver with emissivity coefficient $\epsilon = 0.34$, which is estimated emissivity coefficient from the experiment.

The influence of inverse Richardson number and wind speed on the convective heat losses is shown in Fig. 6 for various values of wind yaw angle and for a cavity temperature of 300 °C, a tilt of 15°, an aspect ratio of 1.5 and aperture ratio of 0.5. The effect of yaw angle on the convective heat losses from a heated cavity can be divided into 3 regions of yaw angles for low inverse of Richardson number ($1/Ri < 8.53$), i.e. $V < 4$ m/s, namely:

- For small yaw angle ($\alpha < 22.5^\circ$), the mixed convective heat losses are higher than the natural convective heat losses (which occurs at 0 m/s);
- For medium yaw angle ($\alpha \sim 45^\circ$), the mixed convective heat losses are similar to the natural convective heat losses; and
- For large yaw angle ($\alpha > 77.5^\circ$), the mixed convective heat losses are lower than the natural convective heat losses.

The role of yaw angle is shown in Fig. 6b. It can be seen that increasing the yaw angle acts to push the flow back toward the natural convection regime. This implies that large yaw angle inhibit the transport of gas through the aperture. It might also increase the size of the stagnant zone. As wind speed increases, more air flow into the cavity, hence it increase the size of convective zone in the cavity, which also increase the heat transfer coefficient. For $\frac{1}{Ri} > 19$ (wind speeds > 6 m/s), its influence on convection can be divided into three regimes. For large yaw angle ($> 77.5^\circ$) the mixed convective heat transfer is approximately $\frac{1}{4}$ of that for small yaw angle ($< 22.5^\circ$) while for medium yaw angle ($\sim 45^\circ$) it is approximately $\frac{1}{2}$ of that for small yaw angle, as seen in Fig. 6a. Such change is because high wind speed increases the size of the convective zone leading to the increase in heat losses. Moreover, a sharp decline in heat loss is noticeable when the yaw angle is varied from 22.5° to 45° . That is, head-on wind enhances mixing between hot and cold air in the heated cavity, while side-on wind inhibits it.

The experimental data is also compared with 2 types of equations to characterise the effect of wind speed and yaw angle on the convective

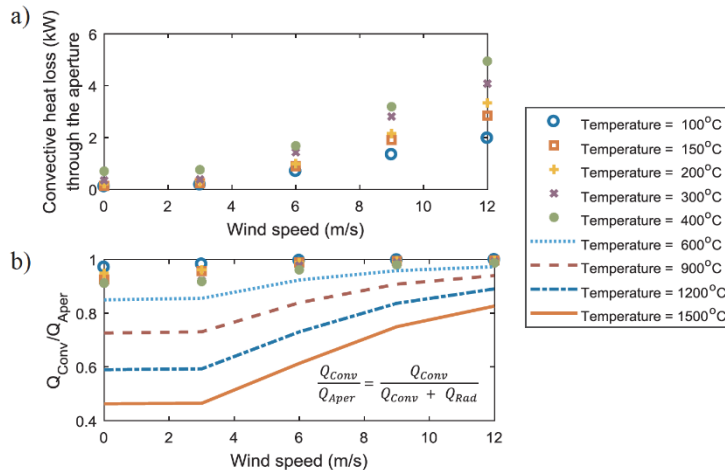


Fig. 5. Variation of (a) the convective heat loss and (b) Q_{Conv}/Q_{Total} through the aperture as a function of wind speeds for a series of uniform wall temperatures. Other conditions: yaw of 0°, tilt of 15°, aspect ratio of 1.5 and aperture ratio of 0.5. The symbols correspond to measurements, while the lines are calculated analytically with the equation shown, assuming a solar cavity receiver with emissivity coefficient $\epsilon = 0.34$.

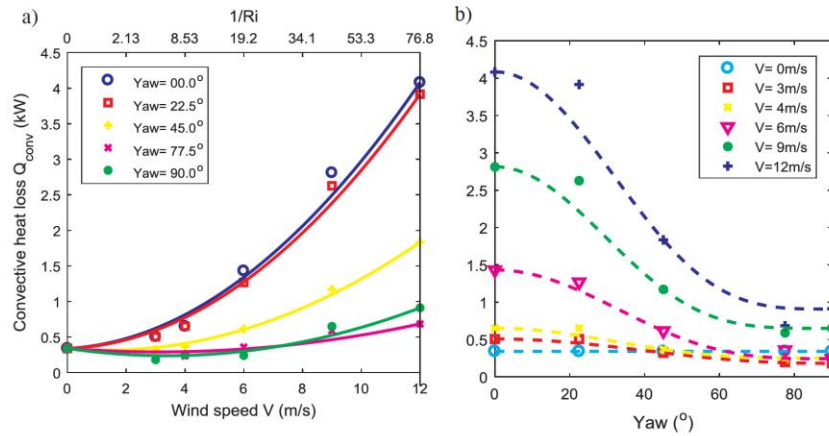


Fig. 6. Variation of the convective heat losses through the aperture with wind speeds for various values yaw angle. For the case with: wall temperature of 300 °C, tilt of 15°, aspect ratio of 1.5 and aperture ratio of 0.5.

heat losses. A second order polynomial function was used for the effect of wind speed and a cosine function for the effect of yaw angle. The coefficients for these functions are displayed in Tables 4 and 5.

The experimental results in this study shows that the convective heat losses are highest for head-on winds ($\alpha \sim 0$). This finding is in agreement with the study of Prakash et al., 2009, who experimented on a cavity with similar aspect ratio and diameter. Nonetheless, our results do not agree with other studies in the literature. While it is hard to ascertain the exact reason for the differences. It appears that geometry and aperture size play an important role. For example, the geometry in the paper by Prakash et al., 2009 incorporate a heated pipe outside the cavity and the cavity in Wu et al., 2015 do not have an aperture. Those variations in aperture shape change the flow around the cavity, and appear to have impact of the findings. Therefore a very simple geometry is used in this study in order to make the outcomes as generic as possible. On the operating range side, Ma, 1993 and Flesch et al., 2015, for example, have reported a much lower inverse of Richardson number in their study as compared to the current study.

Nonetheless, most studies seems to agree that side-on winds have greater effect on heat losses, and for aspect ratios less than 1.1. While cavities with aspect ratio larger than 1.5 it is found that, head-on winds have the greater impact. It is worth noting, is that size of the cavity have a huge impact on the mixed convective heat losses, as it will also vary the turbulence lever, absolute Grashof number and Reynolds number and hence it is not possible to match the conditions of all these studies. Therefore the inverse of Richardson number, which related to the Grashof number and Reynolds number, is used in this study instead.

The distribution of heat loss from the various sections of the heated cavity is presented in Fig. 7. It can be seen that approximately 88% of the convective heat loss is from the lower surface of the heated cavity for a wind speed of 0 m/s. This is quantifies the extent to which natural convection dominates under this condition. Less than 7% of the heat is lost from the upper part of the cavity and less than 1% from the upper rear of the cavity receiver.

As $1/Ri$ is increased to ~ 8 ($V \sim 4$ m/s), the total convective heat loss increases by a factor of approximately 2 and the distribution changes. In addition, the heat loss from lower half of the chamber is approximately double that from the upper half of the chamber. The total convective heat loss from the lower half surface is decreased from 88% to 65%. This shows that natural convection and forced convection (buoyancy and inertial) are both important and the heat losses are in the combined convection mode. In addition the proportion of heat lost

from the upper and end surfaces increases as yaw angle is increased from 0° to 45° , but decreases again as yaw is increased further to 90° .

For higher $1/Ri \sim 40$ (wind speed ~ 9 m/s), the total heat loss is increased by a factor of approximately seven relatively to the zero-wind speed case and the distribution is much more uniform. Approximately, 45% of the total losses occur from the lower surfaces, a loss that is similar to that from the upper surfaces ($\sim 40\%$). Clearly the mode of inertial/ forced convection dominates for this wind speed. The total heat loss from the heated cavity decreases by $\sim 50\%$ and $\sim 75\%$ by increasing the yaw angle from 0° to 90° for $1/Ri = 8$ and 40 (wind speed = 4 and 9 m/s), respectively.

For high wind speed, the heat loss distribution for different sections of the cavity are similar. This is due to the high velocity in the cavity to carry the cool air in and hot air out much faster than the no wind conditions. Therefore the temperature distribution inside a heated cavity under very windy condition is small. This was also shown in the study of (Lee et al., 2017). Therefore the effect of stagnant and convective zone disappears and only the convective zone within the cavity in this case, hence the contribution of the heat losses from difference section are similar.

The absolute distribution of heat loss from the various sections of the heated cavity for all $1/Ri$ is presented in Fig. 8, with the fractional distribution presented in Fig. 7. The total heat losses do not change greatly for $1/Ri$ below 4.8 (wind speeds below 3 m/s), although the distribution does. While approximately 57% of the power is lost from the lower front section of the heated cavity at 0 m/s, an increase in wind speed to 3 m/s reduces their heat loss to below 50%. It also causes an additional $\sim 10\%$ more heat to be lost from the lower rear and upper front sections. For wind speed above 6 m/s ($1/Ri > 19$), the heat loss from the lower front section drops sharply from approximately 57% to 30%. For $1/Ri$ between 43 and 77 (wind speeds between 9 m/s and 12 m/s), the distribution of heat loss is independent of wind speed to

Table 4

List of coefficients of the functions used for the lines of best fit in Fig. 6a.

$Q_{conv} = a_i \times (V + b_i)^2 + c_i$					
α	0°	22.5°	45°	77.5°	90°
a_i	0.02415	0.02369	0.01337	0.005028	0.009043
b_i	0.458	0.2907	-1.346	-3.145	-3.37
c_i	0.3337	0.3375	0.3159	0.2901	0.2374

Table 5
List of coefficients of the functions used for the lines of best fit Fig. 6b.

$Q_{conv} = a_i \times \cos\left(\frac{\pi\alpha}{180}\right)^{b_i} + c_i$						
V	0	3	4	6	9	12
a_i	0	0.3260	0.4009	1.190	2.164	3.177
b_i	0	2.426	3.5630	3.337	4.088	3.546
c_i	0.340428	0.1805	0.2501	0.2413	0.6488	0.9071

within $\pm 1\%$. This implies that the heat loss is dominated by forced convection for $\frac{1}{Ri} > 43$ (wind speed greater than 9 m/s). The dominance of forced convection implies that the absolute heat transfer increases with wind speed in this range, as shown in Fig. 8.

These results are also compared to the results in Fig. 9 obtained from the CFD study of Lee et al. (2017). They have reported the temperature distribution through the vertical axis at various wind speed. For the case with no wind speed, $V = 0$ m/s, the average temperature of the lower front section is less than 15% of the maximum temperature, the less than half of the maximum temperature for the lower rear section while the upper section is higher than the maximum temperature by 85%. In addition, for $V = 4$ m/s, the average temperature of the lower front section is less than 40% of the maximum temperature, the lower rear is less than 55% of the maximum while the upper section is more than 80% of the maximum. The temperature distribution of that CFD study matches the heat flux distribution in the present study, shown in Table 6, well.

Fig. 9 presents the variation of the Nusselt number with inverse of Richardson number $1/Ri$ for various receiver wall temperatures and for a fixed yaw angle ($\alpha = 0^\circ$), tilt angle ($\varphi = 15^\circ$), aspect ratio ($R_{as} = 1.5$) and aperture ratio ($R_{ap} = 0.5$). It can be seen that this dimensionless function collapses all of the relevant data for the case of the head-on wind. This figure combines two correlation equations for different ranges of Ri . The correlation equations for the lines of best fit of Fig. 9 are provided. For $1/Ri < 10$, the correlation is given by Eq. (5), for which the convective heat loss is dominated by natural and mixed convection. An exponential function is used in this region and it is

reasonable because no single mechanism dominates. For $1/Ri > 10$, where forced convection dominates, the correlation is given in Eq. (6), where \overline{Nu} scales with $Ri^{0.5}$. This is consistent with its dependence on the square root of velocity.

$$\overline{Nu} = 23.97 \times \exp^{0.05103Ri} \tag{5}$$

$$\overline{Nu} = 44.1 \times \sqrt{Ri} - 110 \tag{6}$$

The parity plot between the measured and calculated values, presented in Fig. 10, shows that Eqs. (5) and (6) match the experimental result reasonably well. More specifically, the agreement is particularly good for $\overline{Nu} > 250$, where all data points fit to within $\pm 10\%$. Overall, the R-square of the scatter is 0.824 for Eq. (5) and 0.986 for Eq. (6) and more than 95% of the data are within the $\pm 20\%$ of the line. It can also be seen that the two equations result in two points of inflection, consistent with transition between three regimes. That is the rate of increasing heat loss (Nu) firstly increases with $1/Ri$ for lower wind speed ($1/Ri < 10$), then decreases with $1/Ri$ for higher wind speed ($1/Ri > 10$). The correlation equations agree with the experimental data. The size of the cavity, which affects the turbulence level, absolute Grashof number and Richardson number for a given velocity, has a huge impact on the mixed convective losses. Therefore, although non-dimensional numbers are employed in order to generalise the findings, it should be carefully validated before they are applied to a case which has different conditions.

4. Conclusions

This paper reports on an experimental campaign to quantify the heat loss from different parts of a cavity receiver, heated electrically and exposed to different wind speeds ($V = 0-12$ m/s) at various yaw angles ($\alpha = 0^\circ-90^\circ$). The heat losses due to radiation and convection from the various sections of the cavity are quantified at different constant wall temperature in the range of 100–400 °C. It has been found that, for the present scenario of a cavity, with uniform wall temperature distribution and for moderate yaw angles ($\alpha < 45^\circ$), mixed convective heat losses are greater than the natural convective heat losses for $1/Ri < 8.53$ (low wind speed). Nevertheless, for large yaw angle ($\alpha \sim 90^\circ$), there is also a range of wind conditions corresponding to

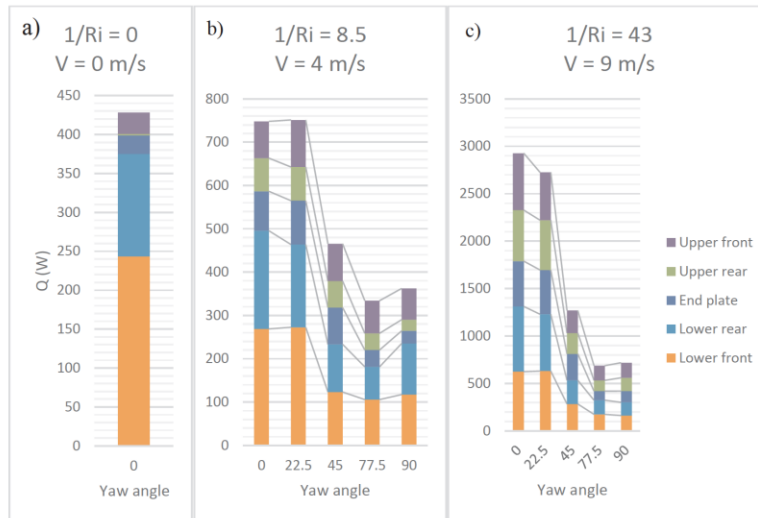


Fig. 7. Heat loss (Q_{com}) over the various sections of the heated cavity (shown in the legend) and for various $1/Ri$ (a = 0, b = 8.5 and c = 43) and yaw angle. Conditions: surface temperature = 300 °C, tilt = 15°, aspect ratio = 1.5 and aperture ratio = 0.5.

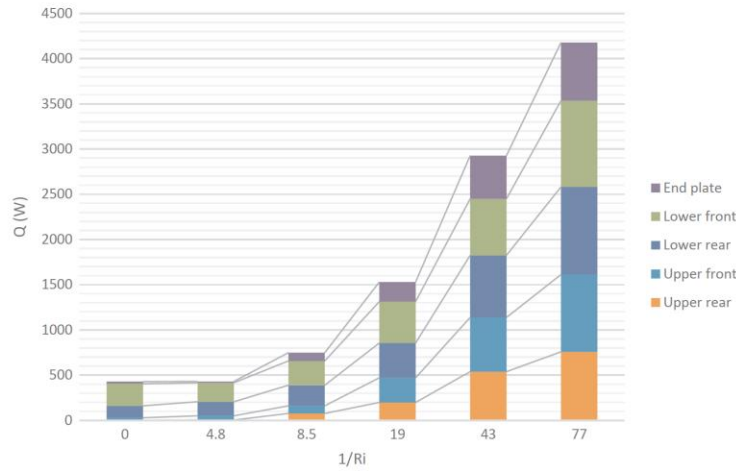


Fig. 8. Distribution of the heat loss ($Q_{c,com}$) from the various sections of the heated cavity plotted for various wind speeds. Conditions: temperature = 300 °C, yaw = 0°, tilt = 15°, aspect ratio = 1.5 and aperture ratio = 0.5.

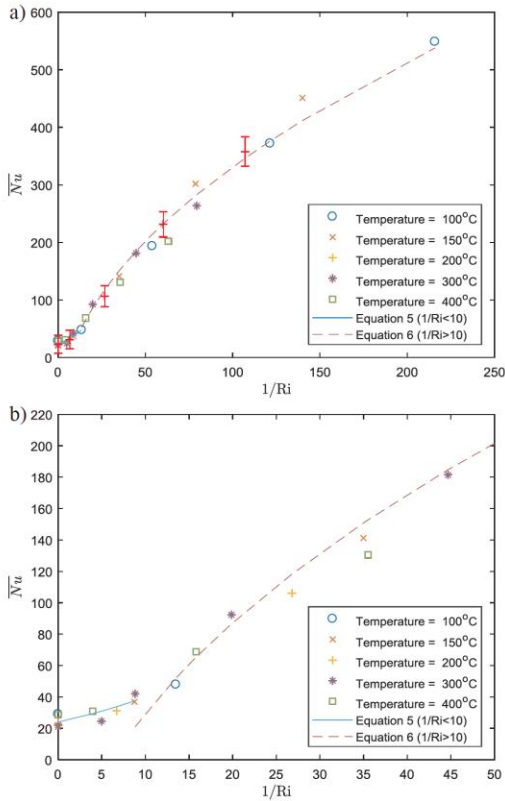


Fig. 9. Dependence of the Nusselt number on the inverse Richardson number for all values of wall temperatures for the heated solar cavity receiver. Conditions: $\alpha = 0^\circ$, $\varphi = 15^\circ$, $R_{as} = 1.5$ and $R_{ap} = 0.5$.

Table 6

Percentage of heat loss from each section of the heated cavity for different wind conditions. Similar condition to Fig. 8.

1/Ri	V (m/s)	Upper front	Upper rear	End plate	Lower rear	Lower front
0	0	6.3%	0.5%	5.5%	30.8%	56.9%
4.8	3	10.5%	1.1%	3.3%	36.2%	48.9%
8.5	4	11.4%	10.2%	12.2%	30.3%	35.9%
19	6	17.9%	12.9%	14.1%	25.1%	30.0%
43	9	20.5%	18.4%	16.3%	23.5%	21.4%
77	12	20.5%	18.1%	15.4%	23.2%	22.8%

$0 < 1/Ri < 19.2$ for which the mixed convective heat losses are lower than the natural convective heat losses from the heated cavity. As wind speed is increased to above $1/Ri > 19$, the convective heat loss can be divided into 3 ranges of yaw angle: (1) for small yaw angles ($\alpha < 22.5^\circ$), the convective heat losses are greatest and uniformly distributed over surface; (2) for medium yaw angle cases ($\alpha \sim 45^\circ$), the convective heat losses are approximately half that for small yaw angles; and (3) for large yaw angles ($\alpha > 77.5^\circ$), the heat losses are approximately one quarter of those for small yaw angles. That is, convective losses are greatest for head-on winds ($\alpha \sim 0$) in this study. It is also noticed in this study that, for heated cavities with aspect ratio larger than 1.5, head-on winds have a greater impact on heat losses. However, side-on winds have a greater impact on heat losses for heated cavities with aspect ratio less than about 1.1. Therefore aspect ratio may be one of the key parameters for the effect of yaw angle on the heat loss from a solar cavity receiver. The interaction between aspect ratio, yaw angle and wind speed need to be further investigated.

The distribution of heat loss from the different parts of the cavity was also quantified for the different operating conditions considered in this study. Approximately 88% of heat is lost from the lower part of the heated cavity for the case of no wind ($V = 0$ m/s), consistent with the well-known dominance of buoyancy and natural convection. As wind speed is increased to $1/Ri < 8.53$ ($V < 4$ m/s), the fractional heat loss from the lower surface decreases from approximately 88 to 65% and the heat transfer is in the mixed regime with buoyancy and inertia both important. Inertia dominates for $1/Ri > 43$ ($V > 9$ m/s) so that convective heat losses are distributed uniformly throughout the cavity.

A correlation equations, which use the Nusselt number as function of the inverse of Richardson number, are given with a very wide range

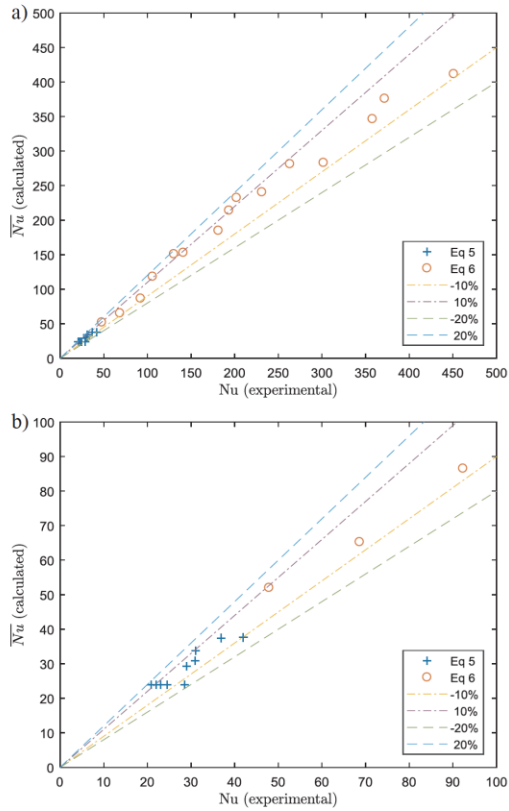


Fig. 10. The parity between the measured Nusselt number and those calculated with Eqs. (5) and (6).

of the inverse of Richardson number and it can be used for various conditions. While this equation works well for the conditions considered in this study, its further application needs to take into account cavity shape, aperture design, tilt angle, yaw angle among other parameters. Also worth noting that, for large scale practical cavity receivers on a solar tower will be subjected to non-uniform incoming flux, and this may result in different heat losses correlation found in this study.

Acknowledgments

This research has been financed by the Australian Renewable Energy Agency (ARENA) and the University of Adelaide, through the Australian Solar Thermal Research Initiative (ASTRI), ARENA1-SRI002.

References

Ávila-Marín, A.L., 2011. Volumetric receivers in solar thermal power plants with central

receiver system technology: a review. *Sol. Energy* 85 (5), 891–910.

Chen, J., Haynes, B., Fletcher, D., 2000. Cobra probe measurements of mean velocities, Reynolds stresses and higher-order velocity correlations in pipe flow. *Exp. Therm. Fluid Sci.* 21 (4), 206–217.

Clausing, A., 1981. An analysis of convective losses from cavity solar central receivers. *Sol. Energy* 27 (4), 295–300.

Collado, F.J., 2008. Quick evaluation of the annual heliostat field efficiency. *Sol. Energy* 82 (4), 379–384.

Flesch, R., Stadler, H., Uhlig, R., Hoffschmidt, B., 2015. On the influence of wind on cavity receivers for solar power towers: an experimental analysis. *Appl. Therm. Eng.* 87, 724–735.

Flesch, R., Stadler, H., Uhlig, R., Pitz-Paal, R., 2014. Numerical analysis of the influence of inclination angle and wind on the heat losses of cavity receivers for solar thermal power towers. *Sol. Energy* 110, 427–437.

Holman, J., 1997. Heat transfer, 8th ed. McGraw-Hill, New York.

Hu, T., Jia, P., Wang, Y., Hao, Y., 2017. Numerical simulation on convective thermal loss of a cavity receiver in a solar tower power plant. *Sol. Energy* 150, 202–211.

Huhn, R., 2006. Beitrag zur thermodynamischen Analyse und Bewertung von Wasserwärmespeichern in Energieumwandlungsketten.

IEA-ETSAP & IRENA, 2013. Concentrating solar power technology brief.

Jafarian, M., Arjomandi, M., Nathan, G.J., 2013. The influence of high intensity solar radiation on the temperature and reduction of an oxygen carrier particle in hybrid chemical looping combustion. *Chem. Eng. Sci.* 95, 331–342.

Kolb, G.J., Ho, C.K., Mancini, T.R., Gary, J.A., 2011. Power tower technology roadmap and cost reduction plan. Sandia National Laboratories, Livermore, CA, Technical Report No. SAND2011-2419.

Lee, K.L., Jafarian, M., Ghanadi, F., Arjomandi, M., Nathan, G.J., 2017. An investigation into the effect of aspect ratio on the heat loss from a solar cavity receiver. *Sol. Energy* 149, 20–31.

Lovegrove, K., Watt, M., Passey, R., Pollock, G., Wyder, J., Dowse, J., 2012. Realising the Potential of Concentrating Solar Power in Australia: Summary for Stakeholders. Australian Solar Institute Pty, Limited.

Ma, R.Y., 1993. Wind Effects on Convective Heat Loss from a Cavity Receiver for a Parabolic Concentrating Solar Collector. Sandia National Laboratories.

Medtherm, C., 2000. HEAT FLUX TRANSDUCERS and INFRARED RADIOMETERS for the DIRECT MEASUREMENT OF HEAT TRANSFER RATES, viewed 09/04/17, < http://www.dr-kubelik.de/cms/tl_files/infomaterial/Heat_Flux_Transducer.pdf > .

Mills, A.F., 1999. Basic heat and mass transfer, vol. 2 Prentice hall Upper Saddle River, NJ.

Paitoonsurikarn, Lovegrove, K., 2003. On the study of convection loss from open cavity receivers in solar paraboloidal dish applications. In: Proceedings of 41st Conference of the Australia and New Zealand Solar Energy Society (ANZSES), Melbourne, Australia.

Paitoonsurikarn, S., Lovegrove, K., 2002. Numerical investigation of natural convection loss in cavity-type solar receivers. *Proceedings of Solar*.

Paitoonsurikarn, S., Lovegrove, K., Hughes, G., Pye, J., 2011. Numerical investigation of natural convection loss from cavity receivers in solar dish applications. *J. Sol. Energy Eng.* 133 (2), 021004.

Paitoonsurikarn, S., Taumoefolau, T., Lovegrove, K., 2004. Estimation of convection loss from paraboloidal dish cavity receivers. In: Proceedings of 42nd conference of the Australia and New Zealand solar energy society (ANZSES), Perth, Australia.

Philibert, C., 2010. Technology roadmap: concentrating solar power, OECD/IEA.

Prakash, M., Kedare, S., Nayak, J., 2009. Investigations on heat losses from a solar cavity receiver. *Sol. Energy* 83 (2), 157–170.

Price, H., 2003. Assessment of parabolic trough and power tower solar technology cost and performance forecasts. In: Sargent & Lundy LLC Consulting Group, National Renewable Energy Laboratory, Golden, Colorado.

Segal, A., Epstein, M., 2003. Optimized working temperatures of a solar central receiver. *Sol. Energy* 75 (6), 503–510.

Siegel, R., 2001. Thermal radiation heat transfer, vol. 1. CRC Press.

Steinfeld, A., Schubnell, M., 1993. Optimum aperture size and operating temperature of a solar cavity-receiver. *Sol. Energy* 50 (1), 19–25.

Tanaka, N., 2010. Technology Road Map, Concentrating Solar Power. International Energy Agency.

Wu, S.-Y., Shen, Z.-G., Xiao, L., Li, D.-L., 2015. Experimental study on combined convective heat loss of a fully open cylindrical cavity under wind conditions. *Int. J. Heat Mass Transf.* 83, 509–521.

Wu, S.-Y., Xiao, L., Li, Y.-R., 2011. Effect of aperture position and size on natural convection heat loss of a solar heat-pipe receiver. *Appl. Therm. Eng.* 31 (14), 2787–2796.

Xiao, L., Wu, S.-Y., Li, Y.-R., 2012. Numerical study on combined free-forced convection heat loss of solar cavity receiver under wind environments. *Int. J. Therm. Sci.* 60, 182–194.

CHAPTER 6

Experimental Investigation Of The Effects Of Wind Speed, Aperture Ratio And Tilt Angle On The Heat Losses From A Heated Cavity

Statement of Authorship

Title of Paper	Experimental investigation of the effects of wind speed, aperture ratio and tilt angle on the heat losses from a heated cavity
Publication Status	<input type="checkbox"/> Published <input type="checkbox"/> Accepted for Publication <input checked="" type="checkbox"/> Submitted for Publication <input type="checkbox"/> Unpublished and Unsubmitted work written in manuscript style
Publication Details	Lee, KL, Chinnici, A, Jafarian, M, Arjomandi, M, Dally, B & Nathan, G, 'Experimental investigation of the effects of wind speed, aperture ratio and tilt angle on the heat losses from a heated cavity', Solar energy, (2018).

Principal Author

Name of Principal Author (Candidate)	Ka Lok Lee		
Contribution to the Paper	Developed the experiment, performed analysis on all data, interpreted data, wrote manuscript and acted as corresponding author.		
Overall percentage (%)	60%		
Certification:	This paper reports on original research I conducted during the period of my Higher Degree by Research candidature and is not subject to any obligations or contractual agreements with a third party that would constrain its inclusion in this thesis. I am the primary author of this paper.		
Signature		Date	29/06/2018

Co-Author Contributions

By signing the Statement of Authorship, each author certifies that:

- i. the candidate's stated contribution to the publication is accurate (as detailed above);
- ii. permission is granted for the candidate to include the publication in the thesis; and
- iii. the sum of all co-author contributions is equal to 100% less the candidate's stated contribution.

Name of Co-Author	Alfonso Chinnici		
Contribution to the Paper	Supervised development of the work , helped to evaluate and edit the manuscript		
Signature		Date	03/07/18

Name of Co-Author	Mehdi Jafarian		
Contribution to the Paper	Supervised development of the work , helped to evaluate the manuscript		
Signature		Date	02,07,2018

CHAPTER 6

Name of Co-Author	Maziar Arjomandi		
Contribution to the Paper	Supervised development of the work , helped to evaluate the manuscript		
Signature		Date	2/07/2018

Name of Co-Author	Bassam Dally		
Contribution to the Paper	Supervised development of the work , helped to evaluate and edit the manuscript		
Signature		Date	2-07-2018

Name of Co-Author	Graham Jerrold Nathan		
Contribution to the Paper	Supervised development of the work , helped to evaluate and edit the manuscript		
Signature		Date	3/7/18

Experimental investigation of the effects of wind speed, aperture ratio and tilt angle on the heat losses from a heated cavity

Ka Lok Lee, Alfonso Chinnici, Mehdi Jafarian, Maziar Arjomandi, Bassam Dally, Graham Nathan

School of Mechanical Engineering, The University of Adelaide, SA 5005, Australia

E-mail address: ka.lee@adelaide.edu.au (K.L. Lee)

Authors email:

alfonso.chinnici@adelaide.edu.au (A. Chinnici)

mehdi.jafarian@adelaide.edu.au (M. Jafarian)

maziar.arjomandi@adelaide.edu.au (M. Arjomandi)

bassam.dally@adelaide.edu.au (B.B Dally)

graham.nathan@adelaide.edu.au (G.J. Nathan)

Abstract

The first systematic experimental study of the combined influences of wind speed (0 - 9 m/s), aperture ratio (0.33 - 1) and tilt angle (15° - 45°) on the convective heat losses from a cylindrical cavity heated with a uniform wall temperature, is presented. The cavity is heated with 16 individually controlled copper surface elements so that both the heat losses from the cavity and the heat flux distribution can be measured and subjected to a controlled convective environment in the open section of a wind tunnel. A complex inter-dependence was found between aperture ratio, wind speed and convective heat losses. In particular, the total heat losses can vary by up to ~75% by varying the aperture ratio from 0.33 to 0.75, for no wind condition, but the effect of aperture ratio is decreased as wind speed is increased. The tilt angle was found to have a small effect on the heat losses relative to the aperture ratio and wind speed. Nevertheless, the minimum overall heat loss occurs for a tilt angle of between 15° and 30° for various wind speeds.

CHAPTER 6

Keywords

Solar receiver; Solar thermal power; Heat loss; Concentrated solar thermal radiation; Temperature distribution; Wind

CHAPTER 6

Nomenclature

Symbols			
A	Area (m ²)	V	Wind speed (m/s)
β	Coefficient of thermal expansion (°C ⁻¹)	ν	Kinematic viscosity of air at reference temperature kg/(s.m)
D	Diameter (m)	α	Yaw angle or incoming wind direction (°)
ϵ	Emissivity coefficient of the internal wall surface	ϕ	Tilt angle of the cavity (°)
g	Gravity (m/s ²)		
Gr	Grashof number = $\frac{g\beta(T_{wall} - T_a)D_{cav}^3}{\nu^2}$	Subscript	
h_c	Convective heat transfer coefficient through the aperture (W/(m ² K))	a	Ambient
k	Thermal conductivity of air at reference temperature (W/(m. K))	as	Aspect
L	Length (m)	ap	Aperture
Nu	Nusselt number = $\frac{h_c D_{cav}}{k_{ref}}$	cav	Cavity
Q	Heat loss (W)	conv	Convection
R	Ratio	rad	Radiation
Re	Reynolds number = $\frac{VD_{cav}}{\nu}$	ref	Reference
Ri	Richardson number = $\frac{Gr}{Re^2} = \frac{g\beta(T_{wall} - T_a)D_{cav}}{\nu^2}$	tot	total
T	Temperature (°C)	w	Wall

1 Introduction

The ongoing development of solar tower thermal energy technology has been driven recently by the low cost of thermal energy storage relative to their electrical energy storage counterparts (Kolb et al. 2011; Philibert 2010; Tanaka 2010). Nevertheless, to capitalise on this, there is an ongoing need to continue to lower the cost of the entire system. One opportunity is to reduce the heat losses, which become increasingly significant with the ongoing drive toward higher operating temperatures to increase the thermal efficiency of the power block (Ávila-Marín, 2011; IEA-ETSAP and IRENA, 2013; Lovegrove et al., 2012; Price, 2003; Segal and Epstein, 2003; Steinfeld and Schubnell, 1993). However, the heat losses from a receiver comprise both radiative and convective component, which are highly complex, so that the underlying mechanisms remain poorly understood. In particular, the heat loss from a solar cavity receiver is influenced by the cavity aspect ratio, aperture ratio, wind speed, yaw angle, tilt angle, mean temperature and temperature distribution. However, little information is available about these effects. Our previous experimental study reported on the interaction between temperature, yaw angle and wind speed (Lee et al. 2018), but a systematic investigation of the effect of wind speed, aperture ratio and tilt angle yet to be reported. Therefore the aim of the present investigation is to meet this need.

The influence of tilt angle on the natural convection heat loss from a solar cavity receiver was first reported via experiments by Clausing (1981,1983), who first introduced the concept of stagnant and convective zones. In the stagnant zone, the air inside the cavity is nearly stationary and the convective heat transfer coefficients are low. However, in the convective zone, the air moves at higher velocity resulting in a much higher heat transfer rates. They also found that the tilt angle has a significant influence on the size of the stagnant and convective zones. The larger the tilt angle, the larger the stagnant zone. Ma (1993) experimentally investigated the effect of wind speed on the convective heat loss using a heated cavity receiver in a wind tunnel. The internal surface of the cavity was heated with a heat transfer fluid, whose temperature change was used to measure the heat losses. They found that the trend of increasing convective heat with wind speed for a side-on wind is independent of the receiver tilt angle. However, for head-on winds, the heat loss is a function of the receiver tilt angle. The influence of head-on wind and side-on wind on cavity receivers with different inclination angles in the range of 0-90° has been analysed numerically by Flesch et al. (2014). They claimed that wind has only a small influence on the convective heat losses from a horizontal cavity receiver. Conversely, in most cases, the losses from cavity receivers increase significantly at high inclination angles. However, the heat losses were found to reduce with increasing wind speed in some cases, although this effect is highly geometry dependent and only occurs for some cavity configurations. This highlights the need for more understanding of the convective losses from cavity receivers.

The ratio of the aperture diameter to that of the cavity has a strong influence on the re-radiation and convection losses from the cavity (Clausing, Waldvogel & Lister 1987; Kim, Yoon & Kang

CHAPTER 6

2009; Steinfeld & Schubnell 1993; Wu, Xiao & Li 2011). The effect of the aperture size on the convective heat loss from a heated cavity was first reported by Clausen et al. (1987), who found that both size and configuration are important. However, this study only considered natural convection, at zero wind velocity. Steinfeld & Schubnell (1993) investigated the effect of the aperture size and operating temperature on the radiative losses from a solar cavity receiver on its heat losses for solar dish system. Kim et al. (2009) measured the heat loss from a cavity receiver from a solar power tower system with four aperture configurations, with no cavity, open cavity (aperture ratio = 1), small centre cavity (aperture ratio = 0.5) and small lower cavity (aperture ratio = 0.5 with aperture opening from the lowest end of the cavity). It was claimed that the convective heat loss increases with wind speed and aperture area, but is not closely related to aperture position or the distance between the aperture and the heated surface. However, the distance between the aperture and the heated surface (aspect ratio) was short and only one aspect ratio was tested in that study. Further work is therefore required to better understand the interactions between wind speed and aperture area on the heat loss from a solar cavity receiver.

Most previous experiments of heat transfer were performed with only a single temperature controller for the entire internal surface. This makes it impossible to achieve a truly uniform internal temperature distribution because the heat transfer across the entire surface is controlled to a single temperature set-point, even though the surface temperature varies spatially. As a result, it is difficult to reliably validate numerical models with existing data, since they require invoking the assumption of a uniform internal wall temperature (Flesch et al. 2014; Hu et al. 2017; Lee et al. 2017; Paitoonsurikarn, Taumoeafolau & Lovegrove 2004; Wu, Xiao & Li 2011; Xiao, Wu & Li 2012), even though this assumption is known to be incorrect. Therefore, there is a need for new experimental data that more accurately reproduces a uniform internal wall temperature. In addition, the interactions between tilt angle and aperture ratio under conditions with wind have not been assessed experimentally, either on the total losses or on the heat losses from different sections of the cavity.

In light of the above gaps in understanding and in available data, the principal objective of the present investigation is to provide direct measurements of the influence of wind speed, aperture ratio and tilt angle on the mixed convection heat losses from a solar cavity receiver with uniform internal wall temperature. In addition, this work aims to resolve the following questions: 1) whether heat flux increases or decreases with tilt angle; 2) how the aperture ratio influences the contribution of convective heat losses to total heat losses; and 3) how wind speed, tilt angle and aperture ratio influence the distribution of heat flux within a uniformly heated cavity.

2 Methodology

Figure 1a) presents the experimental arrangement used in the study. An electrically heated cavity was placed within the open section of the wind tunnel at University of Adelaide's Thebarton laboratory. This provides well-controlled variation in wind speed with negligible blockage, which is low even without the open section. The projected area of the external dimensions of the cavity ($\sim 0.249 \text{ m}^2$) is $\sim 4.1\%$ of the cross-sectional dimensions area of the wind tunnel ($2.75 \text{ m} \times 2.19 \text{ m}$), which is also ~ 330 times larger than the cross-section area of the aperture ($\sim 0.018 \text{ m}^2$). The wind velocities, using air as the working fluid, were measured using multi-hole pressure probe from Turbulent Flow Instrumentation (Lee et al. 2018). The key dimensions of the cavity are shown in Figure 1b). The cavity has an inner diameter $D = 0.3 \text{ m}$ with an aspect ratio $R_{as} = 1.5$ and aperture ratio $R_{ap} = 0.00, 0.33, 0.50, 0.75$ and 1.00 . The internal walls of the cavity are made from copper, because of its high thermal conductivity and safe operating temperature. A mineral fibre of melted rock and chalk (also known as Rockwool), was placed around the sides and end of the cavity as insulation, to reduce the conductive heat loss through the walls of the cavity. The insulation was approximately 40 mm , with losses further reduced by wrapping this with aluminium foil and wires for support.

The surface of the cavity was lined with 16 segments of heating elements that are individually controlled, as shown in Figure 1 and Figure 2. These are arranged to comprise 6 annular rings of 12 heaters, each covering a 180° arc along the length of the chamber to measure separately the upper and lower half, together with another 4 circumferential rings on the back wall. Each heater has its own individual heater code for identification (see Figure 2). Each heater is controlled with a feedback controller, which controls the set-point temperature to the desired value and records the power required to do so. Mica insulators are used to minimise the conductive heat transfer between each heater segment. The configuration is shown in Figure 2. Thermocouples are attached to each copper wall surface to measure its temperature, which is assumed to be uniform due to the high thermal conductivity of copper. The thermocouples used in this study were type K, with a washer/ ring attachment to the copper surface, recorded with a Datataker DT85. These temperatures were also used for the temperature feedback control system using Matlab and Simulink. The output power signal from the computer is converted into DMX signal by Arduino, then control with the DMX lighting system power controllers. The steady-state power required to maintain the system at the set point temperature was measured, with the sum of these corresponding the total heat loss from the system. Steady-state was considered to have been reached when the following conditions were met for 300 seconds: 1) the variation of each measured temperature is below $\pm 0.5^\circ \text{C}$; and 2) the variation of total heat loss is less than $\pm 5\%$ of the total power required for that condition if the total heat loss is above 2 kW or $\pm 100 \text{ W}$ if the heat loss is below 2 kW .

The different contributions to convective and radiative heat losses from the receiver were identified in a series of steps. Firstly the radiative heat loss was determined, being independent of the cavity's orientation. This was performed with the cavity oriented vertically downward (tilt= 90°), because this position minimises the convective heat loss. The total heat losses from the cavity were then measured both with the aperture of the cavity being opened and closed. The power loss for the case with the aperture closed, Q_{wall} , corresponds to the wall losses.

CHAPTER 6

Then, the aperture was opened and the total power loss, Q_{total} , was recorded again. The difference between the cases with the aperture opened and closed presents the heat loss through the aperture, Q_{ap} , calculated as follow:

$$Q_{ap} = Q_{total} - Q_{wall} = Q_{rad} + Q_{conv}. \quad (1)$$

To note that, Q_{ap} was measured for a series of tilt angles, aperture ratio and wind speeds.

The radiative component of heat loss through the aperture is Q_{rad} . A Medtherm 64 series was used to measure the direct radiative heat loss through the aperture (Medtherm 2000). The convective heat loss through the aperture Q_{conv} , was then determined by subtraction. A cross check was performed using the different proportionality constant for radiation, which scales with T^4 , while convection scales with T following previous work (Holman 1997; Siegel 2001).

A systematic study of the influence on the heat losses was assessed for variations in wind speed $V = 0, 3, 4, 6,$ and 9 m/s, aperture ratio $R_{ap} = 0.33, 0.50, 0.75$ and 1.00 , and tilt angle $\varphi = 15^\circ, 30^\circ$ and 45° . This leads to a total of 90 combinations of wind speed, tilt angles and aperture ratios, the details of which are presented in Table 1. Of these, 45 conditions correspond to the case with an open aperture in order to measure the convective and radiative heat losses, and the other 45 cases for the closed aperture to measure the heat loss through the walls.

The temperature of each heated copper surface was measured and controlled individually, which allows heat flux distribution within the cavity to be obtained.

The Richardson number Ri was used to characterise the effect of geometry and wind speed on the relative roles of the buoyancy and inertia forces. The cavity was aligned head-on to the wind for this dimensionless study as the wind has the greatest impact on the heat losses for this orientation. The Ri is the ratio of the buoyancy term to the flow shear term, and can also be expressed in terms of the Grashof and Reynolds numbers, as shown in equation 2.

$$Ri = \frac{\text{buoyancy term}}{\text{flow shear term}} = \frac{Gr}{Re^2} = \frac{g\beta(T_w - T_a)D_{cav}}{V^2} \quad (2)$$

Here g is the acceleration due to gravity, β is the thermal expansion coefficient. Typically, a heated surface is dominated by natural convection for $Ri < 0.1$, and by forced convection for $Ri > 10$, while both are important for $0.1 < Ri < 10$ (Garbrecht, 2017). The Nusselt number, Nu , is calculated using the following equation:

$$\overline{Nu} = \frac{\text{total heat transfer}}{\text{conductive heat transfer}} = \frac{Q_{conv}D_{cav}}{A_{total,cav}(T_{wall} - T_a)}. \quad (3)$$

Here the total inner surface area $A_{total,cav} = 0.495m^2$ and conductivity at the reference temperature, k_{ref} is a function of the reference temperature T_{ref} , which is defined as

$$T_{ref} = \frac{T_{wall}}{2} + \frac{T_a}{2}. \quad (4)$$

CHAPTER 6

The main uncertainties in the experiments are as follows. The maximum uncertainty of the power output from each heater is $\pm 25\text{W}$ ($\sim 3.1\%$), which includes that from the power and temperature measurement ($\pm 0.5^\circ\text{C}$) and their effect on the feedback control system. Although the total maximum uncertainty is $\sim \pm 400\text{W}$, the average error is less than $\pm 3.1\%$ of the maximum power, because the error of random error is reduced by using the 16 results from the heaters. In addition, the uncertainty of the incoming wind speed is $\pm 0.2\text{m/s}$.

Table 1: List of experimental conditions

Velocity (V , m/s)	Yaw angle (α°)	Tilt angle (φ°)	Temperature of the wall (T_w , $^\circ\text{C}$)	Aspect ratio ($\frac{L_{cav}}{D_{cav}}$)	Aperture ratio ($\frac{D_{ap}}{D_{cav}}$)
0,3,6 and 9	0	15, 30 and 45	300	1.5	0.00, 0.33, 0.50, 0.75, 1.00

CHAPTER 6

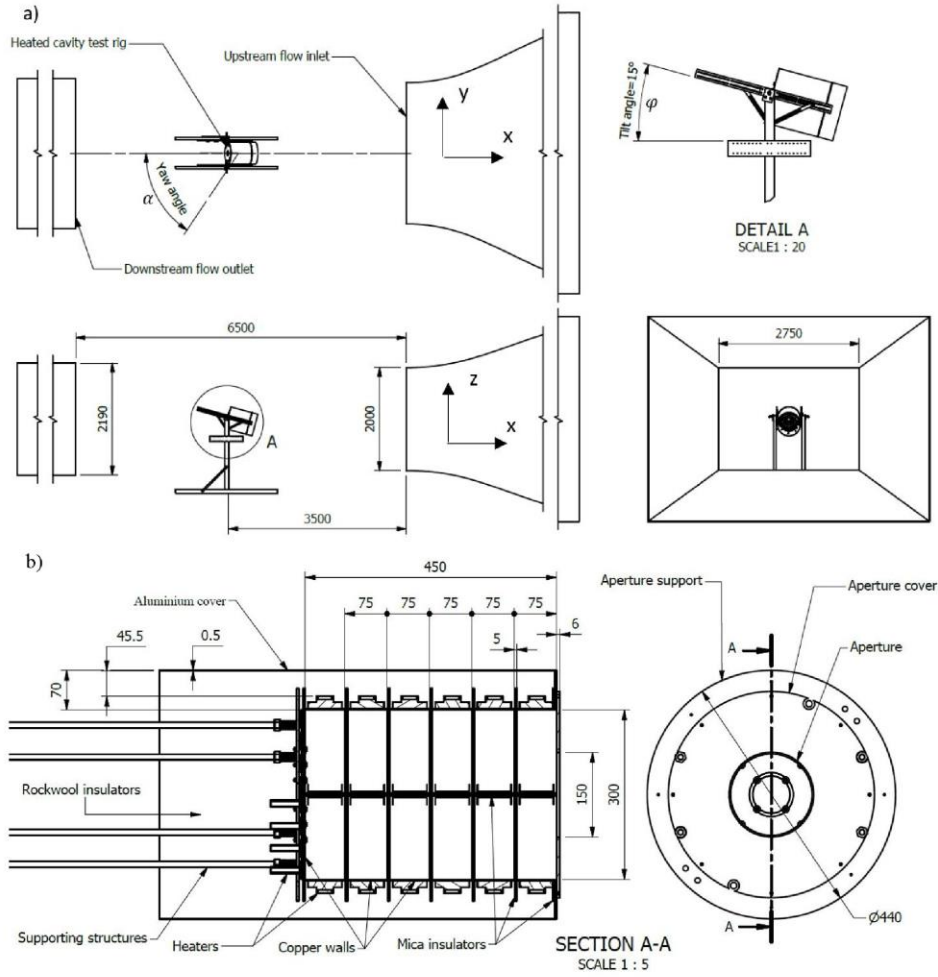


Figure 1: Schematic diagram of a) the heated cavity in the Thebarton wind tunnel and b) the dimensions of the receiver.

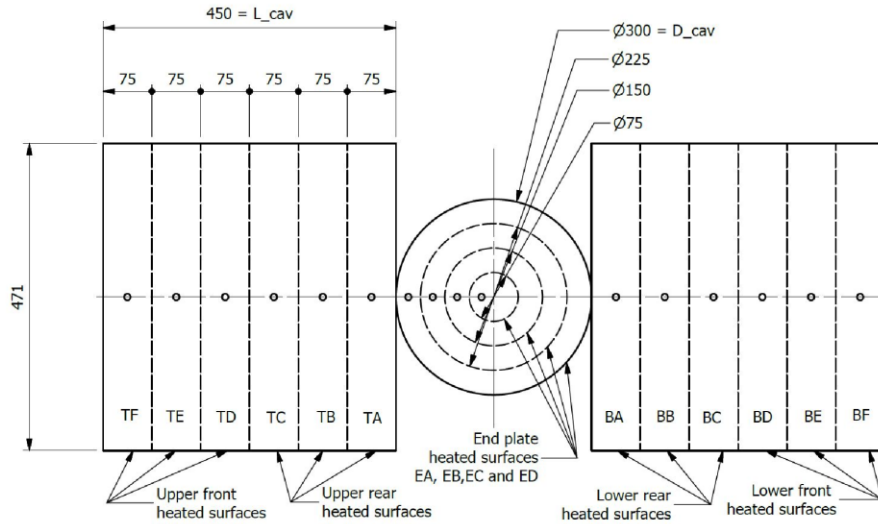


Figure 2: Schematic diagram of the simplified configuration of the internal copper wall surface of the heated cavity (shown unrolled view). The thermocouples are shown as small circles.

3 Results and Discussion

3.1 Absolute convective heat loss

The variation of the convective heat losses through the aperture with wind speed is presented in Figure 3 for various values aperture ratios, but for a constant wall temperature of 300°C , tilt angle of 15° , yaw angle of 0° and cavity length to diameter aspect ratio of 1.5. This case was chosen as a reference case because of its relevance to practical conditions and to match the conditions reported by Lee et al. (2018). The convective heat losses increase with an increase in $1/Ri$ and V , for all the aperture ratios D_{ap}/D_{cav} considered here.

However, the dependence is non-linear. The effect of wind speed is weak for $1/Ri < 8.5$ ($V < 4$ m/s), and strong for $1/Ri > 8.5$ ($V > 4$ m/s). The effect of D_{ap}/D_{cav} is weaker, but is also non-linear. In the low range $1/Ri < 4.8$ (i.e. $V < 3$ m/s), an increase in D_{ap}/D_{cav} increases the convective heat losses. Conversely, for high wind speed cases ($1/Ri > 19$ and $V > 6$ m/s), an increase in D_{ap}/D_{cav} decreases the convective heat losses for $3 < V < 4$ m/s ($4.8 < 1/Ri < 8.5$)

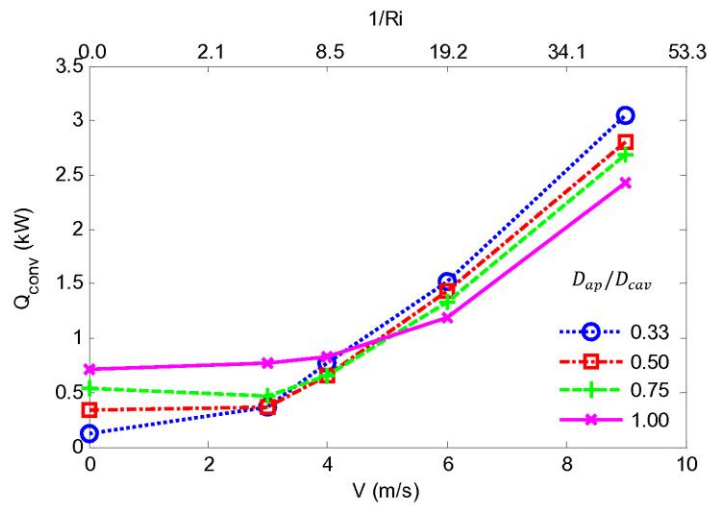


Figure 3: Dependence of the convective heat losses through the aperture on wind speed and inverse Richardson number for a series of aperture ratio. Conditions: wall temperature of 300°C, tilt angle of 15°, yaw angle of 0° and aspect ratio of 1.5.

Figure 4 presents the corresponding dependence of the convective heat losses through the aperture on $1/Ri$ and V for series of D_{ap}/D_{cav} , but for the case of a tilt angle of 30° with the other conditions unchanged. It can be seen that the general trends are the same as for the tilt angle of 15° (Figure 3). However, the effect of aperture ratio on the convective heat loss is even less than for the case of a tilt angle = 15°. In particular, the effect of the aperture ratio is negligible for the higher wind speeds, where $\frac{1}{Ri} > 4.8$ ($V > 3$ m/s) and $D_{ap}/D_{cav} < 0.75$. In addition, the local minimum in convective heat losses at moderate wind speeds is not observed for this orientation. Instead, the slope is weaker, but still positive, throughout the low wind-speed regime.

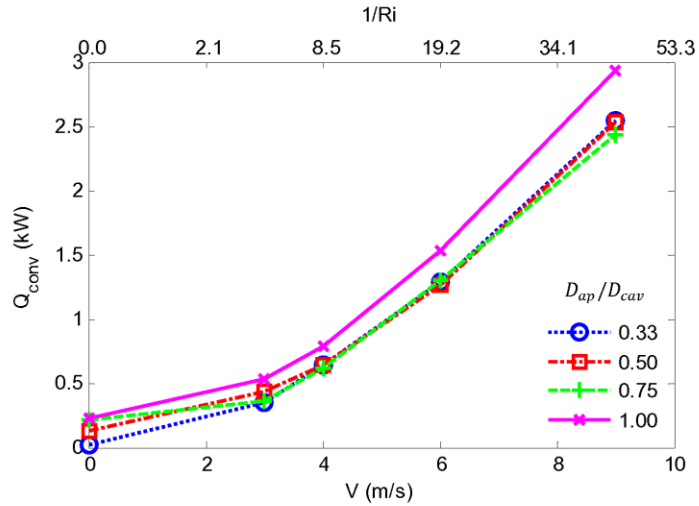


Figure 4: Dependence of the convective heat losses through the aperture on wind speed and inverse Richardson number for a series of aperture ratio. Conditions: wall temperature of 300°C, tilt angle of 30°, yaw angle of 0° and aspect ratio of 1.5.

Figure 5 presents the effects of the aperture ratio and wind speed on the convective heat losses for the 2 values of the tilt angle. For the no wind condition, the convective heat losses increase with the D_{ap}/D_{cav} , while the influence is more complex in the presence of a wind. There is a general trend of the convective heat losses being lower with higher tilt angle (as expected), although there is an exception for the highest value of wind speed ($V = 9$ m/s). For $1/Ri = 8.5$ ($V = 4$ m/s), the tilt angle on the convective heat losses and the convective heat losses are also almost independent of D_{ap}/D_{cav} , although it has a weak local minimum for $0.5 < D_{ap}/D_{cav} < 0.75$. For higher values of $1/Ri = 43$ ($V = 9$ m/s), the convective heat loss decreases with the aperture ratio for both tilt angles, except the case $V=9$ m/s, $\varphi = 30^\circ$ and $D_{ap}/D_{cav} = 1$.

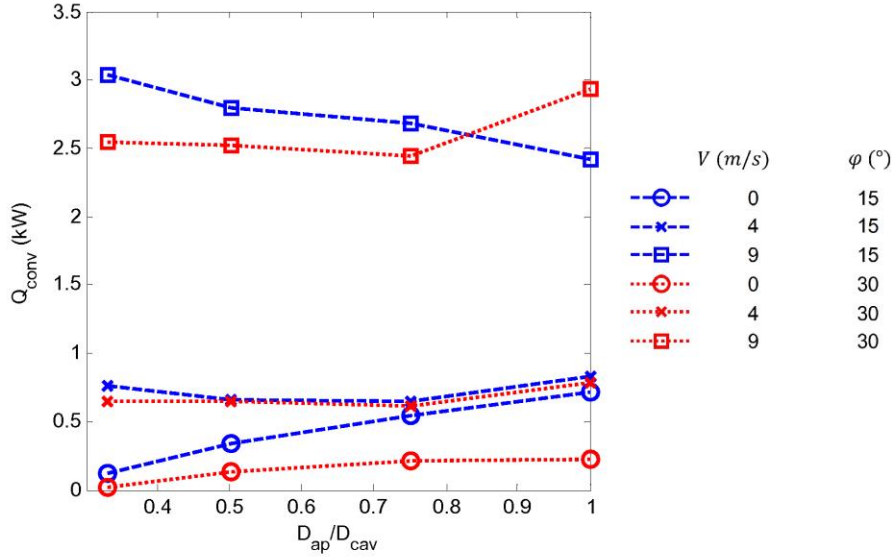


Figure 5: Dependence of the convective heat losses through the aperture on tilt angle, wind speed and inverse Richardson number for a series of aperture ratio. Conditions: wall temperature of 300°C, yaw angle of 0° and aspect ratio of 1.5.

3.2 Relative convective heat loss

The dependence of the relative convective heat losses through the aperture, $Q_v/Q_{v=0}$ on inverse Richardson number and wind speed is presented in Figure 6 for various values of D_{ap}/D_{cav} . It can be seen that the difference between the forced convection and natural convection case increases as D_{ap}/D_{cav} departs from unity. For $D_{ap}/D_{cav} = 0.33$, the corresponding increase is about 25%. That is, the influence of wind speed on the convective heat loss is very high for $D_{ap}/D_{cav} = 0.33$. Referring back to Figure 3, it can be seen that the absolute increase in Q_v is only about 30% at the high wind speed, but rather the bigger difference is the much lower convective heat loss for $V = 0$ m/s with the small aperture. That is, the influence of a small aperture is to greatly reduce natural convective losses, but to slightly increase the forced convective losses at high wind speed.

The dependence of the relative convective heat losses through the aperture $Q_{R_{ap}}/Q_{R_{ap=0}}$ on D_{ap}/D_{cav} is presented in Figure 7 for various values of wind speed. It can be seen that the trend is opposite for high and low values of $1/Ri$. For $1/Ri > 19$ ($V > 6$ m/s), the relative convective heat loss of aperture ratio increase by about 25% as D_{ap}/D_{cav} is decreased from 1 to 0.33. For $1/Ri < 4.8$ ($V < 3$ m/s), the convective losses decrease strongly with a decrease in D_{ap}/D_{cav} . This is the regime in which natural convection is dominant, so that a small aperture inhibits the escape of hot air through the aperture. The case For $1/Ri = 8.5$ ($V = 4$ m/s), shows that the

CHAPTER 6

transition between these two regimes is complex, with $Q_{Rap}/Q_{Rap=0}$ first decreasing by 20% and then increasing back to near unity with a decrease in D_{ap}/D_{cav} .

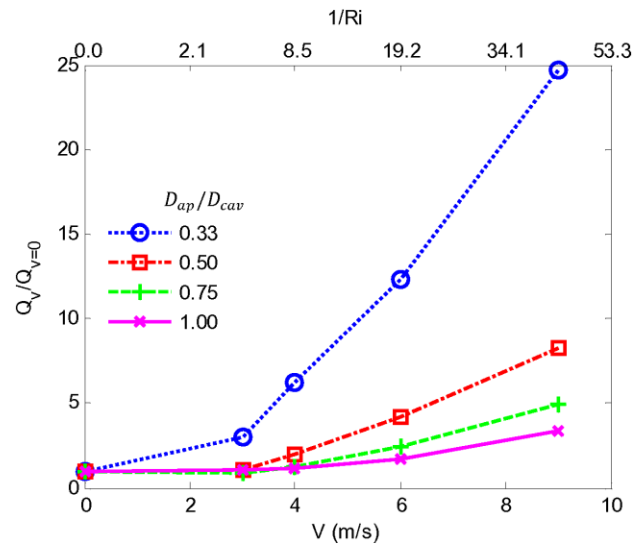


Figure 6: Dependence of the relative convective heat losses through the aperture with wind speed for various values of aperture ratio. Conditions: wall temperature of 300°C, tilt angle of 15°, yaw angle of 0° and aspect ratio of 1.5. The relative convective heat loss $Q_v/Q_{v=0}$ is the ratio between the convective heat loss for a given wind speed and no wind condition.

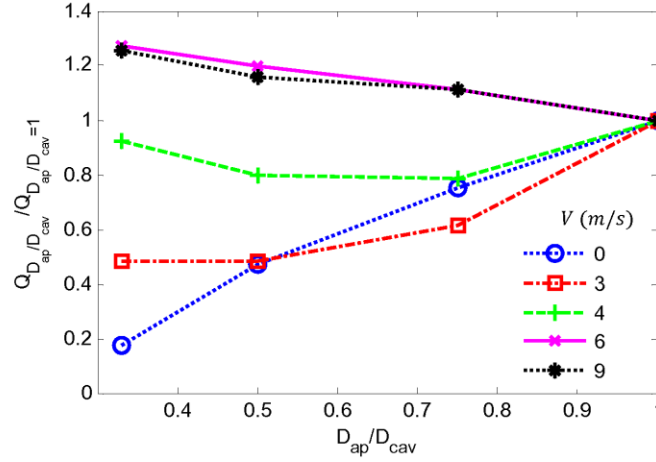


Figure 7: Dependence of the relative convective heat losses through the aperture with aperture ratio for various values of wind speeds. Conditions: wall temperature of 300°C, tilt angle of 15°, yaw angle of 0° and aspect ratio of 1.5. The relative convective heat loss $Q_{D_{ap}/D_{cav}} / Q_{D_{ap}/D_{cav}=1}$ is the ratio between the convective heat loss for a given D_{ap}/D_{cav} and $D_{ap}/D_{cav} = 1$.

3.3 Heat losses distribution

3.3.1 Effect of wind speed and aperture ratio

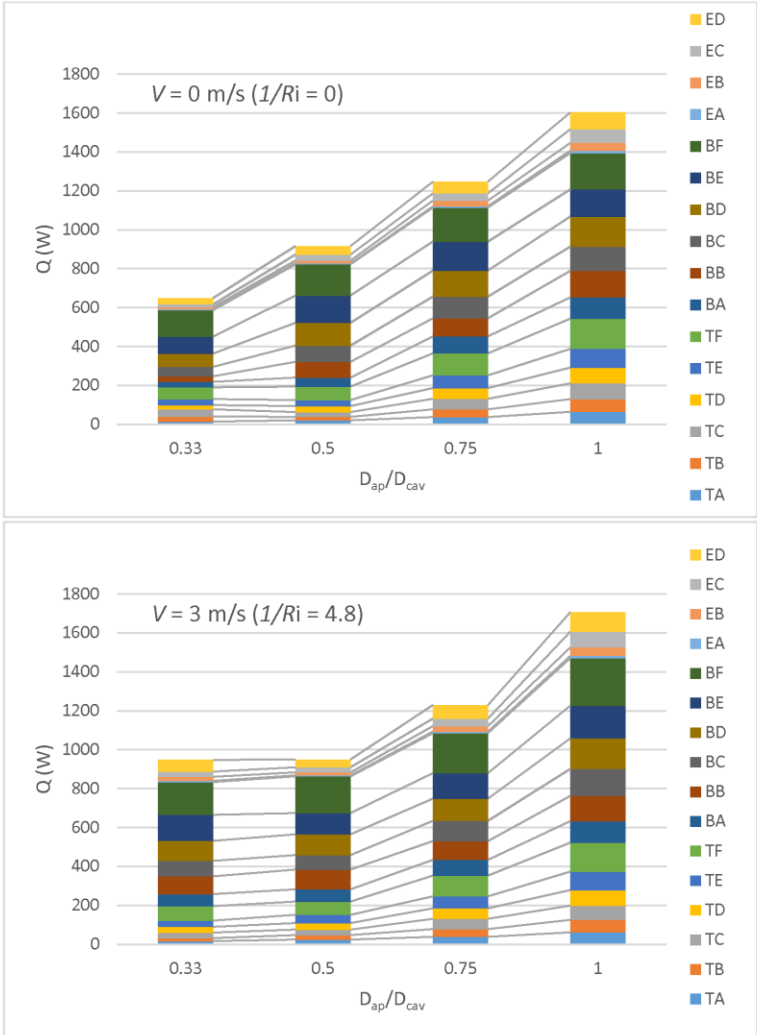
The distribution of the total heat loss from the various surface heated elements in the cavity is presented as a function of aperture ratios for three values of wind speed in Figure 8.

For the no wind condition, increasing D_{ap}/D_{cav} from 0.33 to 0.5, increases the heat losses preferentially from the lower elements, especially from the lower rear section where they are increased by more than 100% although the total heat loss is only increased by approximately 50%. In contrast, increasing D_{ap}/D_{cav} from 0.5 to 1.0 causes the average heat losses to increase by approximately 200% for the upper elements, while average increment of heat loss from the lower elements increases by only approximately 50%.

For $1/Ri < 4.8$ ($V < 3$ m/s), the heat loss from each heater element is similar as D_{ap}/D_{cav} is increased from 0.33 to 0.5. As D_{ap}/D_{cav} is increased from 0.5 to 1.0, the fractional heat loss from the lower elements decreases from 68 to 56%, while that from the upper elements increases from 23 to 31%. It is also worth noting that the heat losses from the lower elements are always more than 50% of the total losses.

For $1/Ri < 43$ ($V < 9$ m/s), the heat losses from the lower elements are less than 50% of the total losses, which is different from the low wind speed cases. In addition, the heat loss from each heater element is similar for D_{ap}/D_{cav} between 0.33 and 1.0. This is because the losses are forced-convection dominated.

CHAPTER 6



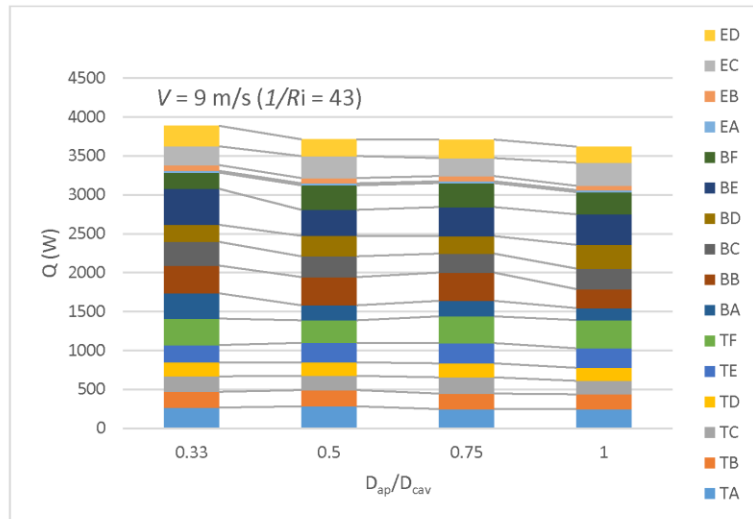


Figure 8: Distribution of the total heat loss from each heater element in the cavity surface as a function of aperture ratio for various wind speeds. Conditions: temperature = 300°C, yaw = 0°, tilt = 15° and aspect ratio = 1.5.

The fractional distribution of heat loss from various section of the heated cavity for various wind speeds and aperture ratios is shown in Figure 9. For the zero and low wind speed conditions ($V < 3$ m/s, $1/Ri < 4.8$), about 60% of the total heat losses are lost from the lower section of the heated cavity for all the aperture ratios tested here. And about 43% of the heat losses are from the lower front section of the heated cavity for $D_{ap}/D_{cav} = 0.33$ and 0.5, but only about 36% are from the $D_{ap}/D_{cav} = 0.75$. This is because increasing in aperture ratio reduce the size of the stagnant zone region, resulting in more heat loss from the upper section.

The heat lost from the lower section of the cavity is about 47% of the total heat losses for all the tested aperture ratios and for $V = 9$ m/s ($1/Ri = 43$). Although the fractional distribution of heat loss is much more uniform for the high wind speed conditions, for the low wind speed cases, the fraction of heat losses from the upper section increases with the aperture ratio. That is although the wind speed has a strong influence on the fractional distribution heat loss for low aperture ratios (0.33 and 0.5), its effect is weakened by increasing D_{ap}/D_{cav} .

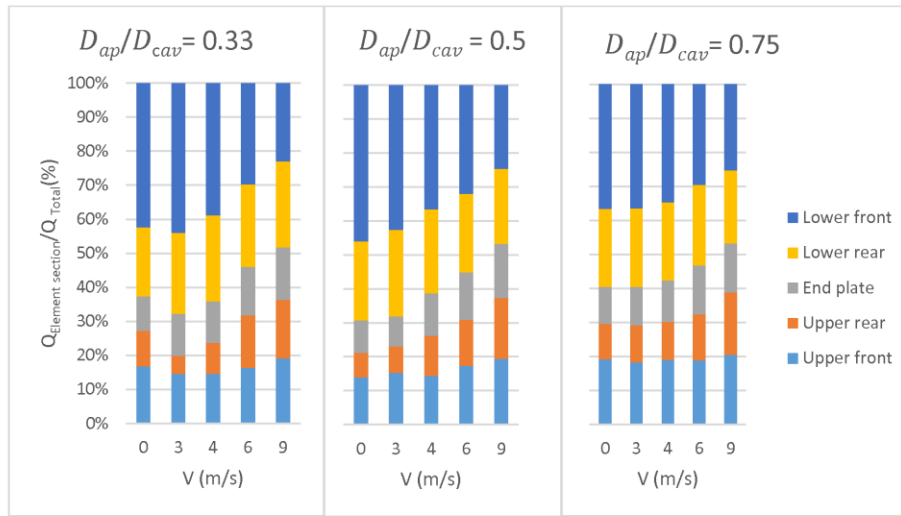


Figure 9: Fractional distribution of the total heat loss from each heater element section in the cavity surface plotted as a function of wind speeds for various aperture ratio. Conditions : temperature = 300°C, yaw = 0°, tilt = 15° and aspect ratio = 1.5.

3.3.2 Effect of wind speed and tilt angle

The absolute distribution of heat loss from each section of the heated cavity is shown in Figure 10 for various wind speeds and tilt angles. For a given wind speed, the total heat loss decreases with an increase in the tilt angle for almost all the cases investigated. However, there exists some combinations of wind speed and tilt angle for which the heat losses increase with the tilt angle. For the zero and low wind speed conditions, the percentage of heat loss from the front sections of the heated cavity is increased with the tilt angle. This is because an increase in the tilt angle causes an increase in the size of the stagnant zone near to the back of the cavity. This, in turn, decreases the natural convective heat losses from the rear sections. Hence, although the absolute heat losses from the front sections are similar, the fractional heat losses from the front sections increases with tilt angle. For the highest wind speed ($V = 9 m/s$, $1/Ri > 43$), the effect of tilt angle on the heat loss distribution of various sections of the heated cavity is very small with a change of $< 1.5%$ for any given rear section and $< 3.3%$ for any given front sections.

Figure 11 presents the heat loss at a given tilt angle normalised by that at 15° with the same wind speed. For the no wind speed condition, the heat loss from the 30° and 45° case are 83% and 77% of that of the 15° case respectively, which is as expected. However, $Q_{\phi}/Q_{\phi=15^{\circ}}$ exhibits a maximum for wind speed $1/Ri = 8$ to 19 ($V = 4$ to 6 m/s). The normalised heat loss for the 30° case is always below that for 100% for these cases. The maximum normalised heat loss of the 45° case is more than the 30° case and it is also above 100%, which was not expected. That is, increasing tilt angle above 30° has a negative effect on the overall heat loss. This will be compounded in practice, because the wind speed at the receiver increase with the tilt angle, since the tower height increases with tilt angle.

CHAPTER 6

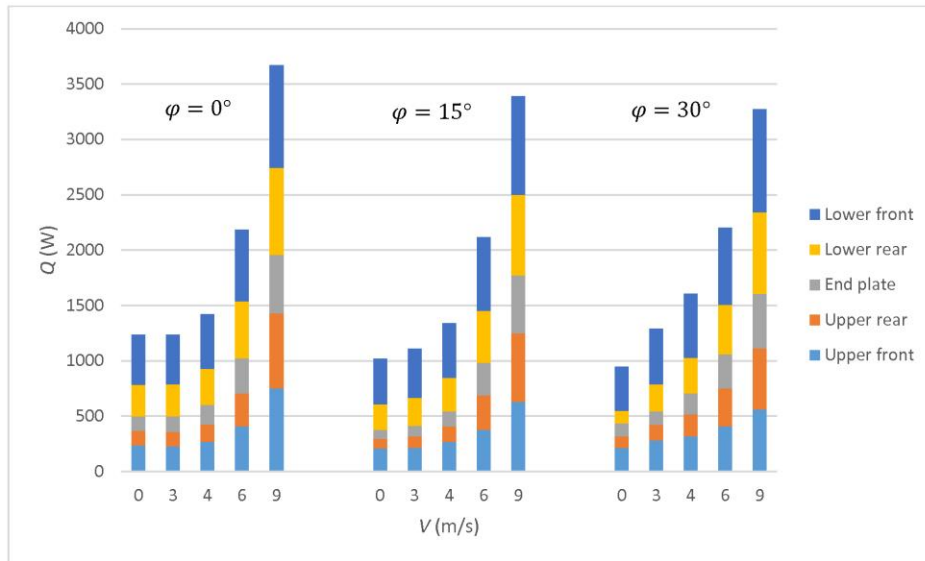


Figure 10: Distribution of the total heat loss from the various sections of the heated cavity plotted as a function of wind speed for three value of tilt angle. Conditions : temperature = 300°C, yaw = 0°, aperture ratio = 0.75 and aspect ratio = 1.5.

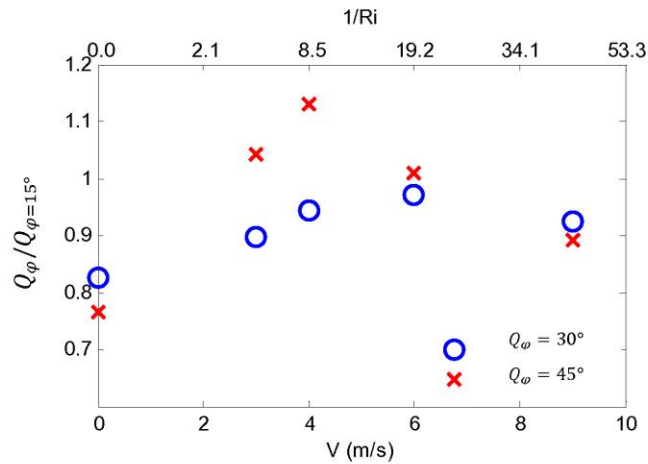


Figure 11: Normalised heat loss from the various sections of the heated cavity plotted for various wind speeds and tilt angle. Conditions: temperature = 300°C, yaw = 0°, aperture ratio = 0.75 and aspect ratio = 1.5.

4 Conclusions

In summary, the dependence of convective heat loss on wind speed, tilt angle and aperture ratio is complex and coupled, despite a general trend of increasing heat loss with wind speed as expected. Introducing a lip at the aperture plane, by decreasing D_{ap}/D_{cav} , acts to inhibit the natural convective losses (at zero wind speed) by up to a factor of 5, but increases the forced

CHAPTER 6

convection losses by a factor of up to 30%. More specifically, for tilt angle = 15° and $1/Ri < 4.8$ ($V < 3$ m/s), the convective heat losses increase with aperture ratio, although this behaviour reverses for $1/Ri > 19$ ($V > 6$ m/s). For the cases with a larger tilt angle of $\sim 30^\circ$, the effect of aperture ratio on convective heat loss is small.

For $1/Ri > 8.5$ ($V > 4$ m/s), the total heat losses are independent of D_{ap}/D_{cav} for a given value of $1/Ri$ to within 10%. On the other hand, for $1/Ri < 4.8$ ($V < 3$ m/s) the total heat loss can vary by up to about 75% by increasing the aperture ratio from 0.33 to 0.75.

For $1/Ri < 4.8$ ($V < 3$ m/s), about 60% of the total heat is lost from the lower section of the heated cavity for the 3 tested aperture ratios. Furthermore, approximately 43% of the heat is lost from the lower front section of the heated cavity for aperture ratio = 0.33 and 0.5, while this only approximately 36 % for the aperture ratio = 0.75 case. This difference is attributed to the decreased size of the stagnant zone at the rear of the cavity. Similarly, the increased uniformity in heat losses with an increase in wind speed is attributed to a decreased significance of the stagnant zone. The same is true for the increased fraction of heat losses from the upper section with an increase in D_{ap}/D_{cav} .

The effect of tilt angle on the total heat loss from the system was found to be relatively small. For $\varphi = 30^\circ$, the heat loss increases from 0 m/s to a local maximum at $1/Ri \approx 19$ ($V \approx 6$ m/s). However, it is always below that from 15° case for all tested wind speeds. Conversely, the heat loss for the 45° case is more than that from the 15° case for $4.8 < 1/Ri < 19$ ($3 < V < 9$ m/s). This shows that there is a slight advantage with respect to heat loss in keeping the tilt angle of a solar cavity below 30° .

Overall the configuration with a tilt angle of 30° has the minimum convective heat loss. Increasing tilt angle from 30° to 45° does not reduce the convective heat loss from the heated cavity for all cases, which is contrary to expectation based on previous work. In addition, although the aperture ratio does influence the convective heat loss, its influence is less than 15% over the range $0.33 < D_{ap}/D_{cav} < 1$ for a tilt angle of 30° and wind speed above 3 m/s. These data highlight the need to consider convective losses in optimising the size, shape and orientation of a cavity receiver, and for more detailed measurements of the flow-field with the cavity to better understand the mechanisms that drive these heat losses.

Acknowledgements

This research has been financed by the Australian Renewable Energy Agency (ARENA) and the University of Adelaide, through the Australian Solar Thermal Research Initiative (ASTRI), ARENA1-SRI002.

References

- Clausing, A 1981, 'An analysis of convective losses from cavity solar central receivers', *Solar energy*, vol. 27, no. 4, pp. 295-300.
- Clausing 1983, 'Convective losses from cavity solar receivers—comparisons between analytical predictions and experimental results', *Journal of Solar Energy Engineering*, vol. 105, no. 1, pp. 29-33.
- Clausing, A, Waldvogel, J & Lister, L 1987, 'Natural convection from isothermal cubical cavities with a variety of side-facing apertures', *Journal of heat transfer*, vol. 109, no. 2, pp. 407-412.
- Flesch, R, Stadler, H, Uhlig, R & Pitz-Paal, R 2014, 'Numerical analysis of the influence of inclination angle and wind on the heat losses of cavity receivers for solar thermal power towers', *Solar energy*, vol. 110, pp. 427-437.
- Holman, J 1997, *Heat transfer*, 8th edn, McGraw-Hill, New York.
- Hu, T, Jia, P, Wang, Y & Hao, Y 2017, 'Numerical simulation on convective thermal loss of a cavity receiver in a solar tower power plant', *Solar energy*, vol. 150, pp. 202-211.
- Kim, JK, Yoon, HK & Kang, YH 2009, 'Experimental study on heat loss from cavity receiver for solar power tower', *Proceedings of ISES World Congress 2007 (Vol. I–Vol. V)*, pp. 1719-1723.
- Kolb, GJ, Ho, CK, Mancini, TR & Gary, JA 2011, 'Power tower technology roadmap and cost reduction plan', *Sandia National Laboratories, Livermore, CA, Technical Report No. SAND2011-2419*.
- Lee, KL, Chinnici, A, Jafarian, M, Arjomandi, M, Dally, B & Nathan, G 2018, 'Experimental investigation of the effects of wind speed and yaw angle on heat losses from a heated cavity', *Solar energy*, vol. 165, pp. 178-188.
- Lee, KL, Jafarian, M, Ghanadi, F, Arjomandi, M & Nathan, GJ 2017, 'An investigation into the effect of aspect ratio on the heat loss from a solar cavity receiver', *Solar energy*, vol. 149, pp. 20-31.
- Ma, RY 1993, *Wind effects on convective heat loss from a cavity receiver for a parabolic concentrating solar collector*, Sandia National Laboratories.

CHAPTER 6

Medtherm, C 2000, 'Heat flux transducers and infrared radiometers for the direct measurement of heat transfer rates', viewed 09/04/17, <http://www.dr-kubelik.de/cms/tl_files/infomaterial/Heat_Flux_Transducer.pdf>.

Paitoonsurikarn, S, Taumoefolau, T & Lovegrove, K 2004, 'Estimation of convection loss from paraboloidal dish cavity receivers', *Proceedings of 42nd conference of the Australia and New Zealand solar energy society (ANZSES), Perth, Australia*.

Philibert, C 2010, *Technology roadmap: concentrating solar power*, OECD/IEA.

Siegel, R 2001, *Thermal radiation heat transfer*, vol. 1, CRC press.

Steinfeld, A & Schubnell, M 1993, 'Optimum aperture size and operating temperature of a solar cavity-receiver', *Solar energy*, vol. 50, no. 1, pp. 19-25.

Tanaka, N 2010, 'Technology Road Map, Concentrating Solar Power', *International Energy Agency*.

Wu, S-Y, Xiao, L & Li, Y-R 2011, 'Effect of aperture position and size on natural convection heat loss of a solar heat-pipe receiver', *Applied thermal engineering*, vol. 31, no. 14, pp. 2787-2796.

Xiao, L, Wu, S-Y & Li, Y-R 2012, 'Numerical study on combined free-forced convection heat loss of solar cavity receiver under wind environments', *International Journal of Thermal Sciences*, vol. 60, pp. 182-194.

CHAPTER 7

The Influence Of Wall Temperature Distribution, Wind Speed And Tilt Angle On The Heat Losses From A Heated Cavity

Statement of Authorship

Title of Paper	The influence of wall temperature distribution, wind speed and tilt angle on the heat losses from a heated cavity
Publication Status	<input type="checkbox"/> Published <input type="checkbox"/> Accepted for Publication <input checked="" type="checkbox"/> Submitted for Publication <input type="checkbox"/> Unpublished and Unsubmitted work written in manuscript style
Publication Details	Lee, KL, Chinnici, A, Jafarian, M, Arjomandi, M, Dally, B & Nathan, G, 'The influence of wall temperature distribution, wind speed and tilt angle on the heat losses from a heated cavity', Solar energy, (2018).

Principal Author

Name of Principal Author (Candidate)	Ka Lok Lee		
Contribution to the Paper	Developed the experiment, performed analysis on all data, interpreted data, wrote manuscript and acted as corresponding author.		
Overall percentage (%)	60%		
Certification:	This paper reports on original research I conducted during the period of my Higher Degree by Research candidature and is not subject to any obligations or contractual agreements with a third party that would constrain its inclusion in this thesis. I am the primary author of this paper.		
Signature		Date	29/06/2018

Co-Author Contributions

By signing the Statement of Authorship, each author certifies that:

- i. the candidate's stated contribution to the publication is accurate (as detailed above);
- ii. permission is granted for the candidate to include the publication in the thesis; and
- iii. the sum of all co-author contributions is equal to 100% less the candidate's stated contribution.

Name of Co-Author	Alfonso Chinnici		
Contribution to the Paper	Supervised development of the work , helped to evaluate and edit the manuscript		
Signature		Date	03/07/18

Name of Co-Author	Mehdi Jafarian		
Contribution to the Paper	Supervised development of the work , helped to evaluate the manuscript		
Signature		Date	02,07,2018.

CHAPTER 7

Name of Co-Author	Maziar Arjomandi		
Contribution to the Paper	Supervised development of the work , helped to evaluate the manuscript		
Signature		Date	2/07/2018

Name of Co-Author	Bassam Dally		
Contribution to the Paper	Supervised development of the work , helped to evaluate and edit the manuscript		
Signature		Date	2-07-2018

Name of Co-Author	Graham Jerrold Nathan		
Contribution to the Paper	Supervised development of the work , helped to evaluate and edit the manuscript		
Signature		Date	3/7/18

The influence of wall temperature distribution, wind speed and tilt angle on the heat losses from a heated cavity

Ka Lok Lee, Alfonso Chinnici, Mehdi Jafarian, Maziar Arjomandi, Bassam Dally, Graham Nathan

School of Mechanical Engineering, The University of Adelaide, SA 5005, Australia

E-mail address: ka.lee@adelaide.edu.au (K.L. Lee)

Authors email:

alfonso.chinnici@adelaide.edu.au (A. Chinnici)

mehdi.jafarian@adelaide.edu.au (M. Jafarian)

maziar.arjomandi@adelaide.edu.au (M. Arjomandi)

bassam.dally@adelaide.edu.au (B.B Dally)

graham.nathan@adelaide.edu.au (G.J. Nathan)

Abstract

An experimental investigation is presented of the effects of wind speed (0 - 9 m/s), yaw angle (0° and 90°), and tilt angle (90°, 15° and -90°) on the convective heat losses from a cylindrical cavity heated with different internal wall temperature distributions. The internal wall comprised 16 individually controlled heating elements to allow the distribution of the surface temperature to be well controlled, while the air flow was controlled with a wind tunnel. It is found that temperature distribution has a strong influence on the convective heat losses, with a joint dependence on the wind speed and its direction. For the no-wind and side-on wind conditions, the measured range of the heat losses varied by up to 50% with a change in the wall temperature distribution. However, for high head-on wind speeds, this variation reduced down to ~20%. In addition, the heat losses from downward tilted were ~3 times larger than the upward facing heated cavity (typical of tower-mounted and beam-down configurations, respectively) Also, the measured heat losses were found to be only slightly dependent on wind speed and direction in contrast with the downward tilted cases.

Keywords

Solar Cavity Receiver; Wind; Concentrated Solar Thermal; Convective Heat Loss

CHAPTER 7

Nomenclature

Symbols			
A	Area (m ²)	V	Wind speed (m/s)
β	Coefficient of thermal expansion (°C ⁻¹)	ν	Kinematic viscosity of air at reference temperature kg/(s.m)
D	Diameter (m)	α	Yaw angle or incoming wind direction (°)
ϵ	Emissivity coefficient of the internal wall surface	φ	Tilt angle of the cavity (°)
g	Gravity (m/s ²)		
Gr	Grashof number = $\frac{g\beta(T_{wall} - T_a)D_{cav}^3}{\nu^2}$	Subscript	
h_c	Convective heat transfer coefficient through the aperture (W/(m ² K))	a	Ambient
k	Thermal conductivity of air at reference temperature (W/(m. K))	as	Aspect
L	Length (m)	ap	Aperture
Nu	Nusselt number = $\frac{h_c D_{cav}}{k_{ref}}$	cav	Cavity
Q	Heat loss (W)	conv	Convection
R	Ratio	rad	Radiation
Re	Reynolds number = $\frac{VD_{cav}}{\nu}$	ref	Reference
Ri	Richardson number = $\frac{Gr}{Re^2} = \frac{g\beta(T_{wall} - T_a)D_{cav}}{\nu^2}$	tot	total
T	Temperature (°C)	w	Wall

1 Introduction

Despite the development of Concentrated Solar Thermal technologies has progressed, the understanding of the influence of wall temperature distribution and wind speed on the heat losses from a heated cavity remains limited. Over the last three decades, resulting in a marked increase in their deployment for power generation and in the development of novel approaches to utilise thermal energy for industrial processes (ASTRI 2017; Chinnici, A et al. 2016; Chinnici, Alfonso et al. 2015; Chinnici, A, Nathan & Dally 2018a, 2018b; Kolb et al. 2011; Philibert 2010; Tanaka 2010). The highly concentrated solar radiation, from a solar field, is collected by a solar receiver, which uses a heat transfer medium to efficiently absorb the radiation. Pre-commercial solar cavity receivers have been operated at temperatures on the order of 1000 °C during short-term trials, which offers potential to achieve higher thermal efficiency than is presently possible (Ávila-Marín, 2011; IEA-ETSAP and IRENA, 2013; Lovegrove et al., 2012; Price, 2003; Segal and Epstein, 2003; Steinfeld and Schubnell, 1993). However, these temperatures result in a significant increase in the heat losses (radiative and convective) from the receiver relative to commercial systems. However, while it is desirable to identify ways to decrease these losses, this is difficult to do because the underlying mechanisms controlling them are still poorly understood. Therefore, further research is required to deepen the understanding of the mechanisms influencing heat losses in solar receivers and, in particular, in solar cavity receivers. More specifically, new measurements are needed of the influence of the controlling parameters of receiver geometry (cavity aspect ratio, aperture ratio), wind speed and direction (yaw angle), cavity orientation (tilt angle), operating temperature, and wall temperature distribution. The overall objective is to meet this need.

A detailed review of previous experimental and numerical studies of the influence of these parameters on the heat losses from solar cavity receivers was reported by Ho and Iverson (2014) and Lee et al. (2018a). These reviews highlighted the role of wind speed and its direction and their strong influence on the mixed, natural and forced convective heat losses from a cavity receiver (Mokhtar, Marwan et al. 2014); (Clausing 1983; Flesch et al. 2015; Ho & Iverson 2014; Lee et al. 2018a; Ma 1993; Taumofolau et al. 2004; Wu et al. 2015). They also highlighted the strong coupling between the heat losses and the geometrical features of the receiver, namely aperture and aspect ratios (Ho & Iverson 2014; Lee et al. 2018b; Wu et al. 2010). In our previous work (Lee et al. 2018a, 2018b), we have systematically assessed the influence of wind speed, yaw angle, aperture ratio, tilt angle and cavity temperature on the convective heat losses from a heated cavity facing downward, for the case of a uniform temperature distribution over the surface of the cavity. These recent data provide further insights into the complex heat loss phenomenon from cavity receivers while also confirming trends from earlier works. However, the majority of presently available data, under well-defined conditions, only consider solar cavity receivers with a uniform wall temperature distribution. Although this approach simplifies the validation of engineering models, in reality, solar receivers are generally characterised by a varied heat flux along the walls of the cavity at different times of the day. Therefore, there is a need to better understand the influence of wall temperature distribution on the heat losses for a range of conditions of relevance to operation. Hence, the overall objective of the present investigation is to assess the effects of the joint

CHAPTER 7

dependencies between temperature distribution and wind speed on the heat losses through the aperture of a heated cavity receiver.

Understanding of the convective heat losses from cavity receivers has been advanced by the numerical studies, some of which have investigated the influence of the temperature distribution (uniform and non-uniform) on the radiation heat losses (Asselineau, Abbassi & Pye 2014; Gil et al. 2015; Sánchez-González, Rodríguez-Sánchez & Santana 2016; Steinfeld & Schubnell 1993). However, the absolute validity of these assessments is not yet known because no data has previously been available with which to validate them (Flesch et al. 2014; Hu et al. 2017; Lee et al. 2017; Paitoonsurikarn & Lovegrove 2003; Paitoonsurikarn, S & Lovegrove 2002; Paitoonsurikarn, Sawat et al. 2011; Wu, Xiao & Li 2011; Xiao, Wu & Li 2012). Furthermore, most previous numerical analyses on convective heat losses have been performed for a uniform wall temperature distribution, probably largely due to a lack of experimental data for model validation (Ho & Iverson 2014; Stalin Maria Jebamalai 2016). Therefore, the present investigation also aims to provide an experimental dataset of convective heat losses from a cavity receiver with uniform and non-uniform temperature distribution, under controlled conditions, to advance the development of the numerical tools needed for optimisation and scale-up.

Advancing understanding requires spanning a range of conditions, including orientation due to the dependence of natural convection on orientation. In addition, despite its lower popularity relative to the tower-mounted receiver due to disadvantages of an extra surface and anticipated higher cost (Kolb et al. 2011; Li, Dai & Wang 2015), the beam-down cavity solar receivers have continued to receive interest due to some (at least partly) compensating advantages. These include a lower wind speed and higher functionality (Leonardi 2012; Mokhtar, M 2011; Segal & Epstein 2008; Wei et al. 2013). Recent studies, utilising new solar field design have also reported good performance for beam-down applications (Li, Dai & Wang 2015; Mokhtar, Marwan et al. 2014). One of the perceived disadvantages of the beam-down configuration is the perceived high natural convective heat loss due to buoyancy (Holman 1997). On the other hand, a beam-up configuration offers the advantages of a beam down without the disadvantages of the secondary reflector, but at the additional cost of a taller tower. Hence all are worthy of further consideration. However, no experimental measurements are available that directly compare the convective heat losses from an upward facing heated cavity a downward facing cavity or a downward tilted heated cavity. For these reasons, we also aim to compare the effect of wind on the heat losses from a downward tilted and an upward facing receiver.

In light of the aforementioned gaps, the key aim of the present investigation is to provide direct measurements of the influence of temperature distribution, tilt angle and wind speed on the mixed convective heat losses from a solar cavity receiver. In particular, the research aims to investigate; i) the effects of the temperature distribution on the convective heat losses as a function of wind speed and direction; ii) the convective heat losses for an upward facing cavity and a downward tilted one (15°) and its effect on the cavity's thermal performance.

2 Methodology

The details of the experimental arrangement used in the study have been published previously by Lee et al. (2018a) so that only a brief overview is shown here. The experimental arrangement has also been reported previously so that it reproduced in the supplement here (Figure S1). A cavity was electrically heated and located within the open section of the University of Adelaide's wind tunnel to generate negligible blockage. The external dimensions of the cavity have a maximum projected area ($\sim 0.249 \text{ m}^2$) of $\sim 4.1\%$ of the wind tunnel, which has a cross-sectional dimension of area $2.75 \text{ m} \times 2.19 \text{ m}$. This is approximately 330 times larger than the projected area of the aperture, which is approximately 0.018 m^2 . Air was used as the working fluid and the velocity in the tunnel was measured using a multi-hole pressure probe from the Turbulent Flow Instrumentation (Lee et al. 2018a). Figure S1b presents the key dimensions of the cavity, which has an inner diameter $D = 0.3 \text{ m}$ with an aperture ratio $R_{ap} = 0.00$ and 0.50 and aspect ratio $R_{as} = 1.5$. The details of the method of recording the power and its errors are reported by Lee et al. (2018a)

The influence on the heat losses was assessed systematically for wind speeds of $V = 0, 3, 6$ and 9 m/s , yaw angle of $\alpha = 0^\circ$ and 90° , 5 profiles of temperature distribution, and tilt angles of $\varphi = 90^\circ, 15^\circ$ and -90° , as shown in Figure S1. This leads to a total of 112 combinations of wind speed, tilt angle, yaw angle and temperature distribution. A summary of the conditions is presented in Table 1. 56 for the case with the aperture opened (to measure the convective and radiative heat losses), and for the 56 cases with the aperture closed (to measure the heat loss through the walls).

Normalised heat loss for the no wind case $Q/Q_{V=0}$ was used to characterise the effect of wind on the heat loss through the aperture. This is defined as the total heat loss through the aperture relative to that for the no wind condition for various temperature distribution, as shown in Table 1 and Table 2. The total heat losses through the aperture for no wind condition is the combination of convective and radiative heat loss at zero wind speed.

Another normalised heat loss for the uniform temperature case $Q/Q_{T=uniform}$ was used to assess the effect of temperature distribution on the heat loss through the aperture. $Q/Q_{T=uniform}$ is defined as the total heat losses through the aperture over the total heat losses through the aperture for the 300°C uniform temperature case for various wind speeds. These were performed with the average temperature of the cavity was kept constant at 300°C .

The air properties, such as thermal expansion, density and kinematic viscosity, were calculated at a reference temperature T_{ref} , which is defined as

$$T_{ref} = \frac{T_w}{2} + \frac{T_a}{2}. \quad (1)$$

Here T_w is the internal wall temperature and T_a is the ambient temperature.

The main uncertainties in the measured data are summarised below, the details are reported by Lee et al. (2018a). The maximum uncertainty of the power output from each heater is $\pm 25 \text{ W}$ ($\sim 3.1\%$), which includes that from the power and temperature measurement ($\pm 0.5^\circ\text{C}$) and their

CHAPTER 7

effect on the feedback control system. Although the total maximum uncertainty is $\sim \pm 400\text{W}$, the average error is less than $\pm 3.1\%$ of the maximum power. This is because the random error is reduced by using the 16 results from the heaters. In addition, the uncertainty of the incoming wind speed is estimated to be $\pm 0.2\text{m/s}$.

Table 1: List of experimental conditions

Velocity V (m/s)	Yaw angle α ($^\circ$)	Tilt angle φ ($^\circ$)	Temperature of the wall T_w ($^\circ\text{C}$)	Aspect ratio $(\frac{L_{cav}}{D_{cav}})$	Aperture ratio $(\frac{D_{ap}}{D_{cav}})$
0,3,6 and 9	0	15	5 various distributions	1.5	0.0 and 0.5
0,3,6 and 9	90	15	4 various distributions	1.5	0.0 and 0.5
0,3,6 and 9	0	-90	3 various distributions	1.5	0.0 and 0.5
0	0	90	100, 200, 300 and 400	1.5	0.0 and 0.5
0	0	15	100, 200, 300 and 400	1.5	0.0 and 0.5
0	0	-90	100, 200, 300 and 400	1.5	0.0 and 0.5

The list of set point temperature for each heater position for various temperature distribution is given in Table 2, while the position can be found in the supplement Figure S2. The temperatures were firstly estimated analytically as a starting point, then the final set point temperatures were chosen based on trial and error in the experiment. This is because it is very complex to analytically estimate the temperature for various temperature distribution and wind conditions. In this study, the range of temperatures is designed to be as wide as possible with the limitation of keeping the maximum variation of the average temperature to be $\pm 10^{\circ}\text{C}$ for the various wind conditions. Although the maximum variation of the average temperature was set at $\pm 10^{\circ}\text{C}$, 90% of the cases are less than $\pm 5^{\circ}\text{C}$ and 80% of the cases are less than $\pm 3^{\circ}\text{C}$. The 10, 5 and 3 $^{\circ}\text{C}$ of error will give a maximum of 3.7%, 1.9% and 1.1% of error in power respectively. The cases with the large temperature difference are the cases with low wind speed and the hotter position away from the aperture. This is because the heat transfer between the hot air near the back of the cavity and ambient air is very low for the low wind speed condition.

Table 2 list of setpoint temperature of each heater position for various conditions

Temperature of the internal walls ($^{\circ}\text{C}$)		Wall position															
Temperature distribution	TA	TB	TC	TD	TE	TF	BA	BB	BC	BD	BE	BF	EA	EB	EC	ED	Average
Head-on $\alpha = 0^{\circ}$ $\varphi = 15^{\circ}$	Uniform	300	300	300	300	300	300	300	300	300	300	300	300	300	300	300	300
	Upper hotter	340	350	360	375	390	400	260	250	240	225	210	200	300	300	300	300
	Lower hotter	260	250	240	225	210	200	340	350	360	375	390	400	300	300	300	300
	Front hotter	275	250	250	300	350	400	250	225	250	300	350	400	300	300	300	300
Side-on $\alpha = 90^{\circ}$ $\varphi = 15^{\circ}$	Rear hotter	350	400	325	275	250	350	400	325	275	225	200	300	300	300	300	300
	Uniform	300	300	300	300	300	300	300	300	300	300	300	300	300	300	300	300
	Upper hotter	340	350	360	375	390	400	260	250	240	225	210	200	300	300	300	300
	Front hotter	275	250	250	300	350	400	250	225	250	300	350	400	300	300	300	300
Beam-down $\alpha = N/A$ $\varphi = -90^{\circ}$	Rear hotter	350	400	325	275	250	350	400	325	275	225	200	300	300	300	300	300
	Uniform	300	300	300	300	300	300	300	300	300	300	300	300	300	300	300	300
	Front /near aperture hotter	250	250	250	300	350	400	250	250	300	350	400	300	300	300	300	300
	Rear /near back wall hotter	325	400	325	275	250	325	400	325	275	250	225	200	300	300	300	300

3 Results

3.1 Head-on wind

The effect of wind speed in the head-on direction, together with that of wall temperature distribution on the convective heat losses through the aperture of a heated cavity is presented in Figure 1. For low wind speed conditions ($Ri < 4.8$, $V < 3\text{m/s}$), the cases featuring the ‘lower section hotter’ and ‘front section hotter’, have a higher convective heat loss than the other cases, including that of the uniform distribution. The higher losses of the ‘lower section hotter’ case, can be deduced to be associated with the added role of natural convection, that is of buoyancy. The higher loss from the ‘front section hotter’ case suggest that close the proximity of the hotter part of the wall to the aperture facilitates increased egress of the hot air than for the reference case. Similarly, for high wind speed condition ($Ri > 19$, $V > 6\text{m/s}$), the ‘front section hotter’ case has the highest measured value of the convective heat loss among all the cases investigated. On the other hand, the ‘lower section hotter’ case features the lowest convective heat loss for high wind speeds. This suggests that a greater fraction of the power lost from the lower section is transferred under these conditions to maintain the temperature of the upper and rear sections. Further evidence for this can be found from our previous study (Lee et al. 2017), which identified a strong flow recirculation transporting the hot air from the lower section toward the rear and the upper section before it leaves the cavity. This flow pattern reduces that heat lost from the other surfaces, and hence the power required to maintain the set point temperature of the lower temperature surface. Therefore, the qualitative trends from the CFD are consistent with the measured trend that the ‘lower section hotter’ case has the lowest convective heat loss behaviour of the cases assessed here for high wind speed condition.

The dependence of the convective heat losses, normalised by the case for no wind on wind speed is presented in Figure 2 for the same conditions as those reported in Figure 1. It can be seen that varying the wall temperature distribution causes up to 50% change in the total natural convection. The ‘upper section hotter’ case has the lowest convective heat loss where natural convection dominates. For $V > 3\text{ m/s}$, the heat transfer moves to the mixed convection regime which greatly reduces this range to $< 20\%$. Consistent with this trend, the ‘lower section hotter’ case has the highest loss for the lower wind speed case and lowest loss for high wind speed. However, the ‘upper section hotter’ case has the lowest average convective heat loss in the range of wind speeds investigated. For the cases with $V > 6\text{ m/s}$ the heat loss plateaus and tends to become independent of the temperature distribution, which also implies that it tends toward that of the uniform temperature distribution case. That is, the shape of the temperature distribution becomes relatively unimportant in the inertia-dominated regime.

CHAPTER 7

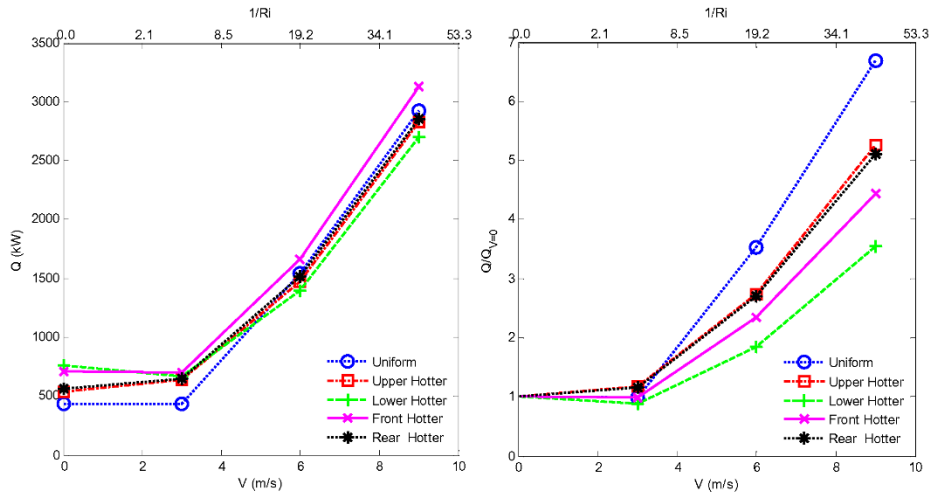


Figure 1 Dependence of the heat losses through the aperture on wind speed for a series of wall temperature distributions. Conditions: tilt angle of 15°, yaw angle of 0°, aperture ratio of 0.5 and aspect ratio of 1.5.

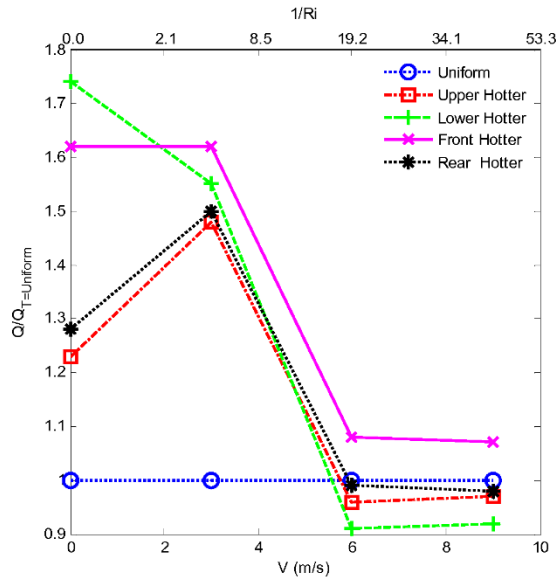


Figure 2 Dependence of the normalised heat losses through the aperture in wind speed for a series of wall temperature distributions. Conditions: tilt angle of 15°, yaw angle of 0°, aperture ratio of 0.5 and aspect ratio of 1.5.

3.2 Side-on wind

The influence of wind speed on the convective heat losses through the aperture for the side-on direction is presented in Figure 3 for several types of wall temperature distribution. The ‘front

section hotter' case has the highest convective heat loss for most of the cases, similar to the head-on wind cases. However, the 'rear section hotter' cases feature the lowest convective heat loss, which is different from the head-on wind cases. This can be attributed to the fact that the relatively cold wind does not penetrate as far into the cavity for the transverse direction as for the head-on direction. This deduction is reasonable for this configuration in which the cavity has an aspect ratio of 1.5 and an aperture ratio of 0.5 so that the distance between the aperture and the back section is 3 times that of the aperture diameter. Hence the 'rear section hotter' case is likely to have the lowest heat loss for those configurations in which a relatively quiescent zone is established at the rear of the chamber.

Figure 4 presents the same data as Figure 3, except that convective heat losses is normalised by the reference case of uniform wall temperature. This highlights the importance of wind speed on the effect of temperature distribution on the normalised convective heat loss. The 'rear section hotter' case has ~40% less convective heat losses than does the distribution with the highest convective loss for all wind speeds assessed here.

Figure 4 also shows that the convective heat losses, which occur in the low wind speed range ($0 < V < 6 \text{ m/s}$, $0 < Ri < 19$) are less than the natural convection. This trend can be attributed to the generation by a side-on wind of a natural "aerodynamic seal" or "air curtain", which helps to mitigate the heat loss from the cavity. However, for $V > 6 \text{ m/s}$, the momentum of the transverse flow becomes so strong that it drives a mixing process between the cold wind and hot air inside the cavity that dominates of the "air curtain". Therefore, the convective heat loss increases strongly with the wind speed, for $V > 6 \text{ m/s}$.

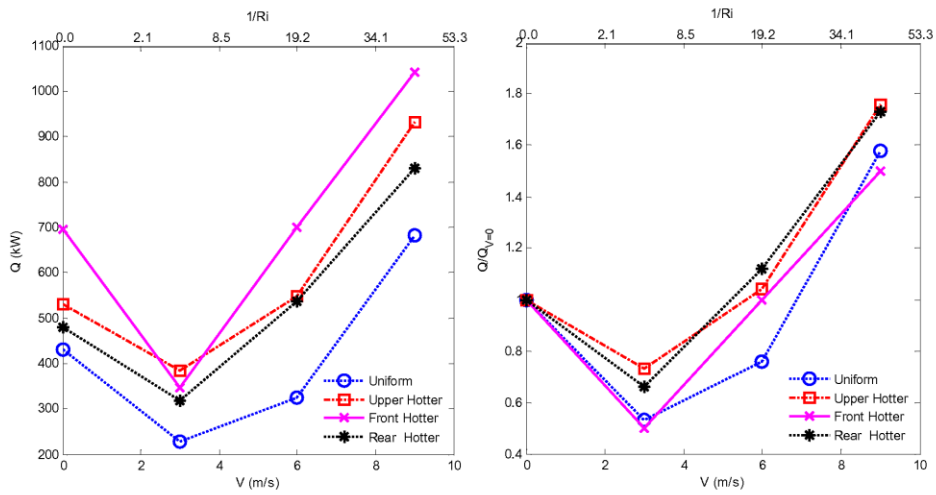


Figure 3 Dependence of the heat losses through the aperture on wind speed for a series of wall temperature distributions. Conditions: tilt angle of 15° , yaw angle of 90° , aperture ratio of 0.5 and aspect ratio of 1.5.

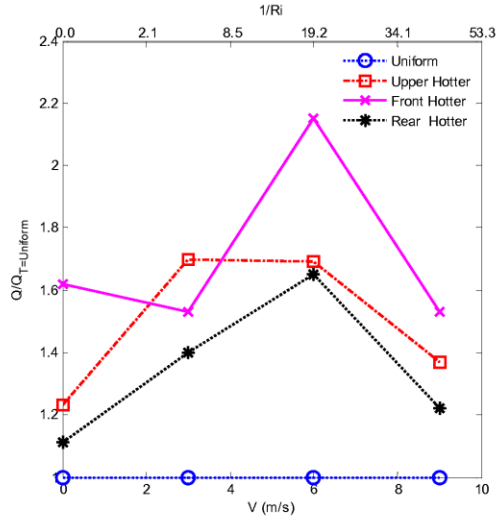


Figure 4 Dependence of the normalised heat losses through the aperture on wind speed for a series of wall temperature distributions. Conditions: tilt angle of 15° , yaw angle of 90° , aperture ratio of 0.5 and aspect ratio of 1.5.

3.3 Upward facing cavity

The influence of wind speed on the convective heat losses through the aperture of an upward facing heated cavity is presented in Figure 5 for three different wall temperature distribution. The convective heat loss through the aperture increases non-linearly with the wind speed, and the case with the hotter surface near to the aperture has the highest heat losses through the aperture, which is consistent with the other cases. The heat losses through the aperture for the ‘near aperture hotter’ cases are approximately 150W higher than the ‘back wall hotter’ cases for all tested wind conditions. It is noteworthy that the wind speed has a particularly strong influence for the upward facing cavity. The convective power losses increase by approximately 50% when the wind speed is increased from 0 to 3 m/s (Ri from 0 to 4.8). For the high wind speed condition ($Ri > 43, V > 9\text{m/s}$), the heat losses are ~ 5 times greater than the natural convection cases. The upward facing solar cavity receiver is also likely to place closer to the ground than the tower mounted case, where it is less windy than the downward facing cavity, which will further reduce the convective heat loss. In addition, the influence of wind is likely to be easier to mitigate by shielding for an upward facing cavity than a tilted one, since the wind direction is always normal to the cavity axis for the vertical orientation but varies in three dimensions for the tilted case.

In contrast to Figure 3 in which the side-on wind was found to initially decrease convective losses for the tilted receiver, this reduction does not occur for the vertical orientation although the wind direction is also perpendicular to the aperture. This is consistent with the vertical orientation avoiding the strong adverse mechanism of the near horizontal orientations in which natural convection establishes a strong recirculation through the aperture.

Figure 6 presents for the vertical orientation the convective heat losses for the three temperature distributions normalised by the case with the uniform wall temperature. The shape of the temperature distribution can be seen to change the total convective heat losses by up to ~60%, which is more significant than the tilted cases. However, the impact of the shape of the temperature distribution decreases with an increase in wind speed to less than 20% for high wind speed condition ($Ri > 43, V > 9 \text{ m/s}$). The total convective heat losses converge with an increase in wind speed to a value that approaches the uniform temperature distribution case. This gives further evidence that both the orientation and temperature distribution become unimportant at sufficiently high wind speeds aligned normal to the cavity axis.

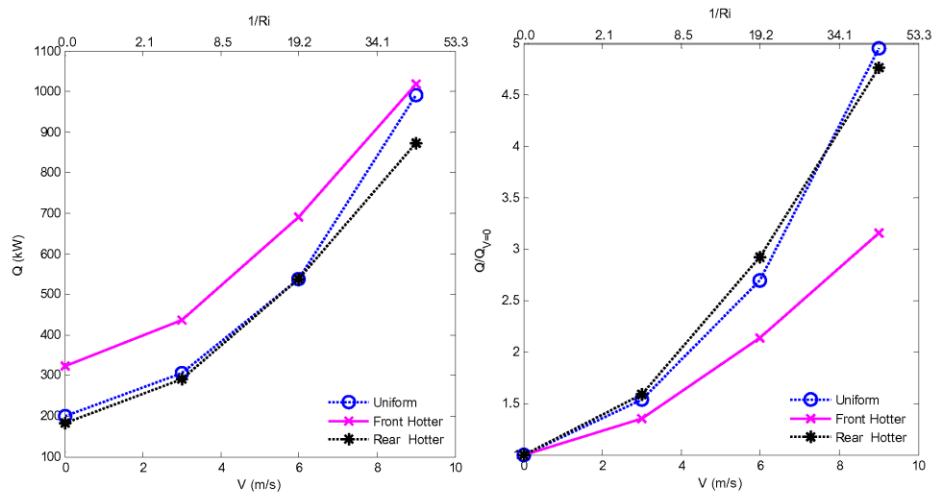


Figure 5 Dependence of the heat losses and normalised heat loss wind speed through the aperture on wind speed for a series of wall temperature distributions. Conditions: tilt angle of -90° , yaw angle of 0° , aperture ratio of 0.5 and aspect ratio of 1.5.

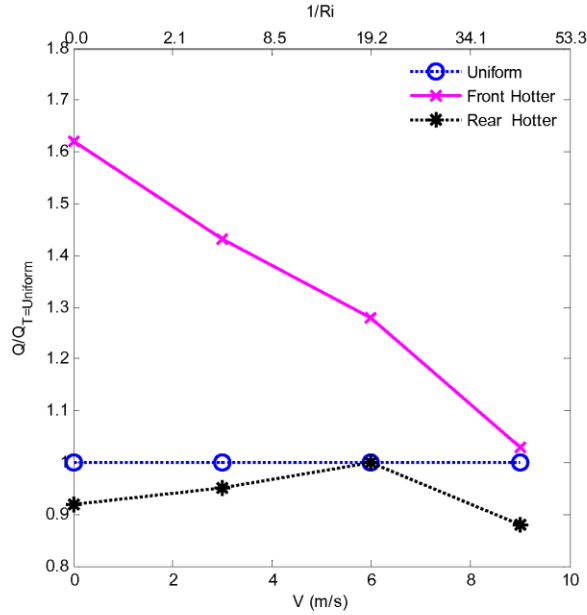


Figure 6 Dependence of the normalised heat losses through the aperture on wind speed for a series of wall temperature distributions. Conditions: tilt angle of -90° , yaw angle of 0° , aperture ratio of 0.5 and aspect ratio of 1.5.

3.4 Temperature and tilt angle

The combined effects of temperature and tilt angle of a heated cavity on convective heat losses through the aperture of a heated cavity are present in Figure 7, incorporating both the beam up ($\varphi = 90^\circ$) and beam down ($\varphi = -90^\circ$) cases. It can be seen that the beam-up has the lowest convection losses as expected, being only 30-40% that of the beam-down. Also the heat loss through the aperture increase non-linearly with temperature. This effect, which is observed for all of the tested tilt angles cases, appears to be related to the influence of radiation heat loss, which has a fourth order dependence on temperature. Worth noting is that the heat loss from the aperture has a complex dependence on tilt angle. The heat losses from the 15° tilted cavity are higher than both the 90° and -90° cases. This indicates that there is at least one tilt angle which will have the highest convective heat loss, although further work is required to determine this. However, this angle is likely to also depend on the cavity dimensions. That is, the heat loss from the $\varphi = -90^\circ$ case may not necessarily be less than the 15° for all geometries, but is expected to depend on the geometry of the cavity, such as aspect ratio and aperture ratio (Bilgen & Oztop 2005). However, the trend is independent of temperature, because the same trend can be observed in Figure 7a for all tested temperatures.

CHAPTER 7

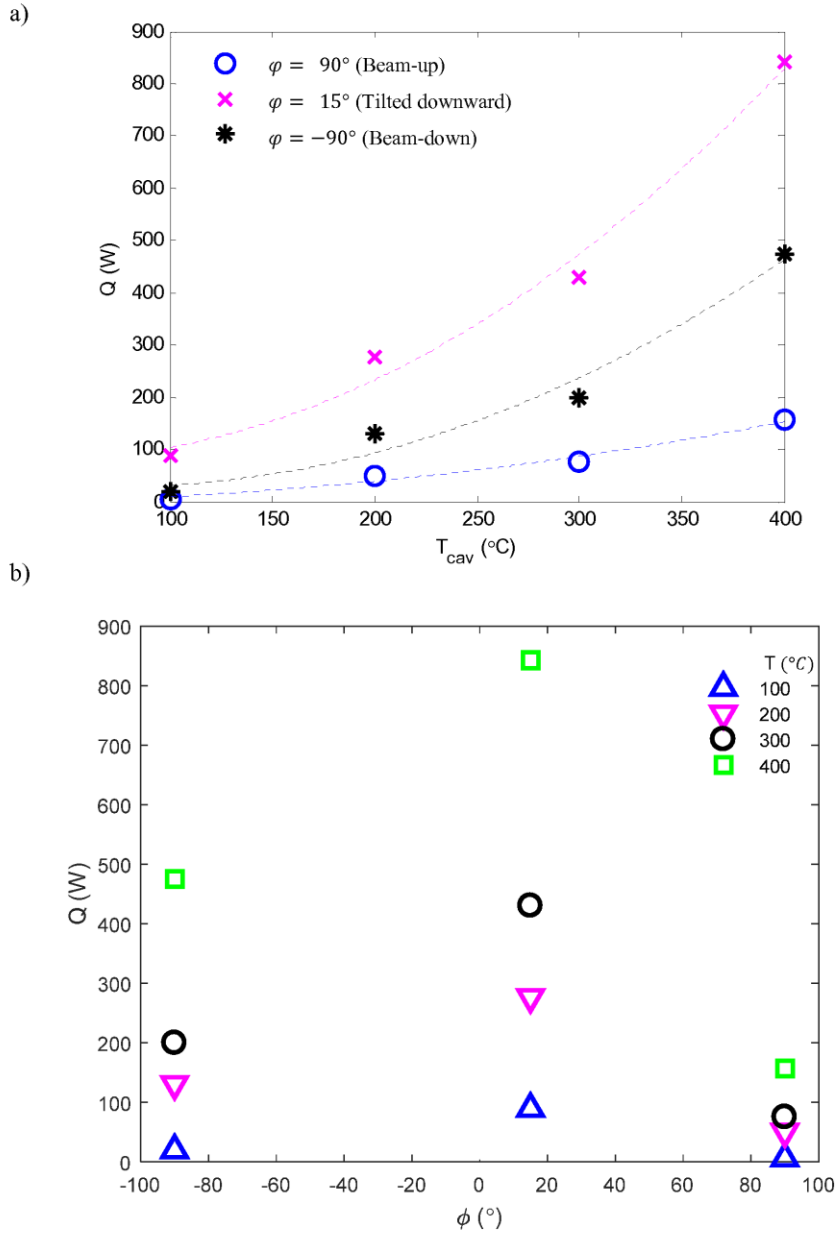


Figure 7 Dependence of the heat losses through the aperture of a heated cavity on temperature and tilt angle. Conditions: no wind, aperture ratio of 0.5 and aspect ratio of 1.5.

The effect of wind speed on normalised heat losses by natural convection for the beam-down case, for various wind directions and the tilt angles is presented in Figure 8. The natural

convection of the ‘beam-down’ was chosen to be the reference case because it has the lowest heat losses. The figure shows that the ‘downward tilted cavity with side-on wind’ case has a very similar trend with the ‘beam-down’ case for wind speed $Ri > 4.8$. This is because, for both cases, the air/ wind flows parallel to the aperture plane. Therefore the flow pattern is expected to be similar for all wind speeds. For these 2 conditions, the increase in heat losses at high wind speed ($Ri < 43$) is up to 4.5 times the value of the natural convection of the ‘beam-down’ case. However, the influence of wind speed on heat losses through the aperture is very high for the head-on wind speed cases, to reach up to 12 times that of the reference case. This highlights the potential benefits of being able to mitigate convective heat loss from for head-on wind directions.

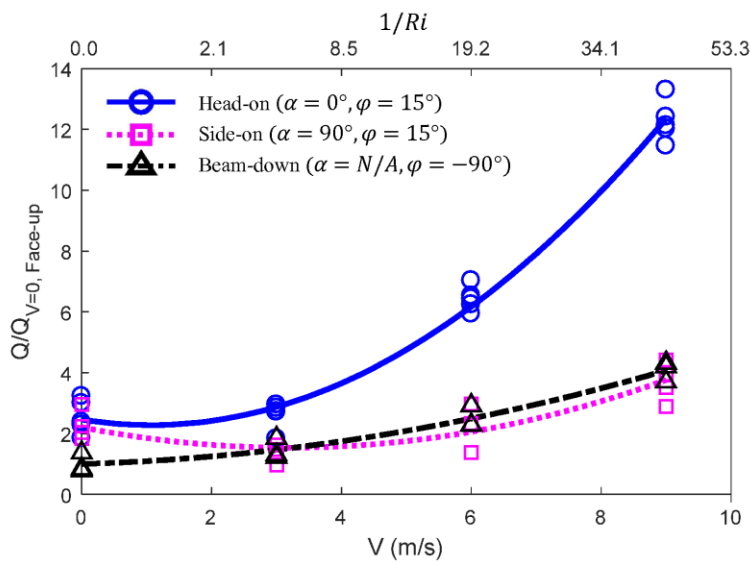


Figure 8 Dependence of the normalised heat losses by natural convection of the ‘beam-down’ case on wind speed for a series of tilt and yaw angles. Conditions: aperture ratio of 0.5 and aspect ratio of 1.5.

The dependence of the inverse of Richardson number on the Nusselt number is presented in Figure 9 for three orientation. It can be seen that the data all collapse very well for the head-on case and quite well for the beam-up case, but is much more complex for the side-on orientation. A strong local minimum in the heat losses at $1/Ri \sim 5$ is clearly observed for of the side-on direction and a very weak minimum is present for a few cases in the head-on direction. This shows that a low velocity cross-flow can inhibit the buoyancy-driven transport of gas through the aperture when the cavity is tilted slightly downward. However, for an upward facing cavity, there is no stagnant zone so that a slight wind does not inhibit buoyancy for this case. Worth noting is that the heat losses from the head-on wind speed case does not vary much between the first 2 data points. Insufficient data are available to identify whether or not a local minimum or maximum is present between $0 < Ri < 5$. In addition, it is also noted that, for high wind speed the heat losses from the head-on cases are about 4 times larger than the side-on cases, agreeing with our earlier study (Lee et al. 2018a). The data also suggests that there may be a

local minimum at $1/Ri \sim 1.25$ for the head-on cases. Figure 9a also shows that, Nu has near linear dependency relationship with $1/Ri$ for $1/Ri > 10$ for the head-on case, hence this behaviour is also expected $1/Ri > 40$ for the side-on cases.

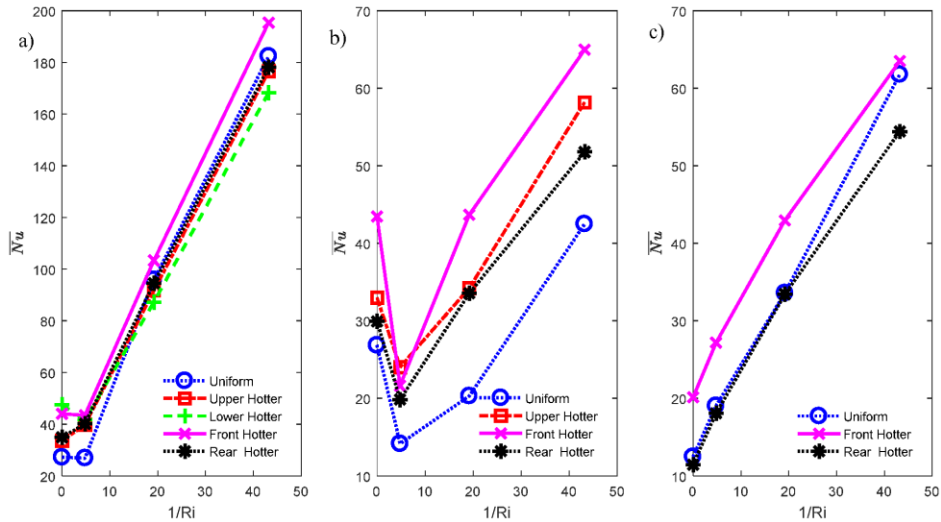


Figure 9 Dependence of the Nusselt number of a heated cavity on the inverse of Richardson number for a series of wall temperature distributions. Conditions: aperture ratio of 0.5, aspect ratio of 1.5, a) head-on ($\alpha = 0^\circ$ and $\varphi = 15^\circ$), b) side-on ($\alpha = 90^\circ$ and $\varphi = 15^\circ$) and c) beam-down ($\alpha = N/A$ and $\varphi = -90^\circ$).

4 Conclusions

The dependence of convective heat loss on wind speed, yaw angle, tilt angle and temperature distribution from a cavity receiver of various geometrical parameters were investigated experimentally in this study. Results point to a complex and joint relationship between the heat loss and the various operating parameters. It is found that there is no heat flux profile that exhibits the best or worst convective heat flux for all orientation. For the downward tilted cavity with the ‘lower surface hotter’ conditions exhibited the maximum heat loss for no wind condition, but minimum heat loss for high wind speed. For this orientation, the ‘upper surface hotter’ cases have the best overall performance for various head-on wind directions, but for the side wind, the convective losses are lowest with the hottest surface at the back. For the beam down case, the heat losses at zero wind were lower with heat flux peaking at the back of the cavity. For the downward tilted cavity, the head-on wind direction has the highest convective losses, which can be ~ 3 times larger than the side-on wind cases. In general, the heat losses from a downward tilted solar cavity receiver ($\varphi = 15^\circ$) tend to be minimised with the upper or rear surface to be hottest. This outcome should be further investigated with the solar optical system.

In general, the convective losses are lowest for the beam-up orientation as expected, but the downward tilted solar cavity receiver ($\varphi = 15^\circ$) has greater losses than the beam down, even

CHAPTER 7

at zero wind, which contradicts the expectation from the literature. Indeed for the high wind conditions, the heat loss from the upward facing cases is approximately 3 times less than the downward tilted cases for head-on wind condition. The main reason for this difference is that the wind direction is always normal to the cavity for the beam-up and beam-down orientations, which is the orientation with the lowest convective losses. These configurations avoid the wind flowing directly into the cavity, which has the greatest convective losses. Furthermore, at high wind speeds, which corresponds to high inverse Richardson number, the heat transfer is momentum dominated, so that the heat losses are controlled by orientation relative to the wind, irrespective of the direction of gravity. Nevertheless, for the downward tilted case, the heat flux profile remains important for convective losses even for the side-on wind case, and is lowest for the uniform temperature case.

Finally, the heat loss from a beam down cavity receiver has a nearly linear dependence on $1/Ri$ throughout the range. This linear dependence shows that natural convection is not significant anywhere. For the downward tilted orientation, the relationship becomes linear for higher wind speed, where momentum dominates over natural convection. The study also suggested that there may be a local minimum of heat loss at $1/Ri \sim 1.25$ for the head-on cases. However, this wind speed is out of the range of the wind tunnel of this study, so requires further work to confirm.

Acknowledgements

This research has been financed by the Australian Renewable Energy Agency (ARENA) and the University of Adelaide, through the Australian Solar Thermal Research Initiative (ASTRI), ARENA1-SRI002.

Supplement

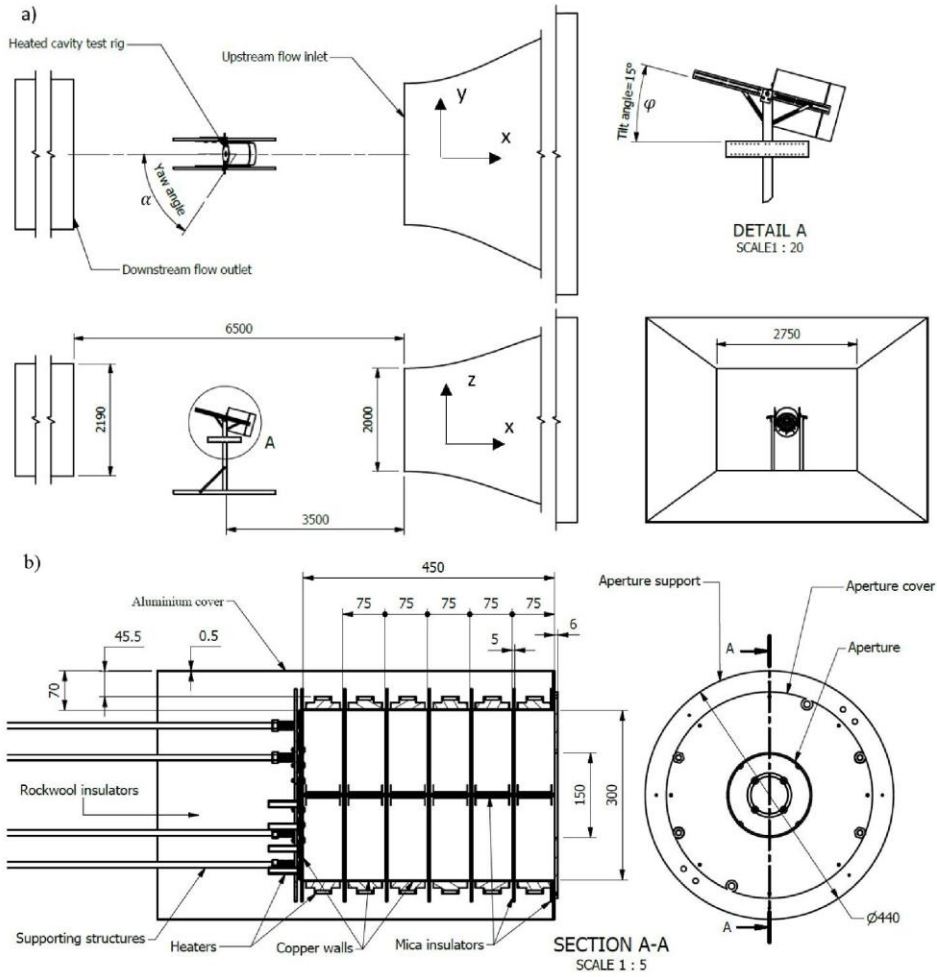


Figure S1 Schematic diagram of a) the heated cavity in the Thebarton wind tunnel and b) the dimensions of the receiver.

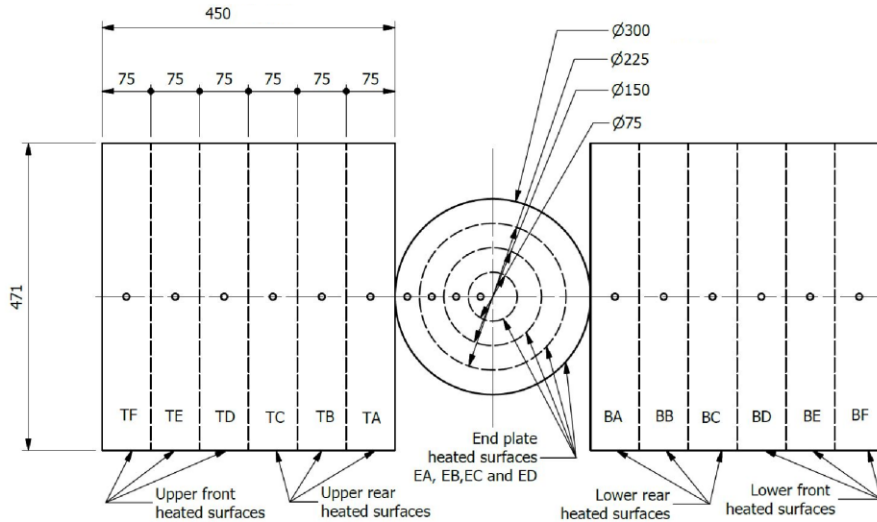


Figure S2 Schematic diagram of the simplified configuration of the internal copper wall surface of the heated cavity (shown unrolled view). The thermocouples are shown as small circles. Please notice that, for the cavity facing upward cases (tilt angle = -90°), upper heaters are the downstream heaters and lower heaters are the upstream heaters.

References

Asselineau, C-A, Abbassi, E & Pye, J 2014, 'Open cavity receiver geometry influence on radiative losses', *Proceedings of Solar2014, 52nd Annual Conference of the Australian Solar Energy Society, Solar2014, ed.(Melbourne, 2014)*.

ASTRI 2017, *ASTRI Milestone 12 Report- For Public Dissemination*, Australian Solar Thermal Research Initiative, <<http://www.astri.org.au/wp-content/uploads/2018/04/iii-ASTRI-M12-2017-Public-Dissemination-Report.pdf>>.

Bilgen, E & Oztop, H 2005, 'Natural convection heat transfer in partially open inclined square cavities', *International Journal of Heat and Mass Transfer*, vol. 48, no. 8, pp. 1470-1479.

Chinnici, A, Arjomandi, M, Tian, Z & Nathan, G 2016, 'A novel solar expanding-vortex particle reactor: experimental and numerical investigation of the iso-thermal flow field and particle deposition', *Solar energy*, vol. 133, pp. 451-464.

CHAPTER 7

Chinnici, A, Arjomandi, M, Tian, ZF, Lu, Z & Nathan, GJ 2015, 'A novel solar expanding-vortex particle reactor: influence of vortex structure on particle residence times and trajectories', *Solar energy*, vol. 122, pp. 58-75.

Chinnici, A, Nathan, G & Dally, B 2018a, 'Experimental demonstration of the hybrid solar receiver combustor', *Applied Energy*, vol. 224, pp. 426-437.

——— 2018b, 'An experimental study of the stability and performance characteristics of a Hybrid Solar Receiver Combustor operated in the MILD combustion regime', *Proceedings of the Combustion Institute*.

Clausing, A 1983, 'Convective losses from cavity solar receivers—comparisons between analytical predictions and experimental results', *Journal of Solar Energy Engineering*, vol. 105, no. 1, pp. 29-33.

Flesch, R, Stadler, H, Uhlig, R & Hoffschmidt, B 2015, 'On the influence of wind on cavity receivers for solar power towers: An experimental analysis', *Applied thermal engineering*, vol. 87, pp. 724-735.

Flesch, R, Stadler, H, Uhlig, R & Pitz-Paal, R 2014, 'Numerical analysis of the influence of inclination angle and wind on the heat losses of cavity receivers for solar thermal power towers', *Solar energy*, vol. 110, pp. 427-437.

Gil, R, Monné, C, Bernal, N, Muñoz, M & Moreno, F 2015, 'Thermal Model of a Dish Stirling Cavity-Receiver', *Energies*, vol. 8, no. 2, pp. 1042-1057.

Ho, CK & Iverson, BD 2014, 'Review of high-temperature central receiver designs for concentrating solar power', *Renewable and Sustainable Energy Reviews*, vol. 29, pp. 835-846.

Holman, J 1997, *Heat transfer*, 8th edn, McGraw-Hill, New York.

Hu, T, Jia, P, Wang, Y & Hao, Y 2017, 'Numerical simulation on convective thermal loss of a cavity receiver in a solar tower power plant', *Solar energy*, vol. 150, pp. 202-211.

Kolb, GJ, Ho, CK, Mancini, TR & Gary, JA 2011, 'Power tower technology roadmap and cost reduction plan', *Sandia National Laboratories, Livermore, CA, Technical Report No. SAND2011-2419*.

Lee, KL, Chinnici, A, Jafarian, M, Arjomandi, M, Dally, B & Nathan, G 2018a, 'Experimental investigation of the effects of wind speed and yaw angle on heat losses from a heated cavity', *Solar energy*, vol. 165, pp. 178-188.

CHAPTER 7

— 2018b, 'Experimental investigation of the effects of wind speed, aperture ratio and tilt angle on the heat losses from a heated cavity', *Solar energy*, vol. under review.

Lee, KL, Jafarian, M, Ghanadi, F, Arjomandi, M & Nathan, GJ 2017, 'An investigation into the effect of aspect ratio on the heat loss from a solar cavity receiver', *Solar energy*, vol. 149, pp. 20-31.

Leonardi, E 2012, 'Detailed analysis of the solar power collected in a beam-down central receiver system', *Solar energy*, vol. 86, no. 2, pp. 734-745.

Li, X, Dai, Y & Wang, R 2015, 'Performance investigation on solar thermal conversion of a conical cavity receiver employing a beam-down solar tower concentrator', *Solar energy*, vol. 114, pp. 134-151.

Ma, RY 1993, *Wind effects on convective heat loss from a cavity receiver for a parabolic concentrating solar collector*, Sandia National Laboratories.

Mokhtar, M 2011, 'The beam-down solar thermal concentrator: experimental characterization and modeling', Master's Thesis. Masdar Institute of Science and Technology, Abu Dhabi, United Arab Emirates.

Mokhtar, M, Meyers, SA, Armstrong, PR & Chiesa, M 2014, 'Performance analysis of masdar city's concentrated solar beam-down optical experiment'.

Paitoonsurikarn & Lovegrove, K 2003, 'On the study of convection loss from open cavity receivers in solar paraboloidal dish applications', *Proceedings of 41st Conference of the Australia and New Zealand Solar Energy Society (ANZSES), Melbourne, Australia*.

Paitoonsurikarn, S & Lovegrove, K 2002, 'Numerical investigation of natural convection loss in cavity-type solar receivers', *Proceedings of Solar*.

Paitoonsurikarn, S, Lovegrove, K, Hughes, G & Pye, J 2011, 'Numerical investigation of natural convection loss from cavity receivers in solar dish applications', *Journal of Solar Energy Engineering*, vol. 133, no. 2, p. 021004.

Philibert, C 2010, *Technology roadmap: concentrating solar power*, OECD/IEA.

Sánchez-González, A, Rodríguez-Sánchez, MR & Santana, D 2016, 'Aiming strategy model based on allowable flux densities for molten salt central receivers', *Solar energy*.

CHAPTER 7

Segal, A & Epstein, M 2008, 'Practical considerations in designing large scale "beam down" optical systems', *Journal of Solar Energy Engineering*, vol. 130, no. 1, p. 011009.

Stalin Maria Jebamalai, J 2016, *Receiver Design Methodology for Solar Tower Power Plants*.

Steinfeld, A & Schubnell, M 1993, 'Optimum aperture size and operating temperature of a solar cavity-receiver', *Solar energy*, vol. 50, no. 1, pp. 19-25.

Tanaka, N 2010, 'Technology Road Map, Concentrating Solar Power', *International Energy Agency*.

Taumoefolau, T, Paitoonsurikarn, S, Hughes, G & Lovegrove, K 2004, 'Experimental investigation of natural convection heat loss from a model solar concentrator cavity receiver', *Journal of Solar Energy Engineering*, vol. 126, no. 2, pp. 801-807.

Wei, X, Lu, Z, Yu, W & Xu, W 2013, 'Ray tracing and simulation for the beam-down solar concentrator', *Renewable Energy*, vol. 50, pp. 161-167.

Wu, S-Y, Shen, Z-G, Xiao, L & Li, D-L 2015, 'Experimental study on combined convective heat loss of a fully open cylindrical cavity under wind conditions', *International Journal of Heat and Mass Transfer*, vol. 83, pp. 509-521.

Wu, S-Y, Xiao, L, Cao, Y & Li, Y-R 2010, 'Convection heat loss from cavity receiver in parabolic dish solar thermal power system: a review', *Solar energy*, vol. 84, no. 8, pp. 1342-1355.

Wu, S-Y, Xiao, L & Li, Y-R 2011, 'Effect of aperture position and size on natural convection heat loss of a solar heat-pipe receiver', *Applied thermal engineering*, vol. 31, no. 14, pp. 2787-2796.

Xiao, L, Wu, S-Y & Li, Y-R 2012, 'Numerical study on combined free-forced convection heat loss of solar cavity receiver under wind environments', *International Journal of Thermal Sciences*, vol. 60, pp. 182-194.

CHAPTER 8

Conclusions And Future Work

The main objective of the research project, reported in this thesis, is to deepen the understanding of heat losses from a heated cavity. The outcomes of this research are needed in order to enable engineers to reliably optimise the design of cavity receivers and minimise heat losses for better efficiency. Experimental and numerical studies have helped to achieve the five main objectives of the project. The research output was published in four journal papers and the key outcomes from the works are highlighted below.

8.1 Key outcomes from the numerical study

The primary contribution of the numerical study is to better understand the effect of interaction between aspect ratio and wind speed on heat losses from a cavity receiver. The focus was to shed light on the temperature and air flow distribution of the air inside the cavity. It has been found that, for the scenario of uniform temperature of the internal cavity walls, a small increase in wind speed above ambient still air (speed of 0 m/s), reduces the combined convective heat loss below the value for natural convection losses (i.e. losses at wind speed of zero). The “critical” values of wind speed, above which heat loss is reduced below the case of natural convection, were found to increase with the aspect ratio.

Furthermore, the higher the aspect ratio, the smaller is the effect of wind speed on the combined convective losses per unit of cavity internal area. This finding shows that, on the one hand, it can be advantageous to use a short cavity under low wind speed conditions while on the other hand, the overall thermal efficiency of a solar

cavity receiver increases with the cavity aspect ratio (for a range of 3 and below). Therefore, there is an advantage to have a long cavity from the convective heat loss point of view, if a solar cavity receiver is placed in a windy location. Nonetheless, when choosing the aspect ratio of a cavity, one needs to take into consideration the aspect ratio of a cavity, one needs to take into consideration the balance between the optical power input and the heat losses from the cavity, as well as the cost of the receiver.

The numerical study also provide information on airflow distribution of the air inside the cavity. It was found that a recirculating interior flow is generated inside the heated cavity for all aspect ratios, with the flow entering from the lower side and recirculating upward from the back of the cavity to leave from the upper side. However, the magnitude of velocity over the surface decreases with an increase in aspect ratio. This further explains why an increase in aspect ratio decreases the average convective heat transfer.

8.2 Key outcomes from the experimental study

The experimental study reported in this thesis, is the first systematic study, which assess the influence of multiple design configuration, and operating conditions on heat losses from a cavity receiver. Those parameters include; wind speed, yaw angle, tilt angle, cavity aperture ratio internal walls temperature and 4 combination of temperature distribution inside a cavity, with 16 well controlled temperature surfaces. The influence of head-on wind speed on the heat losses is found to be

CHAPTER 8

much higher than the side-on wind. At high wind speed ($1/Ri > 19$), the convective heat losses from the head-on wind cases are about 4 times higher than the side-on wind one. Therefore, there is an advantage to locate the solar cavity receiver in a location which prevailing side-on wind most of the time.

Using the experimental observations and data correlation equations for the heat losses from a cavity receiver were developed and tested. These equations, which use the Nusselt number as a function of the inverse of Richardson number, have been developed for a very wide range of the inverse of Richardson number and they are applicable for various operating conditions. The correlation equations are developed for 2 ranges of $1/Ri$ namely; $1/Ri < 10$, dominated by natural convection and $1/Ri > 10$, dominated by forced convection. The correlation equations cover a large range of conditions (up to 200 of the inverse of Richardson number), giving $R^2 = 0.824$ for $1/R < 10$ cases and $R^2 = 0.986$ for $1/R > 10$.

Introducing a lip at the aperture plane, by decreasing the aperture ratio D_{ap}/D_{cav} , acts to inhibit the natural convective losses from a cavity receiver (at zero wind speed) by up of to a factor of 5, but increases the forced convective losses by a factor, by up to 30%. More specifically, for tilt angle = 15° and $1/Ri < 4.8$ ($V < 3$ m/s), the convective heat losses increase with aperture ratio, although this behaviour reverses for $1/Ri > 19$ ($V > 6$ m/s). For $1/Ri < 4.8$ ($V < 3$ m/s) the total heat loss can vary by up to about 75% by increasing the aperture ratio from 0.33 to 0.75.

CHAPTER 8

For tilt angle = 15° condition, about 60% of the total heat is lost from the lower section of the heated cavity. Furthermore, approximately 43% of the heat is lost from the lower front section of the heated cavity for aperture ratio = 0.33 and 0.5, while this drops to approximately 36 % for the aperture ratio = 0.75 case. This difference is attributed to the decreased size of the stagnant zone at the rear of the cavity.

Similarly, the increased uniformity in heat losses with an increase in wind speed is attributed to a decreased significance of the stagnant zone. In addition, although the aperture ratio does influence the convective heat loss, its influence is less than 15% over the range $0.33 < D_{ap}/D_{cav} < 1$ for a tilt angle of 30° and wind speed above 3 m/s ($1/Ri > 4.8$).

The effect of tilt angle on the overall total heat loss from the cavity for various wind speed was found to be relatively small. It was also found that there is a slight advantage with respect to heat loss in keeping the tilt angle of a solar cavity below 30°.

The effect of varying the internal walls' temperature were tested to simulate different 'hot spots' in a solar cavity receiver. It was found that for a downward tilted solar cavity receiver, an "upper or rear surface hotter" cavity has less overall heat losses when compared with other cases. For "upward facing heated cavity", the rear wall hotter cases have lower heat losses than the front hotter cases, which is as expected. It was found that the upward facing cavity has the lowest heat loss

for all wind condition. For high wind speeds, the heat loss from the upward facing cases is approximately 3 times less than the downward tilted cases for head-on wind condition, and similar heat losses with the side-on wind conditions.

The distribution of heat loss from the different parts of the cavity receiver was also quantified for the different operating conditions considered in this study. Approximately 88 % of heat is lost from the lower part of the heated cavity for the case of the no-wind ($V = 0\text{ m/s}$), consistent with the well-known dominance of buoyancy and natural convection. As wind speed is increased to $1/Ri < 8.53$ ($V < 4\text{ m/s}$), the fractional heat loss from the lower surface decreases from approximately 88% to 65 % and the heat transfer is classified in the mixed regime, with buoyancy and inertia both important. Inertia dominates for $1/Ri > 43$ ($V > 9\text{ m/s}$) so that convective heat losses are distributed uniformly throughout the cavity. The heat loss distribution from the different parts of the cavity should be very useful for the development of further models.

8.3 Future Work

Further numerical studies will be needed in order to test the computational CFD models ability to predict the flow and temperature distribution under the conditions investigated in this project. In particular, the new study will be needed to resolve the issue of critical wind speeds under different cavity orientation at which heat losses are reduced below the natural convection value. The “critical” wind speeds, above which the heat loss is reduced below the case of natural convection, was

found for the head-on wind direction. However, the side-on wind was not assessed using CFD. In contrast, the experimental results revealed that a “critical” wind speed was found only for the side-on wind direction. One possible reason for this apparent discrepancy is the difference in their geometries, and may stipulate that this “critical wind speed is possible at a very low wind speed. Furthermore, the experimental study suggested that, the “critical wind speed for the head-on case should occur at low wind speed ($Ri \sim 1.25$). However, this wind speed is out of the testable range of the wind tunnel. It is also worthy of further assess the heat loss from a cavity receiver in this range of low wind speed condition. Moreover, the predicted temperature distribution inside the heated cavity, from the CFD model for various wind speed, agrees reasonably well with the measured heat loss distribution over different wall surfaces of the heated cavity in the experiment. Although flow-field information is not yet available, the present measurements of heat loss distribution over different wall surfaces of the heated cavity, for a series of conditions, can also be used to provide additional data for the validation of further modelling efforts.

Further study is also warranted in developing an approach method to reduce the impact of head-on wind as well as redirecting the air to flow parallel to the aperture, as the impact of head-on wind could be up to 4 times higher than the side-on wind on heat losses. For downward tilted solar cavity, there is a slight advantage with respect to heat loss in keeping the tilt angle of a solar cavity between 15° and 30° , hence future study could look into the effect of other parameters within this range of tilt angles. Further investigations of the “beam-down” orientation is also worth

pursuing. This is because the convective heat losses are about 4 times less than the tower system with head-on wind. Much lower wind speed is also expected from a “beam-down” solar receiver, as it is closer to the ground level. In addition, Further research into matching the solar receiver with the heliostat field to concentrate most of the radiation into the upper rear parts of the cavity will help reduce heat losses from the system, and subsequently increase the efficiency of the concentrated solar receiver. Nevertheless, the experimental results from the studies of this thesis should be further investigate to provide a new correlation for mixed convective heat loss with the parameters, which were assessed in this thesis. Lastly, LCOE should also be assessed for the assessed parameters. Potentially the new correlation for mixed convective heat loss can be used for the LCOE assessment.

References

- ASTRI, 2017. ASTRI Milestone 12 Report- For Public Dissemination. <http://www.astri.org.au/wp-content/uploads/2018/04/iii-ASTRI-M12-2017-Public-Dissemination-Report.pdf>.
- Ávila-Marín, A.L., 2011. Volumetric receivers in solar thermal power plants with central receiver system technology: a review. *Solar Energy* 85(5), 891-910.
- Bader, R., 2011. Optical and thermal analyses of an air-based solar trough concentrating system. Diss., Eidgenössische Technische Hochschule ETH Zürich, Nr. 19772, 2011.
- Barlev, D., Vidu, R., Stroeve, P., 2011. Innovation in concentrated solar power. *Solar Energy Materials and Solar Cells* 95(10), 2703-2725.
- Behar, O., Khellaf, A., Mohammedi, K., 2013. A review of studies on central receiver solar thermal power plants. *Renewable and sustainable energy reviews* 23, 12-39.
- Birol, F., 2017. Key world energy statistics. IEA Publications, International Energy Agency, rue de la Federation, Paris, France.
- Chinnici, A., Nathan, G., Dally, B., 2018. Experimental demonstration of the hybrid solar receiver combustor. *Applied Energy* 224, 426-437.
- Clausing, A., 1981. An analysis of convective losses from cavity solar central receivers. *Solar Energy* 27(4), 295-300.

- Clausing, A., 1983. Convective losses from cavity solar receivers—comparisons between analytical predictions and experimental results. *Journal of Solar Energy Engineering* 105(1), 29-33.
- Deubener, J., Hensch, G., Moiseev, A., Bornhöft, H., 2009. Glasses for solar energy conversion systems. *Journal of the European Ceramic Society* 29(7), 1203-1210.
- Falcone, P., Noring, J., Hruby, J., 1985. Assessment of a solid particle receiver for a high temperature solar central receiver system. Sandia National Labs., Livermore, CA (USA).
- Falcone, P.K., 1986. A handbook for solar central receiver design. Sandia National Labs., Livermore, CA (USA).
- Flesch, R., Stadler, H., Uhlig, R., Hoffschmidt, B., 2015. On the influence of wind on cavity receivers for solar power towers: An experimental analysis. *Applied Thermal Engineering* 87, 724-735.
- Fluent, A., 2016. FLUENT User's Guide 17.0. Ansys Corporation.
- Fluent, A., 2018. FLUENT User's Guide 19.0. Ansys Corporation.
- Garbrecht, O., Al-Sibai, F., Kneer, R., Wieghardt, K., 2013. CFD-simulation of a new receiver design for a molten salt solar power tower. *Solar Energy* 90, 94-106.
- Garcia, A., Torres, J., Prieto, E., De Francisco, A., 1998. Fitting wind speed distributions: a case study. *Solar Energy* 62(2), 139-144.
- Gardon, R., 1961. A review of radiant heat transfer in glass. *Journal of the American Ceramic Society* 44(7), 305-312.
- Hasuike, H., Yoshizawa, Y., Suzuki, A., Tamaura, Y., 2006. Study on design of molten salt solar receivers for beam-down solar concentrator. *Solar energy* 80(10), 1255-1262.
- Hensch, G., Mös, A., Deubener, J., Höland, M., 2010. Thermal resistance of nanoporous antireflective coatings on silica glass for solar tower receivers. *Solar Energy Materials and Solar Cells* 94(12), 2191-2196.
- Ho, C.K., Iverson, B.D., 2014. Review of high-temperature central receiver designs for concentrating solar power. *Renewable and Sustainable Energy Reviews* 29, 835-846.
- Ho, C.K., Khalsa, S.S., Siegel, N.P., 2009. Modeling on-sun tests of a prototype solid particle receiver for concentrating solar power processes and storage, ASME 2009 3rd International Conference on Energy Sustainability collocated with the Heat Transfer and InterPACK09 Conferences. American Society of Mechanical Engineers, pp. 543-550.
- Hogan, R., Diver, R., Stine, W.B., 1990. Comparison of a cavity solar receiver numerical model and experimental data. *Journal of Solar Energy Engineering* 112(3), 183-190.
- Holman, J., 1997. Heat transfer, 8th ed. McGraw-Hill, New York.
- IEA-ETSAP, IRENA, 2013. Concentrating solar power technology brief.
- International Energy Agency, X., 2013. Key world energy statistics. International Energy Agency.
- Jafarian, M., Arjomandi, M., Nathan, G.J., 2013. A hybrid solar and chemical looping combustion system for solar thermal energy storage. *Applied Energy* 103, 671-678.
- James, W., 2011. Zero carbon Australia we can do it. <http://www.skepticalscience.com/print.php?n=647>. (Accessed 19 June 2014).

- Johnston, G., 1995. Flux mapping the 400 m² “Big Dish” at the Australian National University. *Journal of solar energy engineering* 117(4), 290-293.
- Kim, J.K., Yoon, H.K., Kang, Y.H., 2009. Experimental study on heat loss from cavity receiver for solar power tower, *Proceedings of ISES World Congress 2007* (Vol. I–Vol. V). Springer, pp. 1719-1723.
- Kolb, G.J., Ho, C.K., Mancini, T.R., Gary, J.A., 2011. Power tower technology roadmap and cost reduction plan. Sandia National Laboratories, Livermore, CA, Technical Report No. SAND2011-2419.
- Korzynietz, R., Quero García, M., Uhlig, R., 2012. Solugas – future solar hybrid technology, *Proceedings of the International Solar PACES Conference, Marrakesh, Morocco, September*. pp. 11-14.
- Kueh, K.C., Nathan, G.J., Saw, W.L., 2015. Storage capacities required for a solar thermal plant to avoid unscheduled reductions in output. *Solar Energy* 118, 209-221.
- Leonardi, E., 2012. Detailed analysis of the solar power collected in a beam-down central receiver system. *Solar Energy* 86(2), 734-745.
- Li, Q., Zhi, L., Hu, F., 2010. Boundary layer wind structure from observations on a 325m tower. *Journal of wind engineering and industrial aerodynamics* 98(12), 818-832.
- Li, X., Dai, Y., Wang, R., 2015. Performance investigation on solar thermal conversion of a conical cavity receiver employing a beam-down solar tower concentrator. *Solar Energy* 114, 134-151.
- Lovegrove, K., Watt, M., Passey, R., Pollock, G., Wyder, J., Dowse, J., 2012. Realising the potential of concentrating solar power in Australia: summary for stakeholders. Australian Solar Institute Pty, Limited.
- Ma, R.Y., 1993. Wind effects on convective heat loss from a cavity receiver for a parabolic concentrating solar collector. Sandia National Laboratories.
- Mande, O., Miller, F., 2011. Window design for a small particle solar receiver. IECEC 2011.
- McDonald, C.G., 1995. Heat loss from an open cavity. Sandia National Labs., Albuquerque, NM (United States); California State Polytechnic Univ., Pomona, CA (United States). Coll. of Engineering.
- McIntosh, A., Hughes, G., Pye, J., 2014. Use of an Air Curtain to Reduce Heat Loss from an Inclined Open-Ended Cavity.
- Meteotest, 2010. World - Yearly sum of Direct Normal Irradiation (DNI) (1991 - 2010). <http://www.meteonorm.com/>. (Accessed 03/06/2018 2018).
- Mills, A.F., 1999. Basic heat and mass transfer. Prentice hall Upper Saddle River, NJ.
- Mokhtar, M., 2011. The beam-down solar thermal concentrator: experimental characterization and modeling. Master’s Thesis. Masdar Institute of Science and Technology, Abu Dhabi, United Arab Emirates.
- Mokhtar, M., Meyers, S.A., Armstrong, P.R., Chiesa, M., 2014. Performance analysis of masdar city’s concentrated solar beam-down optical experiment.
- Müller-Steinhagen, H., Trieb, F., 2004. Concentrating solar power. A review of the technology. *Ingenia Inform QR Acad Eng* 18, 43-50.

- Nathan, G., Battye, D., Ashman, P., 2014. Economic evaluation of a novel fuel-saver hybrid combining a solar receiver with a combustor for a solar power tower. *Applied Energy* 113, 1235-1243.
- Paitoonsurikarn, S., Lovegrove, K., 2002. Numerical investigation of natural convection loss in cavity-type solar receivers, *Proceedings of Solar*.
- Paitoonsurikarn, S., Lovegrove, K., 2006. A new correlation for predicting the free convection loss from solar dish concentrating receivers, *Solar*. p. 44th.
- Peterson, E.W., Hennessey Jr, J.P., 1978. On the use of power laws for estimates of wind power potential. *Journal of Applied Meteorology* 17(3), 390-394.
- Prakash, M., Kedare, S., Nayak, J., 2009. Investigations on heat losses from a solar cavity receiver. *Solar Energy* 83(2), 157-170.
- Price, H., 2003. Assessment of parabolic trough and power tower solar technology cost and performance forecasts. Sargent & Lundy LLC Consulting Group, National Renewable Energy Laboratory, Golden, Colorado.
- R  nger, M., Pf  nder, M., Buck, R., 2006. Multiple air-jet window cooling for high-temperature pressurized volumetric receivers: testing, evaluation, and modeling. *Journal of solar energy engineering* 128(3), 265-274.
- Romero, M., Steinfeld, A., 2012. Concentrating solar thermal power and thermochemical fuels. *Energy & Environmental Science* 5(11), 9234-9245.
- Rubin, M., 1982. Calculating heat transfer through windows. *International Journal of Energy Research* 6(4), 341-349.
- Salvadore, M.S., Keppler, J.H., 2010. Projected costs of generating electricity, 2010 Edition ed. Paris Dauphine University.
- Segal, A., Epstein, M., 2008. Practical considerations in designing large scale "beam down" optical systems. *Journal of solar energy engineering* 130(1), 011009.
- Shih, T.-H., Liou, W.W., Shabbir, A., Yang, Z., Zhu, J., 1995. A new $k-\epsilon$ eddy viscosity model for high reynolds number turbulent flows. *Computers & Fluids* 24(3), 227-238.
- Siegel, N.P., Ho, C.K., Khalsa, S.S., Kolb, G.J., 2010. Development and evaluation of a prototype solid particle receiver: on-sun testing and model validation. *Journal of Solar Energy Engineering* 132(2), 021008.
- Siegel, R., 2001. *Thermal radiation heat transfer*. CRC press.
- Srilakshmi, G., Venkatesh, V., Thirumalai, N., Suresh, N., 2015. Challenges and opportunities for Solar Tower technology in India. *Renewable and Sustainable Energy Reviews* 45, 698-709.
- Stalin Maria Jebamalai, J., 2016. *Receiver Design Methodology for Solar Tower Power Plants*.
- Steinfeld, A., Schubnell, M., 1993. Optimum aperture size and operating temperature of a solar cavity-receiver. *Solar Energy* 50(1), 19-25.
- Taumoefolau, T., Lovegrove, K., 2002. An experimental study of natural convection heat loss from a solar concentrator cavity receiver at varying orientation, *Proceedings of Solar*.
- Taumoefolau, T., Paitoonsurikarn, S., Hughes, G., Lovegrove, K., 2004. Experimental investigation of natural convection heat loss from a model solar concentrator cavity receiver. *Journal of Solar Energy Engineering* 126(2), 801-807.
- Uhlig, R., Flesch, R., Gobereit, B., Giuliano, S., Liedke, P., 2014. Strategies enhancing efficiency of cavity receivers. *Energy Procedia* 49, 538-550.

- Wei, X., Lu, Z., Yu, W., Xu, W., 2013. Ray tracing and simulation for the beam-down solar concentrator. *Renewable Energy* 50, 161-167.
- Wu, S.-Y., Shen, Z.-G., Xiao, L., Li, D.-L., 2015. Experimental study on combined convective heat loss of a fully open cylindrical cavity under wind conditions. *International Journal of Heat and Mass Transfer* 83, 509-521.
- Wu, S.-Y., Xiao, L., Cao, Y., Li, Y.-R., 2010. Convection heat loss from cavity receiver in parabolic dish solar thermal power system: a review. *Solar Energy* 84(8), 1342-1355.
- Wu, S.-Y., Xiao, L., Li, Y.-R., 2011. Effect of aperture position and size on natural convection heat loss of a solar heat-pipe receiver. *Applied Thermal Engineering* 31(14), 2787-2796.
- Xiao, L., Wu, S.-Y., Li, Y.-R., 2012. Numerical study on combined free-forced convection heat loss of solar cavity receiver under wind environments. *International Journal of Thermal Sciences* 60, 182-194.
- Zhang, H., Baeyens, J., Degève, J., Cacères, G., 2013. Concentrated solar power plants: Review and design methodology. *Renewable and Sustainable Energy Reviews* 22, 466-481.